# Regulatory Networks and Complex Interactions Between the Insulin and Angiotensin II Signaling Systems: Implications for Hypertension and Diabetes

**by**

**Deniz Çizmeci**

**A Thesis Submitted to the**
**Graduate School of Engineering**
**in Partial Fulfillment of the Requirements for**
**the Degree of**

**Master of Science**
**in**
**Chemical and Biological Engineering**

**Koc University**

**September 2012**

Koc University

Graduate School of Sciences and Engineering

This is to certify that I have examined this copy of a master's thesis by

Deniz Çizmeci

and have found that it is complete and satisfactory in all respects,
and that any and all revisions required by the final
examining committee have been made.

Committee Members:

_____

Prof. Yaman Arkun (Advisor)

_____

Prof. Burak Erman

_____

Assoc. Prof. Alper Demir

Date: _____

## ABSTRACT

Clinical evidence shows that there is a correlation between diabetes and hypertension diseases. This thesis applies the tools of systems biology to analyze the structure and the dynamics of the complex cellular networks associated with diabetes and hypertension. The primary research focus is the interaction between Angiotensin II (Ang II) and Insulin AKT signaling pathways. AKT, also known as Protein Kinase B, plays a key regulatory role in metabolic actions of insulin. While being a significant factor in pathophysiology of hypertension, Ang II also induces insulin resistance. We developed dynamic models of the system of interactions among the biomolecules that play important roles in cross-talk between the insulin and Ang II signaling pathways. Embedded feedback structures are revealed. Different scenarios are simulated and dominant dynamic characteristics are investigated. We showed that Ang II inhibits the actions of insulin by interfering with Insulin-AKT signaling reducing insulin-mediated glucose uptake and impairing insulin-mediated vasodilation. Also diabetic state, defined by the poor glucose control, contributes to the progression of hypertension by inducing hyperglycemia. This model provides insight into the complexity of cellular networks governing the development of diseases and hopefully paves the way for proposing targets for therapeutic interventions.

# ÖZET

Klinik veriler diyabet ile hipertansiyon hastalıkları arasında bir ilişki olduğunu göstermektedir. Bu tez, sistem biyolojisi yaklaşımı uygulayarak diyabet ve hipertansiyon hastalıkları ile ilişkilendirilen karmaşık hücresel ağların yapılarını ve dinamiklerini incelemektedir. Öncelikli olarak Angiotensin II (Ang II) ve insülin AKT sinyal iletim ağları üzerine odaklanılmıştır. Protein kinaz B olarak da bilinen AKT, insülinin metabolik etkilerinde merkezi rol oynar. Ang II ise hem hipertansiyon patofizyolojisinde önemli bir etkendir hem de insülin direncine yol açan etkileşimlerde bulunur. Bu çalışmada insülin ve Ang II sinyal ağlarının etkileşiminde önemli rol oynayan molekülleri içeren dinamik modeller oluşturulmuştur. Geri besleme yapıları ortaya çıkarılmıştır. Farklı senaryolar oluşturulup simüle edilerek baskın dinamik özellikler araştırılmıştır. Ang II'nin insülin AKT sinyal iletişim ağına müdahale ederek insülin aracılığıyla gerçekleşen glukoz alımı ve vasodilasyon mekanizmalarına zarar verdiği görülmüştür. Aynı zamanda glukoz kontrolü sağlanamayan diyabet durumunun, hiperglisemi oluşturarak hipertansiyona yol açabileceği gösterilmiştir. Ortaya koyulan model hastalık oluşumunda etkili olan karmaşık sinyal ağlarının anlaşılmasına ve yeni tedavi hedeflerine ışık tutacaktır.

**ACKNOWLEDGEMENT**

I have been more than fortunate to have amazing people in my life who for me define words like trust, encouragement, support, love, patience. I am grateful for the opportunity to thank them, although words couldn't express the full extent of my gratitude.

Above all, I would like to express my sincere appreciation for my thesis advisor Prof. Yaman Arkun. The experience and knowledge he offered me is beyond from this thesis. Without his encouragement and enthusiasm this work would have never been completed. He is an inspiration for me both as an academic and as a person and it is an honor to work with him. I am also grateful to Prof. Burak Erman and Assoc. Prof. Alper Demir for their guidance throughout my study and for their participation in my thesis committee.

I am indebted to my friends for their invaluable companionship. Special thanks to Tuğçe Yıldızoglu and Bahar Degirmenci for their tenderness, moral support and patience during this period. I would like to thank Merve Sancak, Melis Bulutoglu, Sanem Kayandan, Selin Akalın, Tuğçe Acar, Derya Aguday, Selin Kanyas who have brightened my days with joy and laughter. I am happy that I can always trust their endless friendship under any circumstances. I would also like to thank Furkan Anarat for the dare, for the challenge, and for the encouragement and to Hasan Şıldır, İlknur Eruçar, Erhan Atcı, Cemal Erdem, Busra Topal, Emine Guven, Zuhal Tasdemir, Engin Çukuroglu for sharing sharing good times at Koc University.

Last but not least I wish to express my gratitude to my parents, Güler and Hamdi, and my brother, Hakan, for their boundless love, support and sacrifices, for always believing in me, for providing a solid ground to stand on, and for providing me with an inherent sense of security throughout my life. To them I dedicate this thesis.

**TABLE OF CONTENTS**

## LIST OF TABLES

## LIST OF FIGURES

# Chapter 1

## INTRODUCTION

Biological actions are carried out through complex interactions of many cellular agents. Molecular biology enables identification of these agents and their functions. Systems biology integrates the existing knowledge in molecular biology to system level to provide a better understanding of cellular mechanisms. By studying the network of interactions among the biomolecules present in signaling pathways at the systems level, it is possible to understand how the biological functions are regulated and also how the diseases emerge from their deregulations.

Diabetes and hypertension are common diseases affecting millions of people worldwide. Clinical and pharmacological data suggest that diabetes and hypertension diseases are related. Diabetes is often associated with insulin resistance. Insulin resistance can develop through impairments in signaling events downstream of insulin. Renin Angiotensin Sytem (RAS) is found to be activated in hypertension and Ang II is an important vasoconstrictor agent in RAS. Ang II is a key agent since it contributes to hypertension development by increasing blood pressure and impaires insulin signaling as well. Diabetes can induce hyperglycemia and hyperglycemia may lead to hypertension by activating Ang II. This thesis investigates the possible crosstalk between insulin and Ang II signaling pathways using a systems biology approach.

Chapter 2 covers the literature survey which is carried out to identify the biomolecules that play significant roles in diabetes and hypertension development.Their interactions are illustrated in detail. Insulin mediated glucose uptake and vasodilation mechanisms are explained. Available literature knowledge about the crosstalk between insulin and Ang II are reviewed. Blood Pressure mechanisms and the role of Ang II in blood pressure regulation are summarized. Hyperglycemia effects are defined. Embedded feedback structures are listed.

Chapter 3 presents the construction of pathway structures, lumping of interactions and identifications of feedback loops present in the pathway models. There are four models with increasing complexity. The concept of bistability is reviewed and the steady state and dynamic equation sets of the four models are given.

In Chapter 4, steady state and dynamic analysis of the models are presented. Different scenarios with various parameter sets are simulated. Normal and diseased states are identified.

Conclusion is drawn with a summary of findings of this thesis.

# Chapter 2

# LITERATURE REVIEW

## 2.1 Overview

Diabetes mellitus is a prevalent metabolic disease. According to World Health Organization (WHO) fact sheet (World Health Organisation, August 2011), 346 million people worldwide have diabetes and WHO presumes that mortality due to diabetes will double between 2005 and 2030. Glucose homeostasis is regulated by insulin, and diabetes is a chronic disease associated with impaired glucose control (Kahn, 1998). Diabetes can be insulin-dependent (Type 1) or noninsulin-dependent (Type 2). Type 1 diabetes is characterized by deficient insulin production which occurs as a result of destruction of pancreatic β cells whereas Type 2 diabetes is characterized by ineffective use of insulin, called insulin resistance (Kahn, 1998). Blindness, renal failure and cardiovascular diseases are common consequences of diabetes. Data from (National Diabetes Fact Sheet, 2011) shows that in 2005-2008, of diabetes patients aged 20 years or older, 67% had high blood pressure or used hypertension medications. Persons with hypertension are more prone than normotensive persons to develop diabetes (Ando and Fujita, 2006). There is also pharmacological evidence that insulin takes role in coupling blood flow and glucose metabolism and medical studies suggest that drugs such as angiotensin-converting enzyme (ACE) inhibitors or angiotensin II receptor blockers enhance insulin sensitivity and prevent onset of diabetes (Ando and Fujita, 2006; Henriksen, 2007; Henriksen et al., 2001; Nawano

et al., 1999; Perkins and Davis, 2008; Scheen, 2004). These evidences suggest the possibility of crosstalk between insulin signaling pathway and the renin angiotensin system (RAS), an important regulatory mechanism for controlling blood pressure. Moreover, clinical evidence suggests connections between cancer and diabetes (Giovannucci, 2007; Giovannucci et al., 2010; Hsu et al., 2007).

The key component in crosstalk of diabetes, cancer and hypertension is the serine/threonine kinase AKT (also known as protein kinase B). AKT plays a crucial role in processes such as cell survival, proliferation, and glucose metabolism (Altomare and Testa, 2005; Bellacosa et al., 2005; Cong et al., 1997; Liao and Hung, 2010). Disfunctions in insulin mediated activation of AKT can lead to insulin resistance or uncontrolled cell proliferation. RAS activation, Angiotensin II production, inhibits the actions of insulin by interfering with Insulin-AKT signaling pathway reducing insulin-mediated glucose uptake and impairing insulin-mediated vasodilation. Also diabetic state, defined by the poor glucose control, plays an important role in the progression of hypertension by inducing hyperglycemia. These effects are described below in detail.

### 2.2 Insulin AKT Signaling Pathway

AKT is activated by the events downstream of insulin and its activation is essential for insulin mediated glucose transport. This activation is mediated by PI3K and mTOR is linked to the pathway to make it sensitive to nutrients.

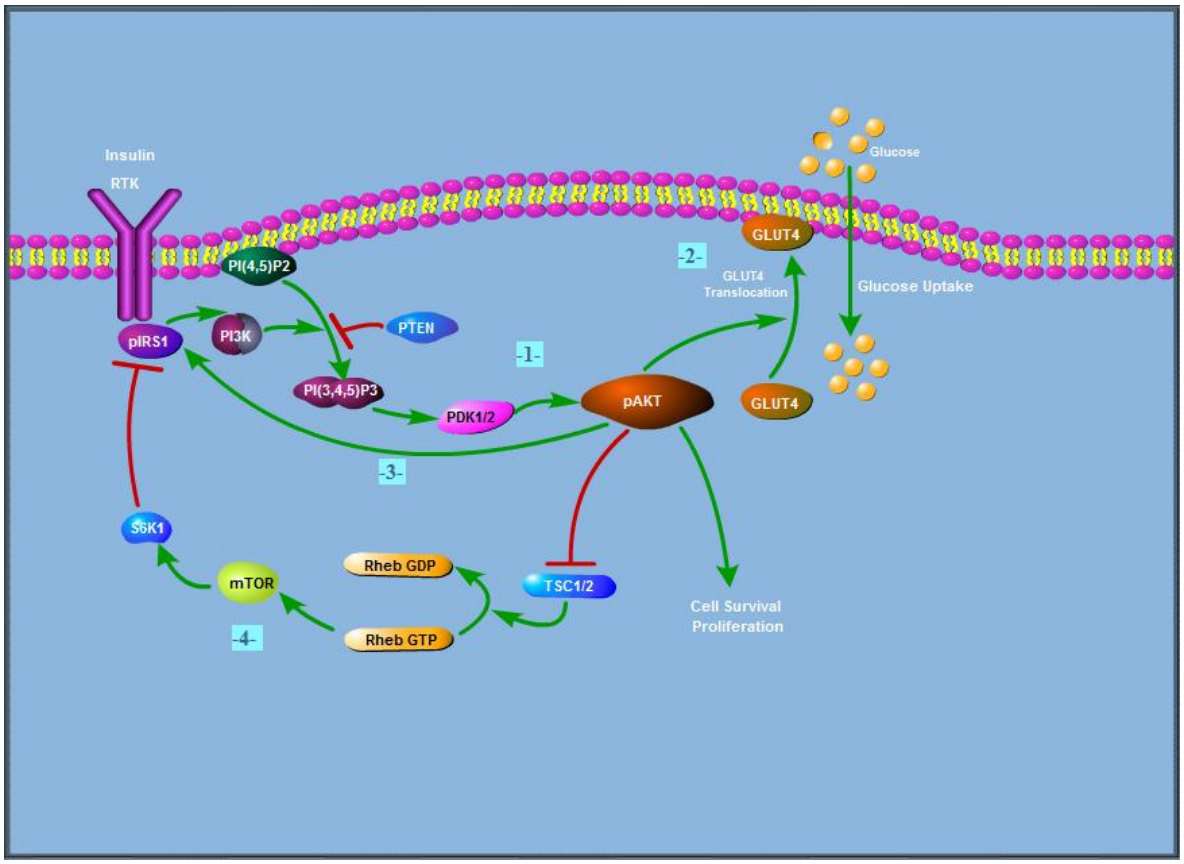


Figure 1. Insulin AKT signaling pathway structure

Table 1. Processes contained in Insulin AKT pathway

| | **Process** | **Reference** |
|---|---|---|
| **1** | pIRS1 → PI3K → PIP2 → PDK1/2 → pAKT | (Franke et al., 1997; Liao and Hung, 2010; Manning, 2004) |
| **2** | pAKT → GLUT4 → Glucose uptake | (Cong et al., 1997; |

| | | |
|---|---|---|
| | | Saltiel and Kahn, 2001; Sowers, 1990) |
| **3** | pAKT → pIRS1 | (Elchebly et al., 1999; Paz et al., 1999; Ravichandran et al., 2001) |
| **4** | pAKT ⊣ TSC1/2 ⊣ Rheb GTP → mTOR → S6K1⊣ pIRS1 | (Guertin and Sabatini, 2005; Hara et al., 1998; Nayak et al., 2011; Raught et al., 2001; Thomas and Hall, 1997; Winter et al., 2011) |

**1: PI3K-dependent signaling and AKT activation**

Growth factors like insulin, insulinlike growth factor IGF-I, and IGF-II activate insulin/IGF-I receptor tyrosine kinases (RTKs) on the cell surface. Activated RTKs autophosphorylate and create phosphotyrosine binding sites for the insulin receptor substrate (IRS). IRSs are phosphorylated by insulin/IGF-I RTKs on tyrosine residues. Phosphorylated IRSs act as binding sites for proteins containing src homology 2 domains, including the p85 regulatory subunit of class I phosphoinositide 3-kinase (PI3K) (Manning, 2004).

PI3Ks are intracellular lipid kinases that phosphorylate the 3'-hydroxyl group of phosphatidylinositols (PIs) and phosphoinositides. They generate PIP3 from PIP2. Subsequently, PIP3 recruits Akt and 3-phosphoinositide-dependent kinase 1 (PDK1) by binding to their PH domain. Akt is activated by phosphorylation on Thr308 and Ser473 via PDK1 and PDK2, respectively (Franke et al., 1997). PP2A dephosphorylates Akt on both Thr-308 and Ser473 sites. PHLPPs also dephosphorylate Akt. The lipid protein phosphatase PTEN negatively regulates Akt activation by converting PI3K-generated PIP3 into PIP2, thus blocking Akt phosphorylation on both Thr308 and Ser473 by PDK1 and PDK2, respectively (Liao and Hung, 2010).

**2: pAKT and glucose uptake**

Plasma glucose homeostasis is maintained during feeding and fasting by regulating the absorption from the intestine, the storage and the release by the liver and the availability for cell uptake via insulin, which is produced in the pancreas, and metabolism by the cells (Saltiel and Kahn, 2001).

Activated AKT (pAKT) enables the translocation of glucose transporter-4 (GLUT-4) from cytosol to the plasma membrane, thus glucose is taken into the cell (Cong et al., 1997; Sowers, 1990). By stimulating the recruitment of GLUT-4 to the cell surface, pAKT plays a key role in the most significant metabolic action of insulin, which is the glucose uptake.

**3: pAKT activates pIRS1**

IRS1 is phosphorylated on serine residues by the activated AKT. This phosphorylation protects IRS1 from the action of protein-tyrosine phosphatases (PTPases) and prevents its dephosphorylation (Paz et al., 1999). PTPases dephosphorylate the insulin receptor, among them PTP1B is found to be upregulated in insulin resistant cells (Elchebly

et al., 1999). pAKT negatively regulates PTP1B and prevents dephosphorylation of IRS1 by PTP1B (Ravichandran et al., 2001). As a result, AKT positively regulates IRS1 function since IRS1 maintains its tyrosine phosphorylated active conformation.

**4: Akt activates mTor**

Nutrient availability is sensed (Hara et al., 1998; Raught et al., 2001) and regulatory signals are transmitted through mTOR (mammalian Target of Rapamycin). pAkt activates mTor by phosphorylating the tuberous sclerosis complex (TSC), heterodimer of hamartin (TSC1) and tuberin (TSC2). The TSC1/2 complex controls the balance between two forms of a small GTPase called Rheb. Rheb-GDP is the inactive form whereas Rheb-GTP directly activates mTor. AKT-dependent phosphorylation of TSC2 inactivates the TSC complex and thus the conversion to the inactive Rheb-GDP form is inhibited (Winter et al., 2011). Since active Rheb-GTP form is favored, mTOR becomes activated. mTOR activates S6K which phosphorylates and inhibits IRS1 (Thomas and Hall, 1997) (Guertin and Sabatini, 2005; Nayak et al., 2011).

## 2.3 Crosstalk with other pathways

### 2.3.1 Angiotensin II and insulin resistance

Insulin has vasodilatory actions on vascular tone mediated by NO which is produced by pAKT. Ang II impaires insulin signaling by interfering with the pathway through several mechanisms.

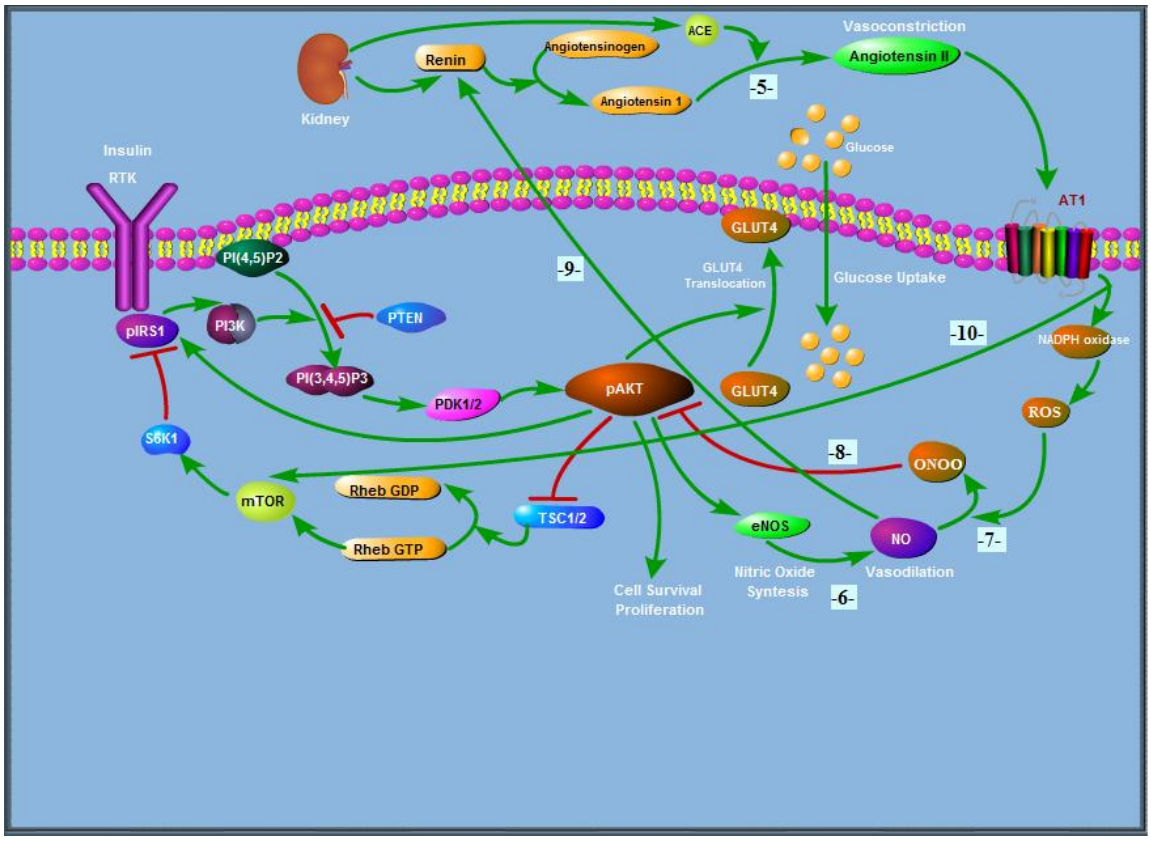


Figure 2. Pathway structure including Ang II effectTable 2. Processes contained in Figure 2

| | **Process** | **Reference** |
|---|---|---|
| **5** | Renin → Angiotensinogen → Angiotensin I →Angiotensin II | (de Kloet et al., 2010) |
| **6** | pAKT → eNOS →NO | (Andreozzi et al., 2004; Zeng et al., 2000) |
| **7** | NO → $ONOO^-$ | (Blendea et al., 2005; Ceriello et al., 2004; Fan et al., 2004; Guo et al., 2003; Pueyo et |

| | | |
|---|---|---|
| | | al., 1998; Sowers, 1990; Ushio-Fukai et al., 1998; Wattanapitayakul et al., 2000; Wei et al., 2006; Wenzel et al., 2008) |
| **8** | $ONOO^-$ ⊣ pAKT | (Carvalho-Filho et al., 2005; Csibi et al., 2010; Yasukawa et al., 2005) |
| **9** | NO → Renin | (Kurtz and Wagner, 1998) |
| **10** | Ang II → mTOR | (Pulakat et al., 2011) |

**5: Angiotensin II production**

Renin is secreted from the kidney and it cleaves angiotensiongen, which is synthesized in the liver, to produce angiotensin I. Then angiotensin converting enzyme (ACE) converts angiotensin I to angiotensin II (de Kloet et al., 2010).

**6: pAKT stimulates NO synthesis**Vasodilator effects of insulin are mediated by the signaling pathway involving IRS-1/PI-3 kinase/Akt/eNOS that leads to increased NO production by endothelium (Zeng et al., 2000). AKT leads to phosphorylation of eNOS on serine 1177. eNOS, endothelial nitric oxide synthase, catalyzes the production of nitric oxide from L-arginine. Thus, Ang II would affect insulin-stimulated production of nitric oxide negatively since it leads to inhibition of AKT activation (Andreozzi et al., 2004).

**7: NO converted to $ONOO^-$ by the action of ANG II**

Ang II is known to generate $ONOO^-$ (Pueyo et al., 1998) (Wattanapitayakul et al., 2000) (Fan et al., 2004) (Ceriello et al., 2004) (Guo et al., 2003). Ang II stimulates production of reactive oxygen species (ROS) such as superoxide $O_2^-$ through activation of NAD(P)H oxidase (Blendea et al., 2005) (Wei et al., 2006) (Wenzel et al., 2008) (Ushio-Fukai et al., 1998). When both $O_2^-$ and NO are synthesized they will react spontaneously to form peroxynitrite ($ONOO^-$) (Sowers, 1990).

**8: $ONOO^-$ inhibits pAKT**

AKT is nitrated in response to ANG II. $ONOO^-$ nitrates AKT and prevents its phosphorylation on Ser473 and Thr308 and thus inhibits its catalytic activity (Csibi et al., 2010). Inhibitory S-Nitrosation of AKT in response to ONOO is shown in (Yasukawa et al., 2005) (Carvalho-Filho et al., 2005).

**9: NO activates renin**

NO regulates renin synthesis and has stimulatory effect on renin secretion through a cGMP mediated mechanism (Kurtz and Wagner, 1998).

**10: Ang II activates mTOR**

ANG II promotes insulin resistance through activation of the (mTOR)/S6 kinase 1 (S6K1) signaling pathway, inhibits insulin metabolic signaling by promoting S6K1-mediated IRS-1 serine phosphorylation (Pulakat et al., 2011).

### 2.3.2 ERK effects

Insulin signaling pathway interacts with MAPK, and activation of pERK impairs insulin signaling through different paths. Ang II induced activation of pERK contributes to this disruption.

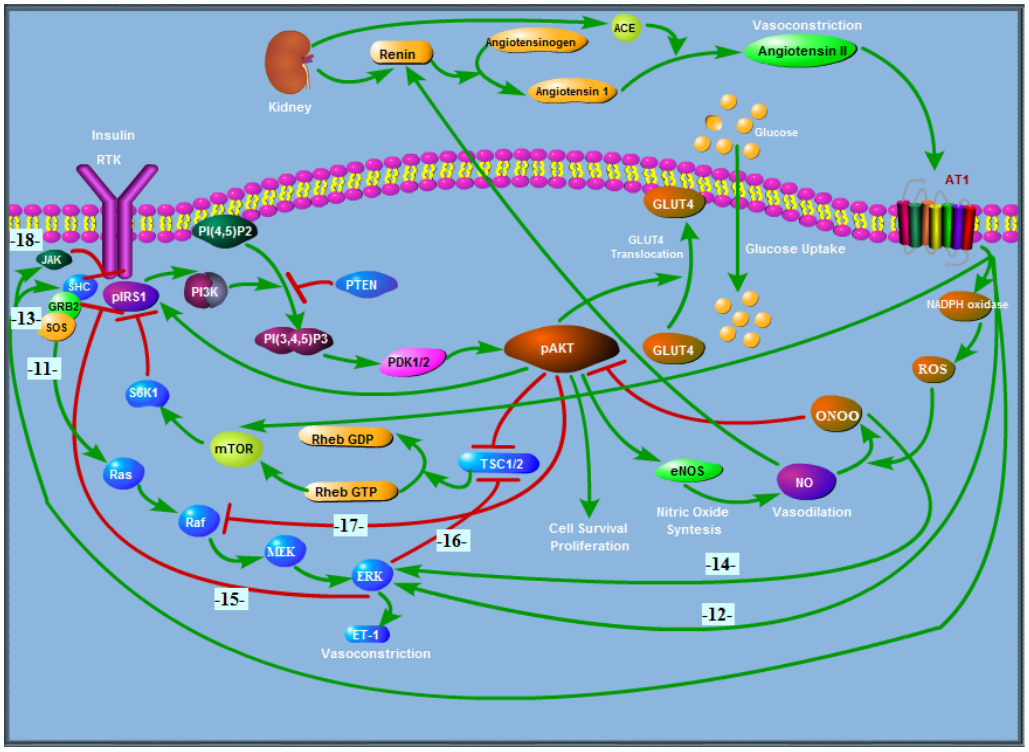


Figure 3. Pathway structure including pERK effects

Table 3. Processes contained in **Error! Reference source not found.**

| | Process | Reference |
|---|---|---|
| **11** | pIRS1 → Shc → Grb2 → SOS → Ras → Raf → Raf → MEK → ERK | (Boulton et al., 1991; Velloso et al., 2006) |
| **12** | Ang II → pERK | (Csibi et al., 2010; Eguchi et al., 2001; Tian et al., 1998) |

| | | |
|---|---|---|
| **13** | ANG II → IRS/Grb2 → pERK | (Velloso et al., 2006) |
| **14** | $ONOO^-$ → pERK | (Csibi et al., 2010; Frank et al., 2000; Pinzar et al., 2005) |
| **15** | pERK ⊣ pIRS1 | (Corbould et al., 2006; Izawa et al., 2005) |
| **16** | pERK ⊣ TSC1/2 ⊣ Rheb GTP → mTOR → S6K1⊣ pIRS1 | (Winter et al., 2011) |
| **17** | pAKT ⊣ Raf → MEK → ERK | (Zimmermann and Moelling, 1999) |
| **18** | ANG II → JAK ⊣ pIRS1 | (Muscogiuri et al., 2008; Velloso et al., 1996) |

**11: pIRS activates pERK through Shc-Grb2-SOS-RAS-RAF-MEK-ERK**

The tyrosine phosphorylated IRS1 catalyzes the tyrosine phosphorylation of Shc. Shc interacts with Grb2 and recruits SOS and induces the activation of Ras; activated Ras stimulate activation of MAPK signaling cascade: the stepwise activation of Raf, MEK, and extracellular signal regulated kinase (ERK) (Boulton et al., 1991) (Velloso et al., 2006).

**12: Ang II activates pERK through the Raf–MEK–ERK pathway**

Ang II activates MAPK via AT1 receptor (Csibi et al., 2010) (Eguchi et al., 2001) (Tian et al., 1998).

**13: Ang II increases IRS/Grb2 association which activates ERK**

Ang II increases pIRS1/Grb2 association and thus activates pERK (Velloso et al., 2006).

**14: $ONOO^-$ activates pERK**

ERK is activated by Ang II mediated ROS dependent mechanism (Frank et al., 2000). $ONOO^-$ nitrates tyrosine residues of ERK1/2. Tyrosine nitration of ERK1/2 enhances their phosphorylation on Thr and Tyr and their subsequent activation (Pinzar et al., 2005) (Csibi et al., 2010).

**15: Ang II activated pERK inhibits pIRS by serine phosphorylation**

Ang II, acting via the type 1 receptor (AT1), increases IRS-1 phosphorylation at Ser312 and Ser616 via JNK and ERK1/2, thus impairs IRS-1 phosphorylation at Tyr612 and Tyr632, two sites essential for engaging the p85 subunit of PI3-kinase. Insulin stimulated IRS-1/PI3K association is inhibited. Ang II-induced ERK1/2 and JNK activations both inhibited insulin-induced IRS-1 tyrosyl phosphorylation but Akt activation was only affected by ERK1/2 activity (Izawa et al., 2005). ERK is found to be activated in insulin resistant cases (Corbould et al., 2006)**.**

**16: pERK activates mTOR**

In addition to AKT activation of mTOR, ERK phosphorylates a distinct site on TSC2 leading to a greater inhibition of Rheb-GDP and activation of mTOR (Winter et al., 2011).

**17: pAKT down regulates pERK**

Akt phosphorylates Raf at serine residue and thus inhibits activation of the Raf-MEK-ERK signaling pathway (Zimmermann and Moelling, 1999).

**18: ANG II activates JAK and JAK decreases IRS1/PI3K activity**

Ang II activates JAK-2, a Janus kinase, induces its association and co immunoprecipitation with IRS-1 and at the same time induces tyrosine phosphorylation of IRS-1. These effects result in increased association of PI3K/IRS1 but the enzymatic activity is decreased (Velloso et al., 1996) (Muscogiuri et al., 2008).

## 2.4 Embedded Regulatory Feedback Structures

Various signaling pathways regulate growth and metabolism. Insulin has a significant role in glucose and vascular homeostasis and in stimulating cell growth (Saltiel and Kahn, 2001). Deregulation of processes downstream of insulin may result in diseases such as diabetes, hypertension or cancer. Feedback structures which emerge from the complex network of signaling pathways cover the underlying regulatory mechanisms of the cell functions and reveal the pathophysiology of diseases.

Glucose level is controlled tightly by insulin. Insulin PI3K dependent activation of AKT mediates GLUT4 translocation and thus the glucose uptake. This is regulated both positively and negatively as explained next.

**pIRS1→pAKT→pIRS1 Positive feedback loop**

pAKT is activated downstream of insulin as explained in Process 1. In turn, pAKT activates pIRS1 (Process 3) and forms a positive feedback loop. Glucose uptake should be sensitive to insulin and this positive feedback regulation ensures the required bistable response (Giri et al., 2004). pAKT should switch between high and low values according to the cellular and extracellular conditions since glucose uptake process, translocation of GLUT4 to the plasma membrane, is an all or none type process Giri et al., 2004). Second property associated with AKT is cell proliferation. Cell proliferation operates also in all or

none manner. These all or none decisions are controlled by insulin. Insulin resistant systems which cannot switch between on-state and off-state leads to diseases. Systems with persistent low pAKT values are associated with diabetes whereas systems with persistent high pAKT values are associated with cancer (Wang, 2010).

**pIRS1→pAKT⊣pIRS1 Negative feedback loop**

pAKT also forms a negative feedback loop by inhibiting pIRS1 through activation of mTOR. Coupling of the negative feedback with the positive feedback enables the fine adjustment of the response dose and provides a stable regulatory response to nutrient level and helps maintain glucose homeostasis. mTOR is involved in many signaling pathways and especially plays significant role in cell growth, proliferation, survival and protein synthesis. mTOR pathway is found to be activated in cancer and drugs that inhibit mTOR are used for anticancer therapy (Inoki et al., 2005; Tee and Blenis, 2005). As opposed to its cancer developing effects elsewhere, in this particular system, mTOR acts to reduce cancer. Through inhibition of pIRS1, mTOR decreases the level of pAKT which is one of the agents responsible for cell proliferation. In other words, mTOR inhibition may reduce cancer through other mechanisms which are not considered in this study, but does drive cancer progression through elevating pAKT levels and driving uncontrolled cell proliferation. This can explain the findings that mTOR inhibition for cancer treatment being less effective than expected (Carracedo et al., 2008).

Furthermore, pERK is, like pAKT, an agent responsible for growth and activated by pIRS1. If mTOR is inhibited, the negative feedback to pIRS1 is weakened and elevated pIRS1 levels activate pERK through pIRS1 → Shc → Grb2 → SOS → Ras → Raf → Raf → MEK → ERK path. pIRS1 activates ERK and contributes to MAPK signaling events such as proliferation, cell survival, apoptosis. Coupling this effect with pIRS1→pAKT⊣pIRS1

negative feedback loop, if mTOR is inhibited ERK levels increase and cell proliferation is enhanced (Carracedo et al., 2008).

The relative strengths of the pIRS1 positive and negative feedback loops determine the phenotypes of the system such as normal, diabetes, or cancer.

Also, vasodilator actions of insulin are mediated by nitric oxide (NO). Since pAKT stimulates NO production through pAKT → eNOS →NO path, proper regulation of pAKT by these positive and negative feedback loops is crucial in insulin's vascular effects.

**NO→ANG II→ROS⇥NO Negative feedback loop**

NO is converted to ONOO by the actions of ANG II. Conversion of NO to ONOO is important for preventing accumulation of NO (Pacher et al., 2007). This feedback loop helps to balance NO level. However, in Ang II overactive systems, such as hypertension, NO will decrease through this mechanism. Since NO is a vasodilator agent, decreasing NO levels would further increase blood pressure.

**pAKT→NO→ONOO⇥ pAKT / pAKT→NO→ANG II→ROS→ONOO⇥pAKT / NO→ANG II→ROS⇥NO Negative feedback loop**

There are at least two feedback loops through which pAKT is inhibited: first through direct inhibitory nitration by ONOO and second through activation of Ang II which produces ONOO. NO stimulates renin production and thus activates Ang II. ONOO is produced by ROS and NO.

**pIRS1→pAKT→NO→ANG II ⇥pIRS1 Negative feedback loop**

Second important mechanism of Ang II impairment of insulin signaling is through inhibition of IRS1. Stimulation of NO production downstream of pIRS1 contributes to IRS1 inhibition by activating Ang II.

**pIRS1→pERK⇥ pIRS1 Negative feedback loop / pIRS1→pAKT→NO→ANG II→pERK⇥pIRS1 Negative feedback loop**

pERK is activated by IRS1 for insulin mediated actions such as cell proliferation through two mechanism: one directly and the other one is downstream of pAKT and involves activation of Ang II. However these have inhibitory actions on IRS1 as disturbance.

**pIRS1→pAKT ⇥pERK⇥pIRS1 Positive feedback loop**

pERK inhibits pIRS1. However, pAKT is able to prevent this inhibition by inhibiting pERK. Two negative interactions in a loop form a positive feedback. Accordingly, inhibitory actions of pAKT on pERK may have a beneficial outcome since it can repair pIRS1 which is inhibited by pERK.

## 2.5 Blood Pressure Control and Hypertension

Arterial Pressure is known to be regulated by several feedback mechanisms.(Guyton et al., 1974) These mechanisms can be divided into two groups according to their response times, namely rapid and long-term pressure control mechanisms. Rapidly acting pressure control mechanisms operate by vasoconstriction or vasodilation of the arterioles. In a situation where the body needs a fast action such as severe bleeding, these mechanisms ensure that the pressure is immediately returned to a level sufficient enough for survival. On the other hand the short-term rapid actions do not have strong lasting effects to be able to bring the pressure to the normal level dictated by the tissue conditions. However, the long term pressure control has the capacity to adjust the pressure to the required steady-state level. Thus, the long term regulation plays a significant

role in responding to the metabolic demands. The study of hypertension i.e., constantly elevated blood pressure, is concerned with the abnormalities originating from or related to the long term pressure control mechanism (Guyton, 2006).

### 2.5.1 Renal body fluid volume feedback mechanism

The dominant controller of the long-term pressure level is a renal-body fluid volume feedback mechanism. Operation of this mechanism can be summarized as: an increase in arterial pressure causes the kidneys to excrete markedly increased quantities of urine. This, in turn, decreases the level of body fluids and eventually decreases the arterial pressure toward normal. This autoregulation is shown in Figure 4 (Guyton, 2006).

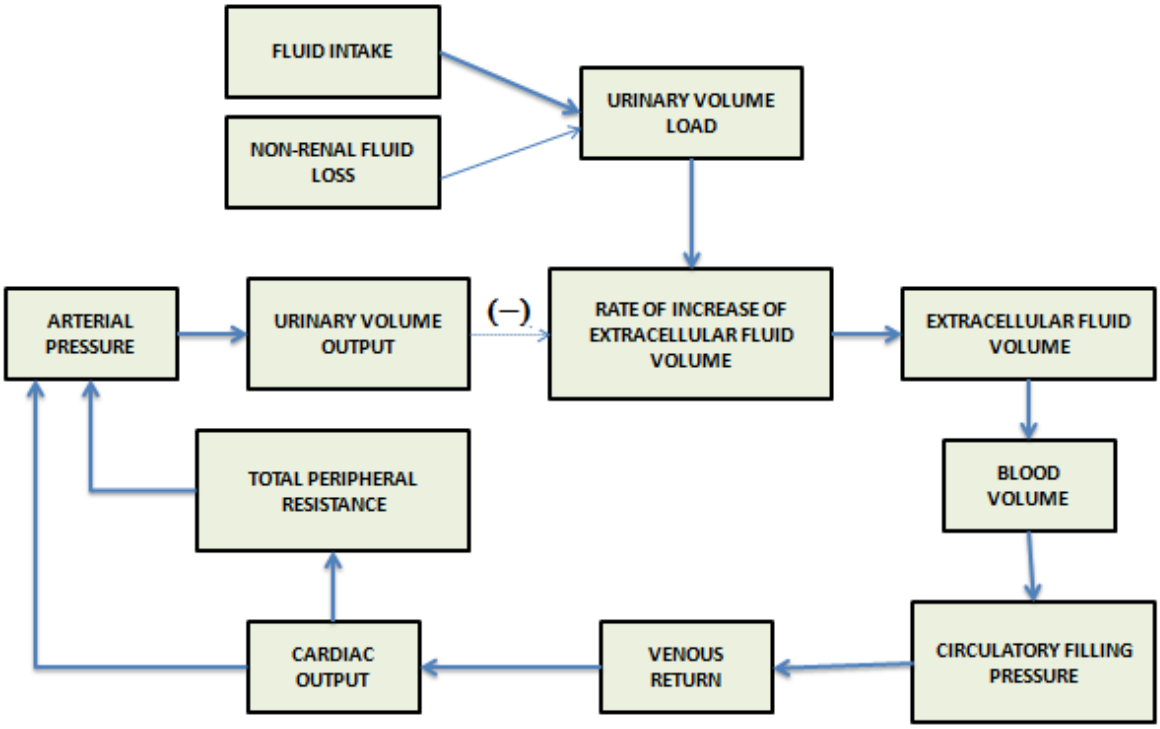


Figure 4. Renal-body fluid mechanism block diagram (Guyton et al., 1974)

A slight rise in arterial pressure results in marked increase in urinary volume output. The rate of increase of extracellular fluid volume is decreased by the increase in urinary volume output and increased by the increase in urinary volume load. Urinary volume load

is determined by the fluid intake and non-renal fluid loss. An increase in fluid intake increases the urinary volume load. An increase in non-renal fluid loss decreases the urinary volume load. Under steady state conditions the rate of change of extracellular fluid volume must be equal to zero. Steady-state condition is maintained by balancing the urinary load with the urinary output. Increase in extracellular fluid volume increases the blood volume following by the increase in circulatory filling pressure, venous return, and cardiac output. Increase in cardiac output causes an increase in arterial pressure but more importantly it increases total peripheral resistance by a mechanism called autoregulation and the increase in total peripheral resistance causes increase in arterial pressure. All in all, this mechanism is a slowly acting negative feedback control system of the integral control type where a change in the arterial pressure is followed by the events that bring the pressure back to its normal basic level given enough time to do so (Guyton et al., 1974).

The equilibrium point for blood pressure control is dictated by the kidneys. Kidneys regulate blood pressure by maintaining water and sodium balance. At steady state the urinary volume load must be equal to the urinary volume output so that constant dehydration or edema developments are avoided. At steady state there is a corresponding arterial pressure value for any given urinary volume load level. This relation is illustrated with the renal function curve as shown in Figure 5. Long term mean arterial pressure reference level can change due to a persistent change in the level of salt and water intake. Abnormalities in the kidney function may shift the renal function curve as well (Guyton, 2006).

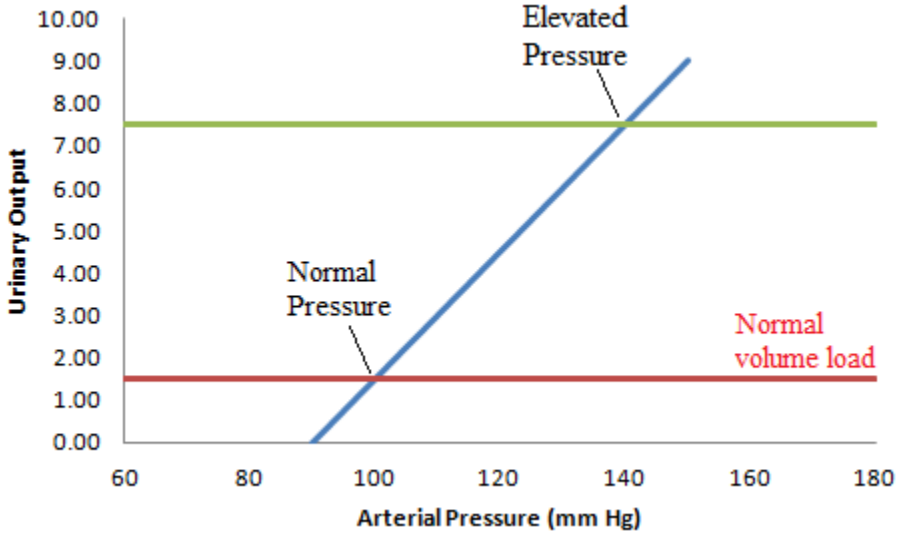


Figure 5. Renal function curve. Urinary volume load is a determinant of the reference level for Arterial pressure. Pressure will be regulated for normal and elevated volume loads.

### 2.5.2 Glomerular Filtration Rate Control, Afferent Efferent Arterioles

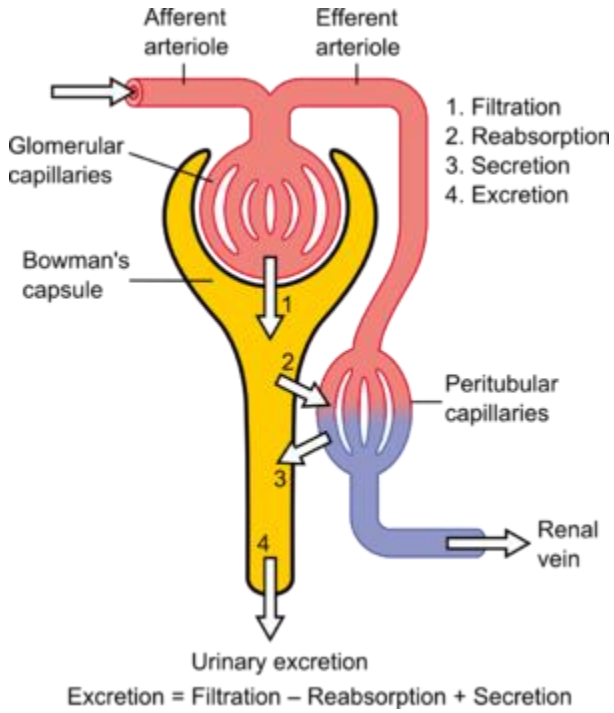


Figure 6. Nephron (Guyton, 2006)

The basic physiologic mechanism of the kidney can be explained by studying the nephron.(Gookin et al., 2010) Kidneys filter blood to remove water soluble waste products from the body and excrete them in the urine. They also regulate the recovery of sodium and water to alter the volume and composition of the body fluids. Blood flows through the afferent arteriole and exits through the efferent arteriole. After entering, blood is distributed to glomerular capillaries. Twenty percent (filtration fraction) of the plasma fluid is filtered from the glomerular capillaries into the Bowman's capsule. The volume of the filtered fluid per unit time is defined as the glomerular filtration rate (GFR). Increases (decreases) in glomerular hydrostatic pressure increases (decreases) GFR. The kidney should regulate GFR at a constant level to avoid glomerular injury and carry out reabsorption and waste

elimination functions properly. Glomerular hydrostatic pressure is maintained by controlling the efferent and afferent arteriolar resistances. Increasing the resistance of the afferent arteriole (constriction) reduces the blood that enters into the glomerulus and hydrostatic pressure is decreased. With a decrease in hydrostatic pressure the filtration force is decreased; therefore, GFR decreases. The filtration fraction doesn't change since it is the ratio of GFR to renal plasma flow, where both decreases at the same time. Similarly, decreased resistance of the afferent arteriole (relaxation) increases renal blood flow, GFR and does not change FF. Increasing the resistance of the efferent arteriole (constriction) prevents the outflow of the blood. In a mild to moderate constriction, renal blood flow is not significantly altered. Hydrostatic pressure is increased and this results in increase in GFR. FF is also increased. Similarly, decreased resistance of the efferent arteriole (relaxation) decreases renal blood flow, GFR and FF. An increase in blood pressure increases glomerular hydrostatic pressure and GFR (Gookin et al., 2010).

Myogenic mechanism, tubuloglomerular feedback, renin activation

The kidney is able to control GFR by mechanisms such as tubuloglomerular feedback or the myogenic mechanism. As the pressure increases, the stretch receptors at the afferent arteriole become activated and they constrict the afferent arteriole and thus decrease GFR bringing it back to normal. This is the myogenic control mechanism. The other mechanism, tubuloglomerular feedback, involves macula densa cells to sense NaCl within the tubule lumen and secrete substances such as ATP, Adenosine to constrict the afferent arteriole. In the case where there is a decrease in blood pressure, the stretch receptors are not activated and afferent arteriole is relaxed by the myogenic mechanism. Macula densa cells sense the decrease in the rate of delivery of NaCl within the tubule lumen and decreases the release of substances that constrict the afferent arteriole. Another mechanism through which kidney responses to drop in blood pressure, includes the

production of renin and subsequent constriction of the efferent arteriole. Renin activation leads to production of the powerful vasoconstrictor agent ANG II. ANG II constricts efferent arteriole and increases glomerular hydrostatic pressure (Gookin et al., 2010).

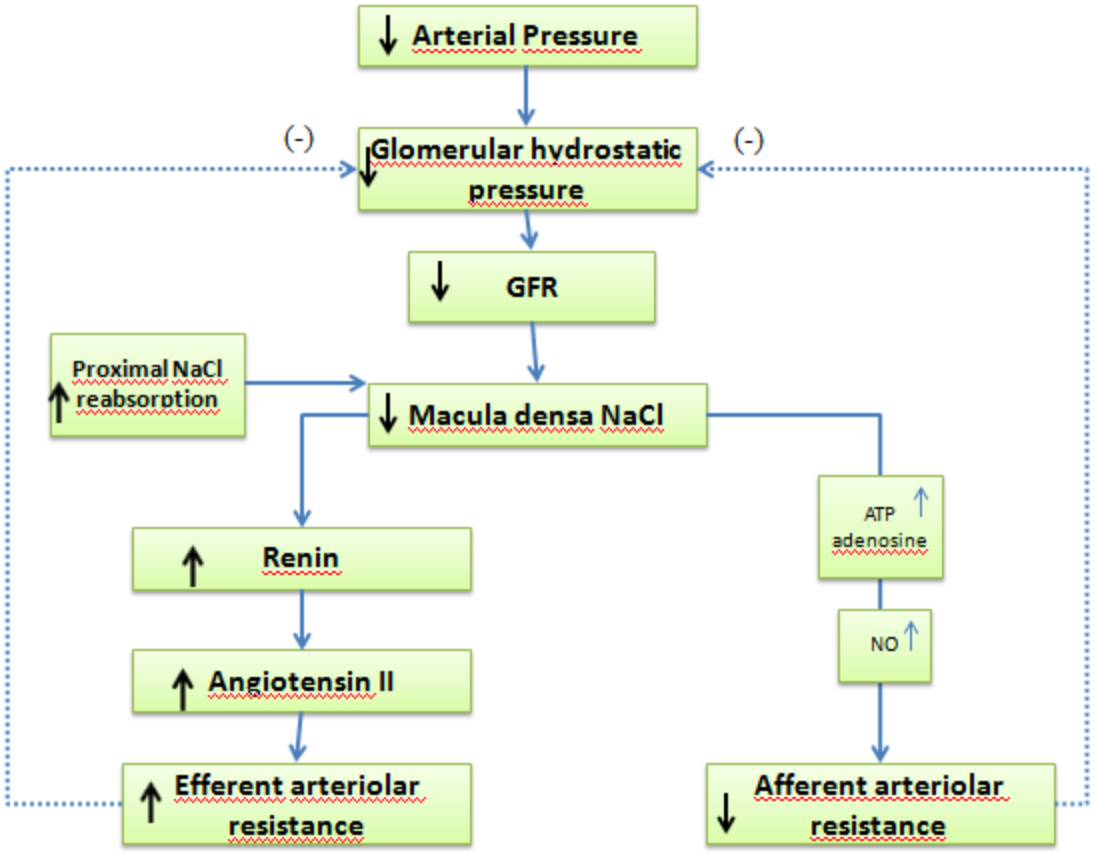


Figure 7. GFR regulation

### 2.5.3 Reabsorption mechanism, Aldosterone production

Renin is released from JG cells, passes out of the kidneys and circulates throughout the body. A small amount of renin remains for intrarenal functions. Renin itself is not a vasoactive substance. Angiotensin II is produced from renin. Angiotensin II can directly

elevate arterial pressure by rapid vasoconstriction in many areas of the body (Guyton et al., 1974). Another aspect of the regulation of blood pressure is related to the ability of Angiotensin II to affect sodium and extracellular fluid homeostasis by the stimulation of aldosterone production. Aldosterone increases reabsorption of ions and water in the kidney, increasing blood volume and, therefore, increasing blood pressure. The body regulates extracellular fluid (ECF) volume and arterial pressure within narrow limits despite wide variations in dietary sodium intake. Aldosterone mechanism ensures that the system is adjusted to the alterations in intake and prevents sodium sensitivity. As the intake is increased, EFV increases and elevates BP. Aldosterone reabsorption mechanism acts to decrease the retention of salt and water to bring EFV and BP back to normal (Guyton, 2006).

### 2.5.4 RAS activation and hypertension

Abnormal cases

1. Hypertension

Hypertension is accompanied with overstimulation of the Renin Angiotensin System. Ang II plays a significant role in the regulation of the blood pressure as explained earlier. However, excess Ang II level contributes to hypertension development by enhancing the regulatory actions beyond the normally required levels for maintaining blood pressure.

Angiotensin II overstimulation by abnormalities such as tumor:

Excess amounts of Ang II may be formed by a tumor developed in juxtaglomerular cells making them secrete large quantities of renin. In turn, the presence of high level Ang II pushes renal-body fluid mechanism to become set to a higher arterial pressure as depicted in Figure 9.

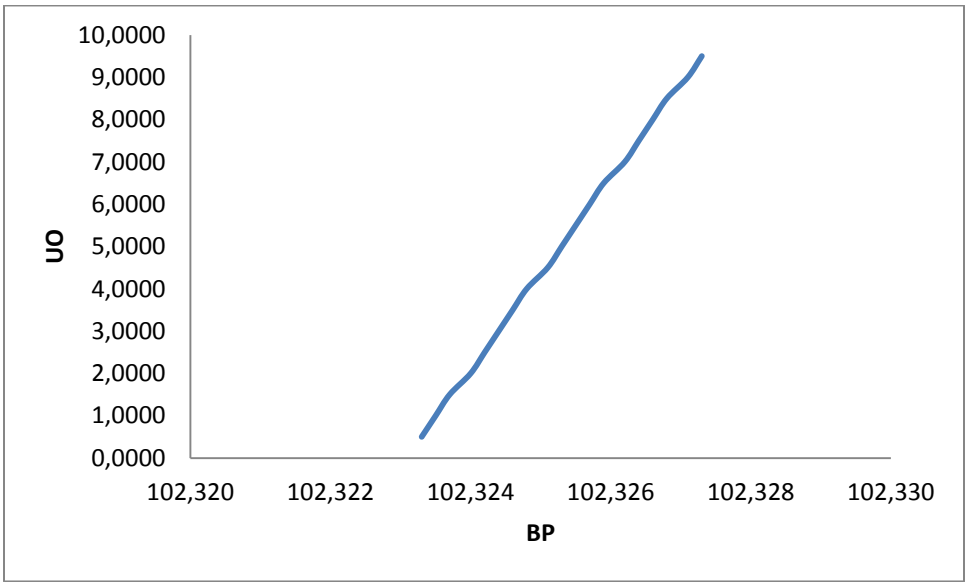


Figure 8. Renal function curve for kidneys stimulated by excess aldosterone. Excess aldosterone is a factor that can increase pressure level of the renal function curve.

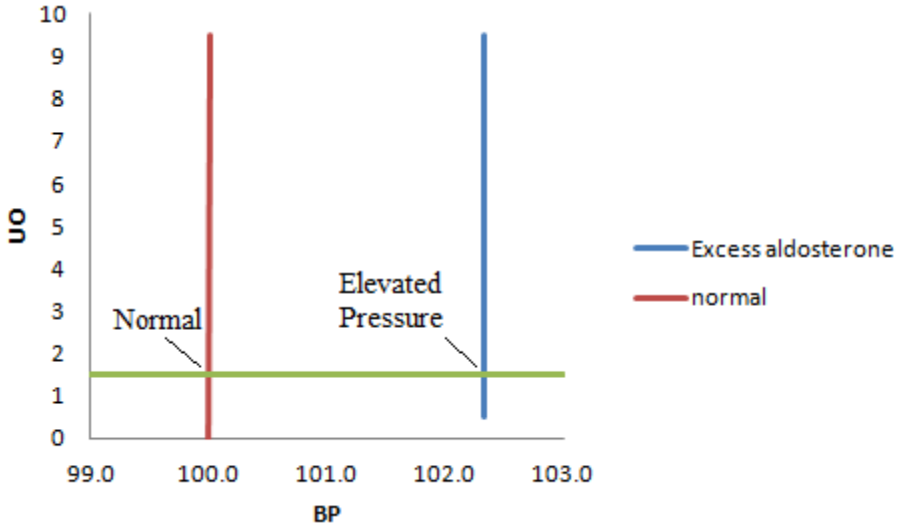


Figure 9. Comparison of the renal function curve for normal and excess aldosterone stimulated conditions. The curve shifts towards higher pressure level. For a given volume load, the pressure level is higher in the excess aldosterone stimulated condition.

Also, some parts of the kidney may get diseased and become ischemic. These parts secrete renin and consequently Ang II is formed and the remaining kidney mass retains salt and water contributing to the hypertension development (Guyton, 2006).

A tumor in one of the adrenal glands may develop and secret large quantities of aldosterone. Aldosterone increases reabsorption of salt and water, reducing the loss of these in the urine causing increase in extracellular fluid volume. And, if salt intake is increased in this state of sodium and water retention, the consequence would be a more severe elevation in blood pressure (Guyton, 2006).

The co-occurance of diabetes and hypertension can be a consequence of Ang II overstimulation as well. Overactivation of Renin Angiotensin System contributes to hypertension development and at the same time it has inhibitory actions on insulin signaling system causing insulin resistance.

### 2.5.5 Hyperglycemia

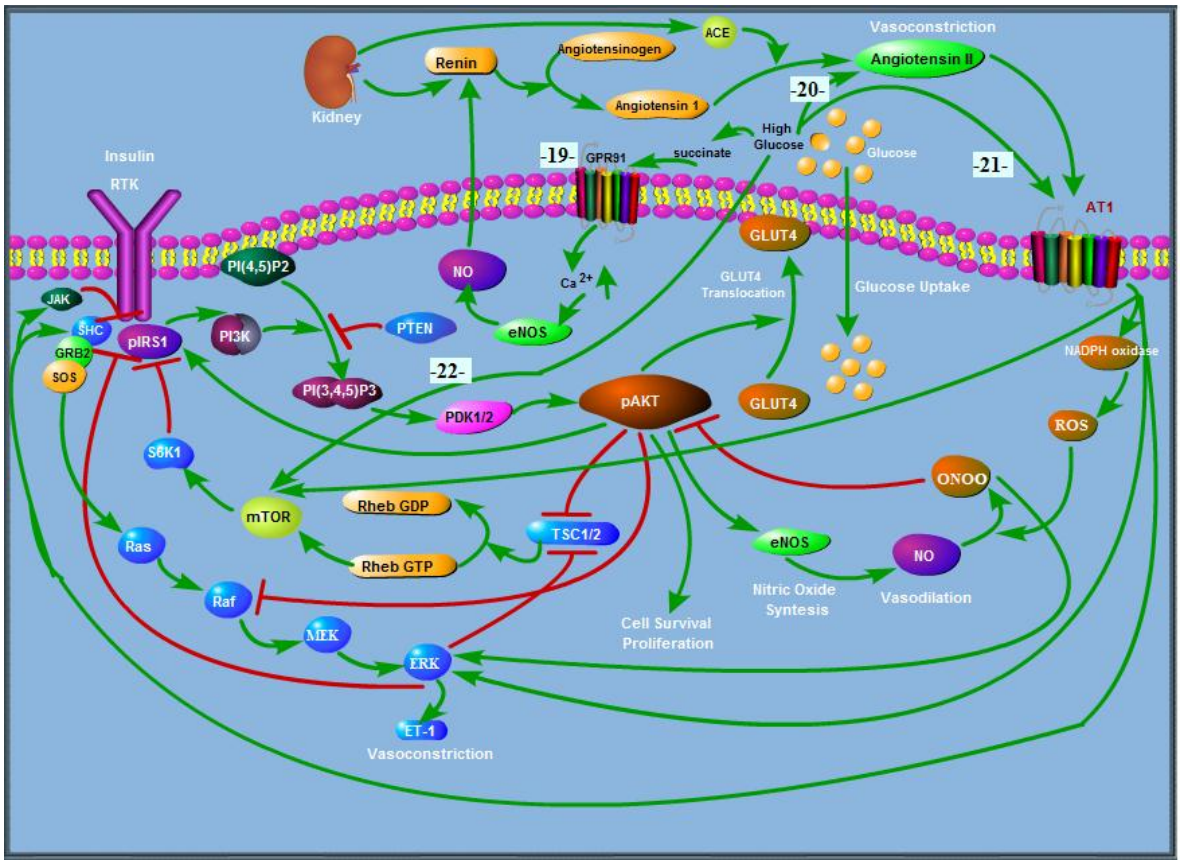


Figure 10. Pathway structure including hyperglycemia effects

Table 4. Processes contained in Figure 10

| | Process | Reference |
|---|---|---|
| **19** | High glucose → succinate → GPR91 → $Ca^{2+}$ → eNOS → NO → renin | (Peti-Peterdi et al., 2008) |
| **20** | High glucose → Ang II | (Miller, 1999) |
| **21** | High glucose → ROS | (Inoguchi et al., 2000; Yu et al., |

| | | |
|---|---|---|
| | | 2011) |
| **22** | High glucose → mTOR | (Crouthamel et al., 2009**)** |

Ang II overstimulation by Hyperglycemia

In uncontrolled diabetes blood glucose level increases. High glucose, hyperglycemia, promotes diabetic nephropathy . Clinical trials show that poor glucose control plays a role in the progression of renal disease. Studies suggest this to be the outcome of glucose-mediated activation of RAS. Through the activation of RAS, Ang II increases intraglomerular pressure and thus can lead to glomerular injury. This effect is mediated by the tubuloglomerular feedback mechanism. Also, glucose is reabsorbed along with sodium in the proximal tubule. Delivery of increased glucose increases sodium reabsorption. Hyperglycemia activates the glucose-sodium cotransport mechanism and increases the normally enhanced proximal tubular sodium reabsorption and leads to increased renin activation (Miller, 1999).

However there is an alternative explanation for the renin activation other than the origination from the primary effects of glucose on proximal tubule salt reabsorption that secondarily activates macula densa mediated feedback mechanisms. Recently, it is proposed that there exists a direct link between high glucose levels and renin activation mediated by the G-protein-coupled receptor GPR91 and succinate (Process 19 in Figure 10). High glucose levels lead to accumulation of succinate which activates GPR91. Through the activation of GPR91 endothelial cytosolic calcium is increased causing production of prostaglandins and NO. Prostaglandins and NO activate renin release from the juxtaglomerular apparatus (JGA). Glomerular hyperfiltration and JGA renin activation are observed in diabetes. Since prostaglandins and NO are vasodilator agents that cause relaxation of the afferent arteriole they can also explain the development of hyperfiltration (Peti-Peterdi et al., 2008).

There is evidence that hyperglycemia induce RAS and NO activation and it is argued that NO activates RAS (Lansang and Hollenberg, 2002). Intracellular Ca2+ is increased by shear stress activates eNOS by promoting the binding of calmodulin. AKT activates eNOS and increases the affinity of eNOS for calmodulin. eNOS catabolizes L-arginine to NO. NO stimulates guanylate (G-) cyclase and increases cGMP levels. cGMP activates cGMP-dependent protein kinase (PKG). PKG may reduce the force and rate of contraction. cGMP inhibits PDEIII. This may result in an increase in cAMP and cAMP-dependent protein kinase (PKA). PKA in turn activates Ca2+ channels, increasing the rate of contraction. Renin is activated by PKA and inhibited by PKG. The net effect of NO on renin release is argued to be stimulatory (Kurtz and Wagner, 1998).

Hypertension is accompinied by an increase in ANG II and an absence of hyperfiltration. In response to hyperglycemia ANG II is overstimulated and blood pressure may increase. At the early stages of diabetes NO mediate the increase in glomerular filtration rate and prevent hypertension. But if hyperfiltration continues over time it may ultimately cause glomerular injury (Brands and Fitzgerald, 2002).

# Chapter 3

# METHODS AND MODELS

## 3.1 Systems Biology Approach and Pathway Model Development

Current approach to understand biological functioning of cells uses system-level analysis. Advances in molecular biology enable the identification of genes and proteins. Nevertheless it is insufficient to reveal the complete picture of how biological mechanisms are designed to work. Systems biology aims to build on the existing knowledge about individual parts of the cell (genome sequencing, protein-protein interactions, etc.) and analyzes the structure and dynamics of the network of biomolecules (Kitano, 2002).

Within this framework, this thesis analyzes the structure and the dynamics of the complex cellular networks associated with diabetes and hypertension. For this, first, the biomolecules and their specific interactions are identified by carrying out an extensive literature research. By studying the organization of these interacting molecules, expanded models are created starting from a base signaling pathway. Next feedback mechanisms and their corresponding functional properties are defined. Steady-state and dynamic behaviors are analyzed for various conditions (e.g. modified rate constants, feedback strengths) to generate biologically relevant representations and uncover the organizing principles of normal regulatory functions and development of disease states.

Biological processes are complex large-scale systems. They consist of components shared in common among various pathways with different functions. Complete and detailed understanding of cell behavior and simulation of all the proteins and interactions is a very difficult task. Nonetheless, simplified models with only sufficient accuracy and coverage focusing on particular functioning of the cell can provide useful insight. Creating such a pathway model can still be challenging since the proposed model should include the necessary details capturing the regulatory function or the disease mechanism under study. At the same time models should not be too complex to be analyzed. Thus, the objective of this study is to identify the significant interaction paths related to diabetes and hypertension, and develop a meaningful mathematical model that is amenable to analysis. Known regulatory relations and interactions between biomolecules are integrated to the model systematically. Wherever it is necessary and makes sense, interactions are lumped to reduce the complexity of the network under study.

The first part of this work focuses on building the pathway structure model that represents the biological phenomena under study. The model is constructed in four consecutive steps with increasing complexity. First each model is illustrated with its components and interactions to define the cause-effect relationships that govern the physical structure of the pathway. Next some components are lumped to simplify the model. Finally the feedback loops underlying the signaling pathway are identified.

The starting point of this study was the model of the AKT signaling pathway proposed in (Wang, 2010). Wang developed a mathematical model of the AKT signaling pathway to investigate system-level mechanisms of cell growth and metabolism. The model centers on mTOR which senses the level of nutrients, insulin growth factor which activates the pathway, and pAKT (phosphorylated AKT) that adjusts the growth. pAKT is the key component of the pathway since its activation characterizes the phenotypes.

Biological events related to Insulin/PI3K dependent activation of pAKT and the role of mTOR signaling are illustrated in Figure 11.

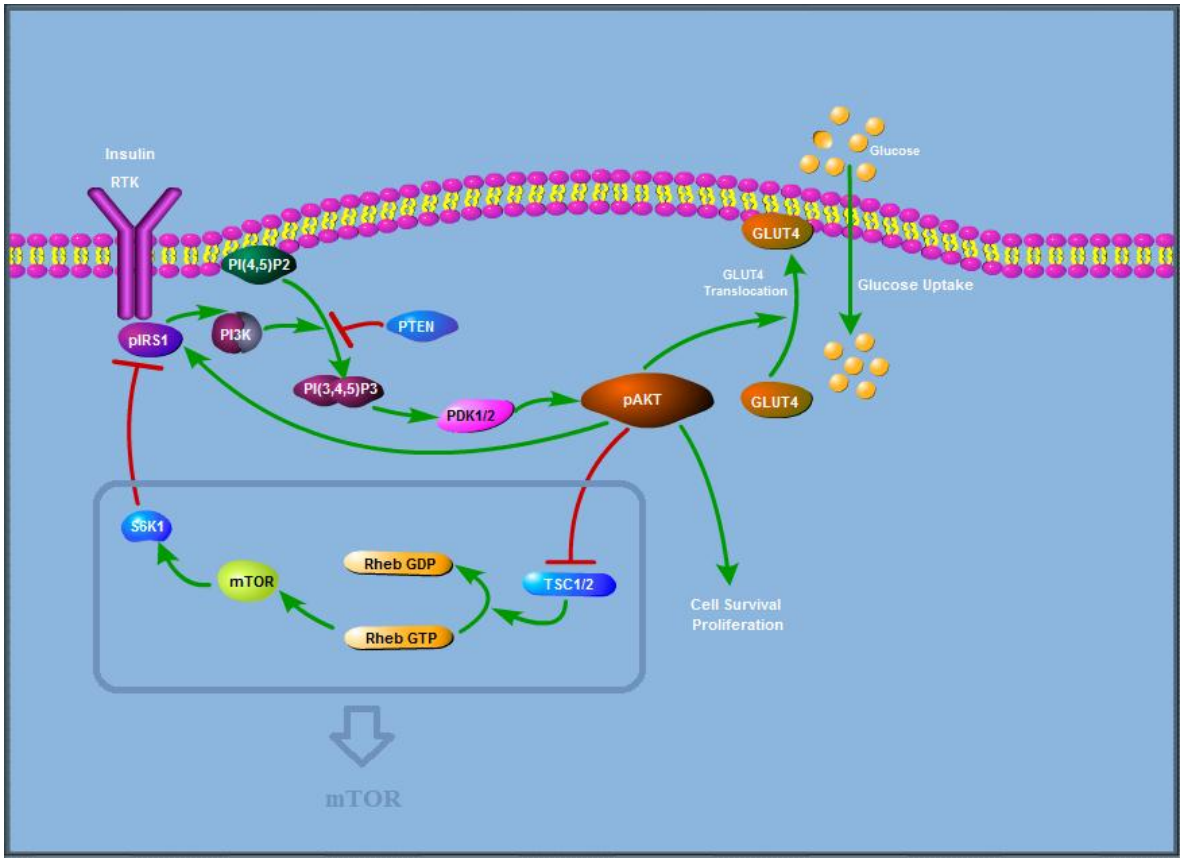


Figure 11. Insulin signaling pathway structure

Wang's model includes activation of pAKT as a phosphorylation and dephosphorylation cycle mediated by E1 and E2 enzymes. The effectors shown in Figure 11 such as TSC1/2, S6K1 are lumped and represented for simplicity by mTOR only. Positive feedback is generated by activation of pIRS1 by pAKT. Negative feedback regulation is mediated by

mTOR which inhibits pIRS1. This simplified AKT pathway structure is denoted as Model 1 and shown in

$$AKT + E_1 \underset{a_1}{\overset{d_1}{\leftrightarrows}} AKT{:}E_1 \xrightarrow{k_1} pAKT + E_1$$

$$pAKT + E_2 \underset{a_2}{\overset{d_2}{\leftrightarrows}} pAKT{:}E_2 \xrightarrow{k_2} AKT + E_2$$

Figure 12. Regulatory feedback structure is illustrated in Figure 13.

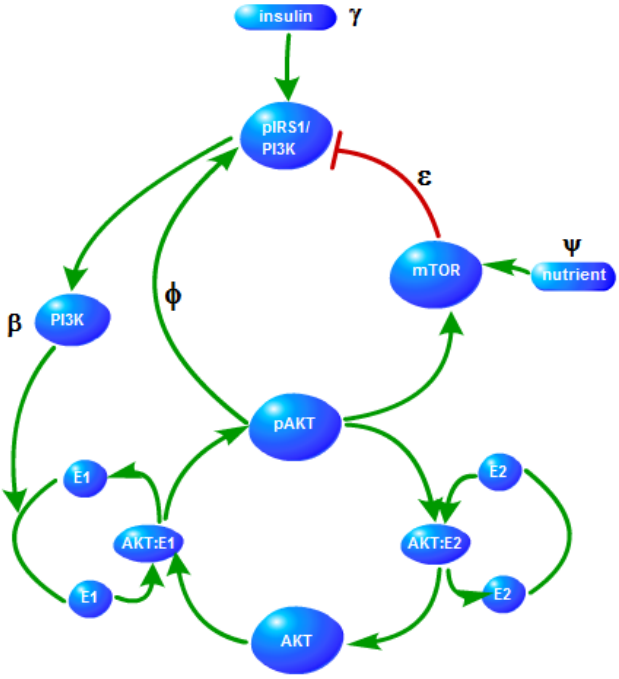


$$AKT + E_1 \underset{a_1}{\overset{d_1}{\rightleftarrows}} AKT{:}E_1 \xrightarrow{k_1} pAKT + E_1$$

$$pAKT + E_2 \underset{a_2}{\overset{d_2}{\rightleftarrows}} pAKT{:}E_2 \xrightarrow{k_2} AKT + E_2$$

Figure 12. Model 1 lumped pathway structure (Wang, 2010)

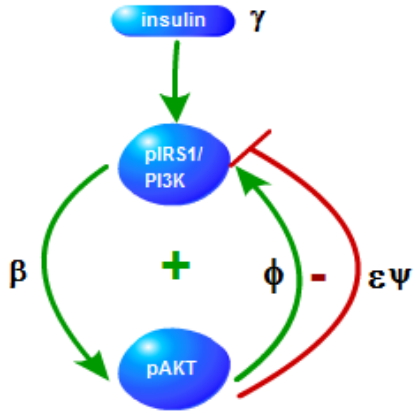


Figure 13. Model 1 feedback loops

Table 5. Parameters of Model 1(Wang, 2010)

| Parameters | Description |
|---|---|
| $\mathbf{a_1, d_1, k_1, a_2, d_2, k_2}$ | Rate constants of PdPC |
| **β** | The strength of the edge pIRS1 → $E_1$ |
| **γ** | The insulin level |
| **δ** | The decay rate of pIRS1 |
| **Φ** | The strength of the positive feedback pAKT→ pIRS1 |
| **Ψ** | The nutrient level |
| **ε** | The strength of the negative feedback pAKT→ pIRS1 |
| + | Positive feedback loop |
| - | Negative feedback loop |

Wang performed bifurcation analysis of this system and generated the parameter space for the normal bistable response and disease phenotypes such as cancer and diabetes. Since the relationship between diabetes and hypertension is a focus of this study, we have advanced the model by including new biomolecules. In particular, Ang II plays a significant role in development of hypertension and in crosstalk with insulin signaling. Therefore, the next model, Model 2, mainly analyzes the inhibitory actions of Ang II and how the system may shift to diabetes regime. Figure 14 illustrates the production of Ang II and subsequent generation of Reactive Oxygen Species (ROS) that decreases the vasodilator Nitric Oxide (NO) availability and inhibits pAKT which impairs the glucose uptake. Another inhibitory activity of Ang II is through the activation of mTOR. Production of Ang II by the stimulation of renin and the activation of the Angiotensin receptor and downstream effectors are lumped as Ang II and illustrated in Figure 15. Figure 16 summarizes the feedback loops underlying Model 2 and has 1 positive and 5 negative feedback loops.

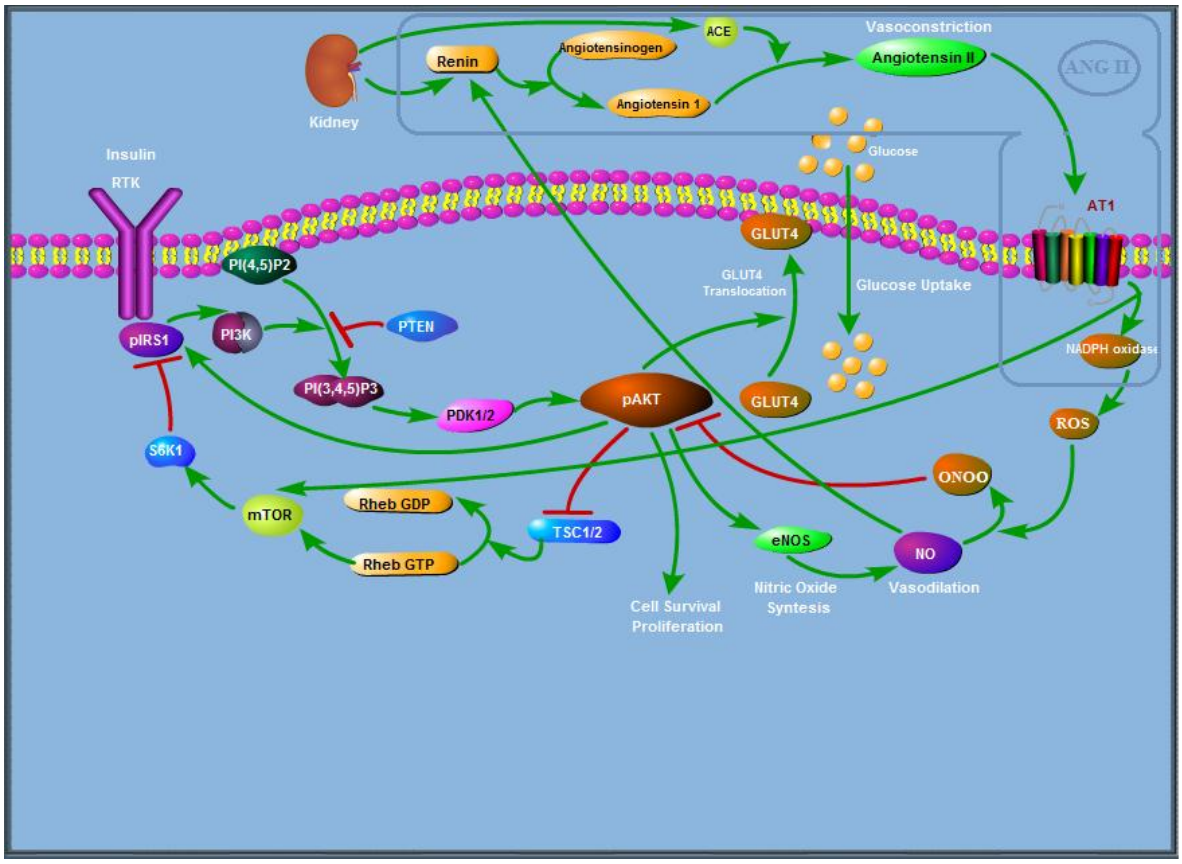


Figure 14. Model 2 pathway structure

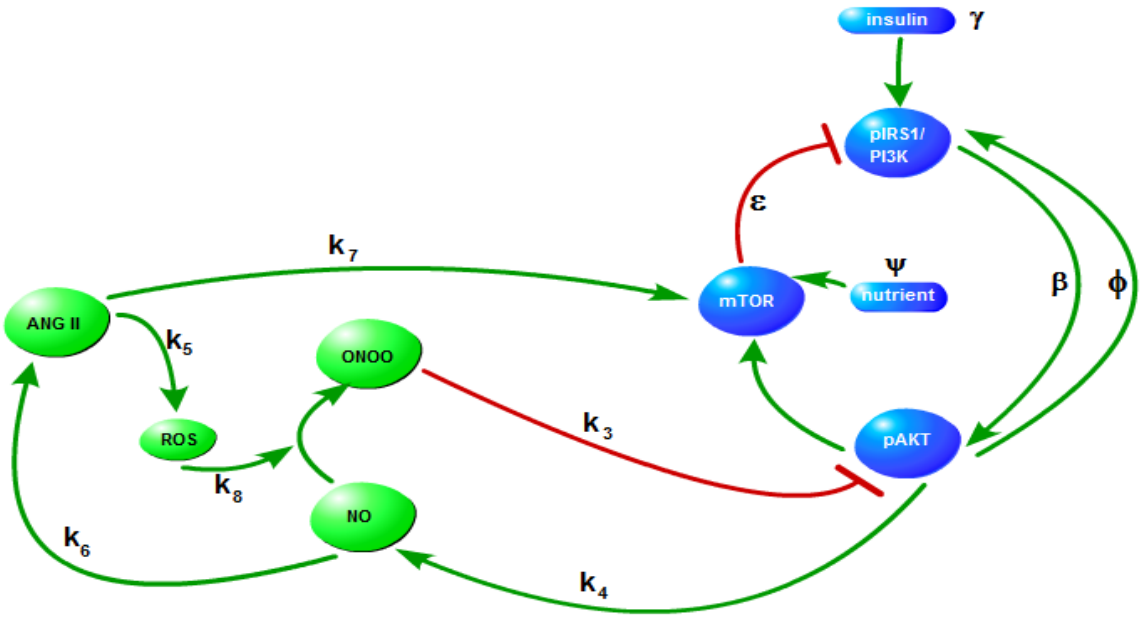


Figure 15. Model 2 Lumped Pathway Structure

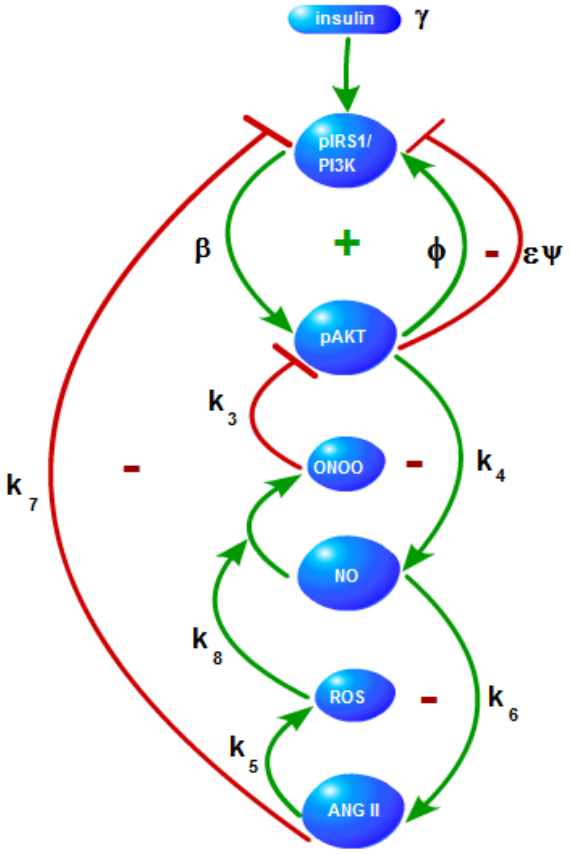


Figure 16. Model 2 Feedback Loops

Table 6. Parameters of Model 2

| Parameters | Description |
|---|---|
| $k_3$ | $ONOO^-$ inhibits pAKT |
| $k_4$ | pAKT stimulates NO production by activating eNOS |
| $k_5$ | Ang II, AT1 and NADPH oxidase depended generation of ROS |
| $k_6$ | NO stimulates renin production and subsequent Ang II production |
| $k_7$ | Ang II inhibits pIRS1 by activating mTOR |
| $k_8$ | ROS and NO react to form $ONOO^-$ |

Table 7. Feedback Loops

(+) pIRS1→pAKT→pIRS1

(-) pIRS1→pAKT⊣pIRS1

(-) pAKT→NO→ONOO⊣pAKT

(-) NO→ANG II→ROS⊣NO

(-) pAKT→NO→ANG II→ROS→ONOO⊣pAKT

(-) pIRS1→pAKT→NO→ANG II ⊣pIRS1

Further search for new interactions revealed that MAPK signaling pathway is also involved in this system (Figure 17). The components of the MAPK pathway Ras, Raf, MEK and ERK are lumped as pERK (phosphorylated ERK) (Figure 18). As shown in Figure 19 the crosstalk between pERK and the rest of the model results in activation as well as inhibition of pERK and pERK has inhibitory effects on the insulin signaling. One positive and two negative feedback loops are introduced in Figure 19. Also, ANG II inhibits pIRS1 mediated by JAK.

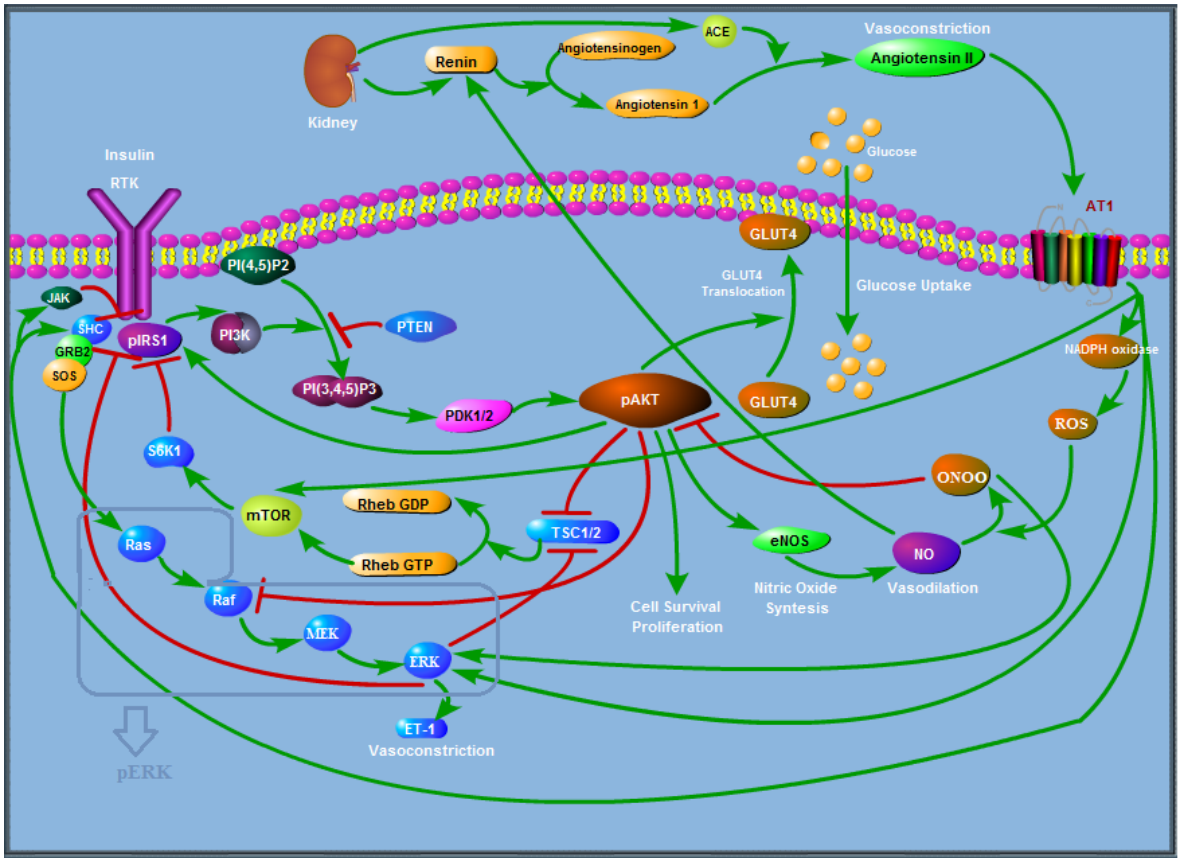


Figure 17. Model 3 Pathway Structure

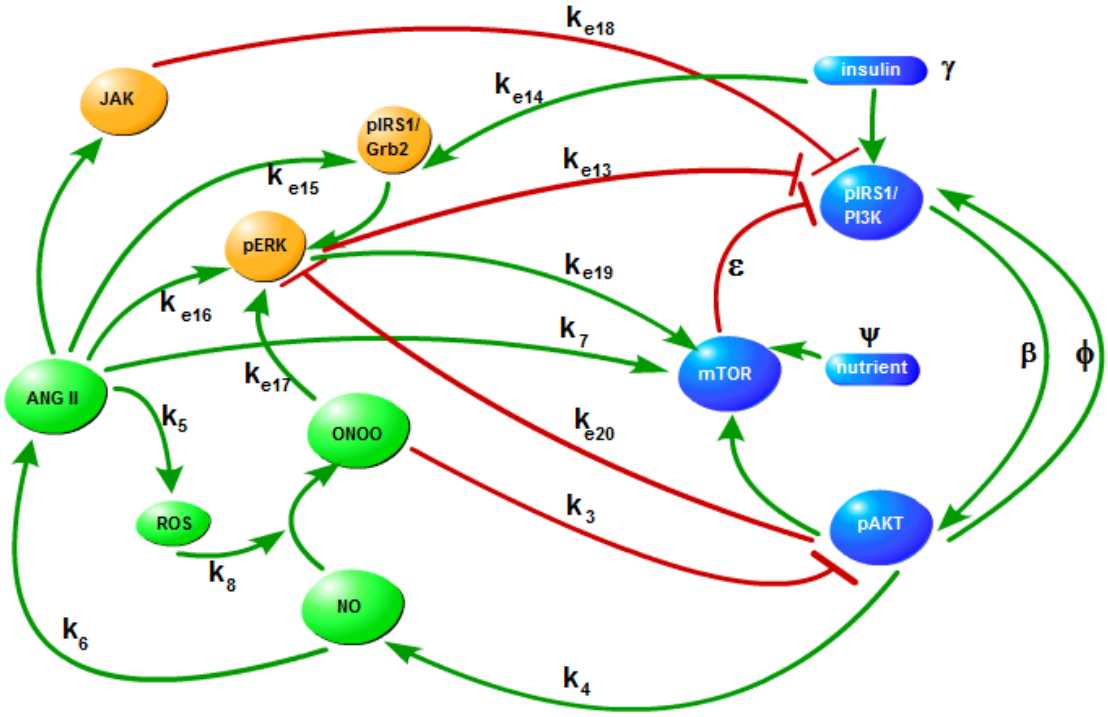


Figure 18. Model 3 Lumped Pathway Structure

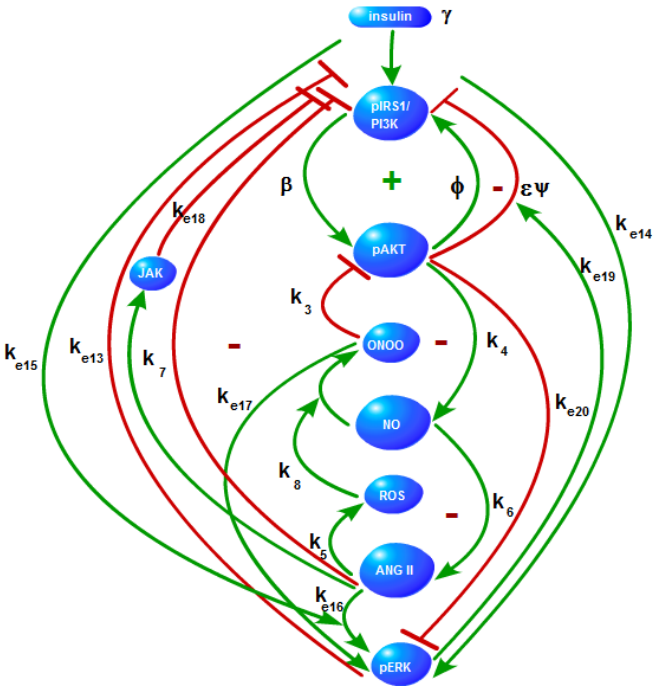


Figure 19. Model 3 Feedback Loops

Table 8. Parameters of Model 3

| Parameters | Description |
|---|---|
| $k_{e13}$ | pERK inhibits pIRS1 |
| $k_{e14}$ | Insulin dependent activation of pERK |
| $k_{e15}$ | Ang II and pIRS1 dependent activation of pERK |
| $k_{e16}$ | Ang II directly activates pERK |
| $k_{e17}$ | ONOO activates pERK |
| $k_{e18}$ | pIRS1 inhibition through JAK |
| $k_{e19}$ | pIRS1 inhibition through mTOR |
| $k_{e20}$ | pAKT inhibits Raf |

Table 9. Feedback Loops

(+) pIRS1→pAKT→pIRS1

(-) pIRS1→pAKT⊣pIRS1

(-) pAKT→NO→ONOO⊣pAKT

(-) NO→ANG II→ROS⊣NO

(-) pAKT→NO→ANG II→ROS→ONOO⊣pAKT

(-) pIRS1→pAKT→NO→ANG II ⊣pIRS1

(-) pIRS1→pERK⊣pIRS1

(+) pIRS1→pAKT ⊣pERK⊣pIRS1

(-) pIRS1→pAKT→NO→ANG II→pERK→⊣pIRS1

As explained in literature review section of this thesis hyperglycemia is an important phenomenon in the crosstalk of diabetes and hypertension. Model 4 (Figure 20) covers hyperglycemia related interactions. The simplified version can be seen in Figure 21 and the events corresponding to the interactions are summarized in Table 10.

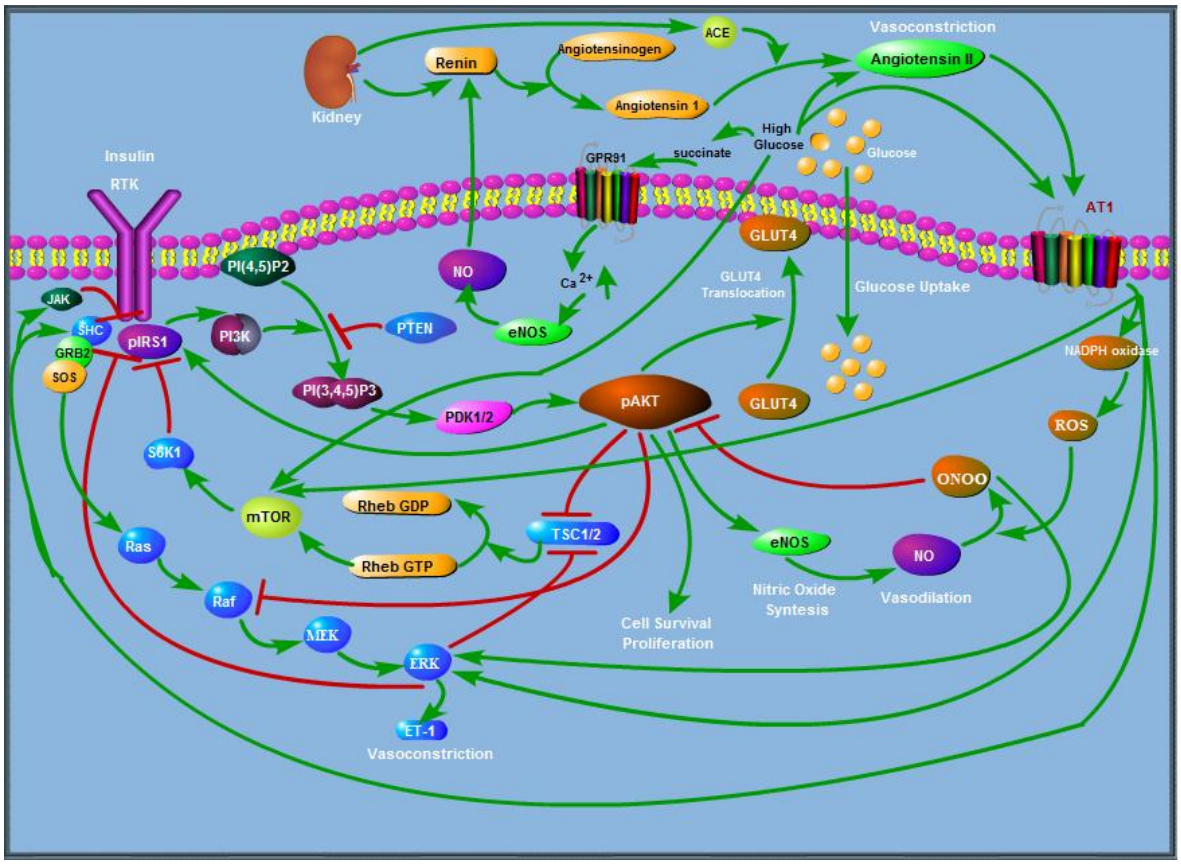


Figure 20. Model 4 Pathway Structure

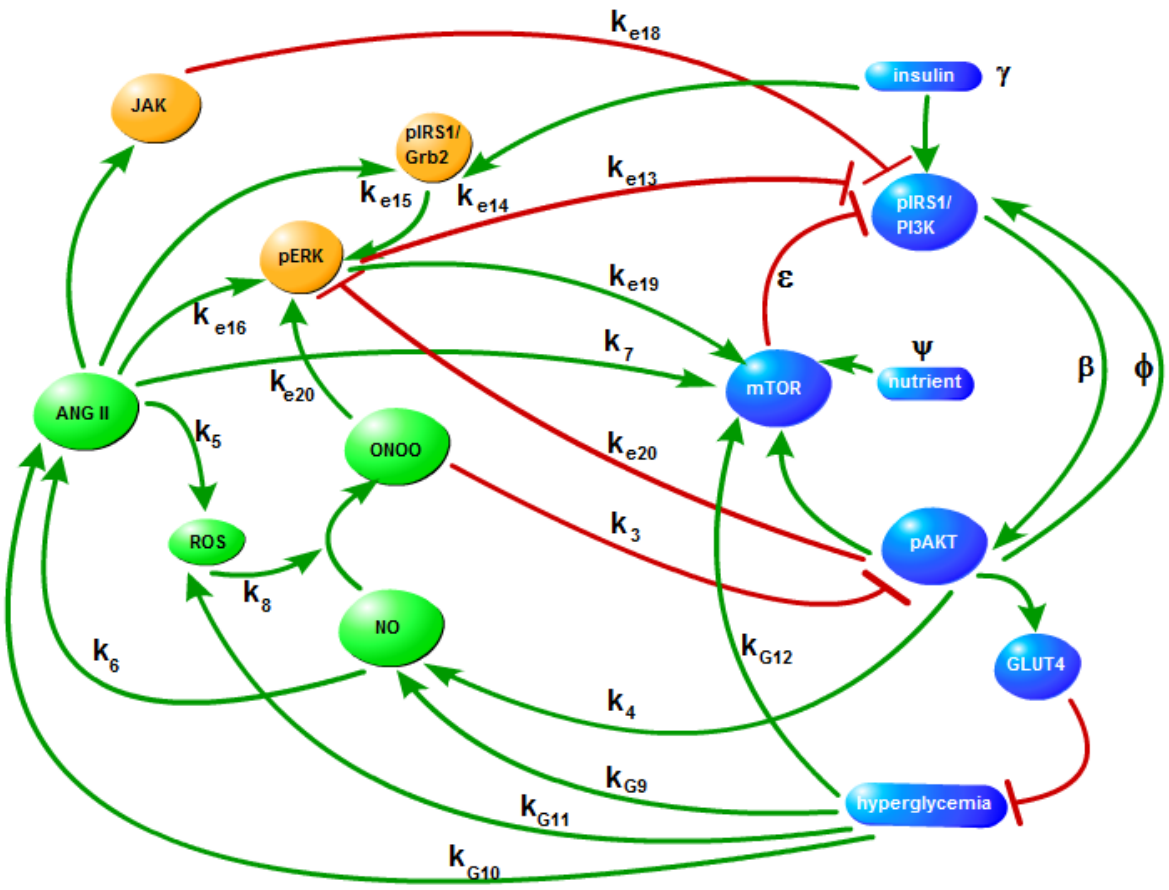


Figure 21. Model 4 Lumped Pathway Structure

Table 10. Parameters of Model 4

| Parameters | Description |
|---|---|
| $k_{G9}$ | Hyperglycemia induced succinate and GPR91 mediated activation of NO |
| $k_{G10}$ | Hyperglycemia activates Renin Angiotensin System |
| $k_{G11}$ | Hyperglycemia induced production of ROS |
| $k_{G12}$ | Hyperglycemia activates mTOR |

### 3.2 Coupled Feedback Loops and Bistability

System behavior emerges from the organization of components into a complex network structure. Information is carried through the network to coordinate cellular activity. Properties such as feedback, non-linearity, and stability are common in regulatory networks. This thesis analyzes the system behavior of insulin signaling and blood pressure regulation within the aspect of feedback design principles and parameter sensitivity.

Biological networks are designed to cope with changes in its components and to withstand external perturbations (Barkai and Leibler, 1997; Little et al., 1999). Signals have various defined roles in cells and they must be tightly regulated in order for the cell to function properly and to avoid failure. Through feedback mechanisms cells can assure precise, robust and multifaceted signaling (Freeman, 2000). Feedback loops are ubiquitously identified subnetworks of biological systems.


Figure 22. Single feedback loops with two components A and B.

In a network, each component directly influences the next component and also influences indirectly all other components, including itself thus forming a feedback loop. When the component ultimately activates itself as a result of this course of interaction, the feedback loop is termed as positive. Negative feedback loops are formed when the resulting effect is repressive. Figure 22 illustrates positive and negative feedback loops in a simple

system with two components, green and red arrows represent activation and inhibition respectively. Feedback loops with an odd number of negative interactions are negative.

Negative feedback is usually used to control output parameters within certain ranges and provide homeostasis preventing over-activation (Brandman and Meyer, 2008; Freeman, 2000; Kim et al., 2008). The importance of a negative feedback is that it provides stability (Becskei and Serrano, 2000); it can be used to suppress disturbances and noise (Kim et al., 2008) and it can speed up the response (Brandman and Meyer, 2008; Kim et al., 2008). Positive feedback loops act to amplify the output (Brandman and Meyer, 2008; Freeman, 2000). Also, they can elongate the signaling time to reach the steady state and are beneficial for careful decision making in crucial processes like cell proliferation and apoptosis (Brandman and Meyer, 2008; Kim et al., 2008). Another significant contribution of a positive feedback is that it can lead to bistability (Ferrell and Xiong, 2001).

Frequently biological networks consist of several feedback loops that are coupled with each other.(Kim et al., 2008) demonstrated that coupled feedback loops enforce actions which are not possible by single feedback loops. They discovered that coupled positive feedbacks can amplify signals and induce bistability; coupled negative feedbacks maintain homeostasis; coupled positive and negative feedbacks strengthen regulation capacity for better responses regarding time and magnitude. (Kim et al., 2008; Kwon and Cho, 2008) argue that signaling networks consist of coupled feedback loops to enhance robustness in the system. In this thesis, coupled feedback loops of insulin/Ang II crosstalk system are studied to investigate their role in normal regulatory mechanisms such as glucose uptake and vasodilation-vasoconstriction balance. Furthermore, bistability and parameter sensitivity analysis is carried out through network simulations to reveal the interactions and feedback loops, and their parameter regions, which are significant in disease development such as cancer, diabetes, and hypertension.

Graded processes generate output as a smoothly varying function of the input. However, this type of a response may be inadequate for biological processes where the nature of the system requires shut down or full activation depending on the cellular conditions. Bistability is a recurrent motif of processes such as differentiation, cell cycle progression biochemical memory production, apoptosis, signal propagation and immune cell activation (Bagowski and Ferrell, 2001; Becskei et al., 2001; Ferrell, 2002; Laurent and Kellershohn, 1999; Ozbudak et al., 2004; Pomerening et al., 2003; Reynolds et al., 2003; Smolen et al., 1998; Teruel and Meyer, 2002; Thron, 1997; Xiong and Ferrell, 2003) where the system switches between two stable steady states. Signaling networks that produce bistability exhibit steady states of either a low activity or a high activity. Even if the system has the capacity for bistability, it shows bistable behavior only under certain conditions. Signaling networks which consist of feedback loops can be analyzed for the conditions that induce monostability or bistability (Sobie, 2011).

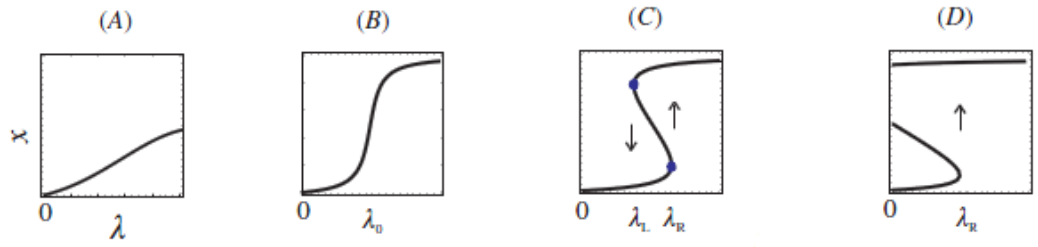


Figure 23. Response curves x(λ) ), where λ and x are insulin and activated pAKT respectively.. (A) The monotone type with low sensitivity. (B) The monotone type with high sensitivity. (C) The toggle switch. (D) The one-way switch. Adapted from (Wang, 2010).

Base model of this thesis is AKT signaling pathway proposed in Wang (2010). AKT promotes cell proliferation and glucose uptake and this is controlled by insulin. Wang developed steady state regulatory curves of insulin vs activated AKT to reveal the regulatory mechanisms that correspond to the phenotypes constrained by the system. He argued that a normal response is a toggle switch, shown in Figure 23 (C), resulting from the bistability nature of the system. The system needs to be able to alternate between low and high activated AKT levels. For certain values of the system parameters, such as increased positive feedback strength, the response becomes a one-way switch, Figure 23 (D), and this is characterized as a cancer state since a one-way switch enforces the system to stay in the activated state AKT persistently that drives uncontrolled cell proliferation. A similar response is observed in Xenopus oocyte maturation system where the system has all-or-none character and once it has matured it remains in the mature state (Ferrell and Xiong, 2001). However the irreversibility is a desired property for this maturation system. Another type of a response curve in Wang is the monotone type with low sensitivity, Figure 23 (A). This corresponds to diabetes where the system loses its bistability character and cannot switch to higher activated AKT values, thus glucose uptake is impaired. Insulin signaling pathway contains feedback regulations that can ensure bistability and the switch like response required for glucose uptake (Giri et al., 2004). This thesis investigates new feedback regulations and disturbances that affect the bistability of the system by developing new models, steady state analysis and dynamic simulations.

### 3.3 Mathematical Modeling

Mathematical modeling is a tool for understanding biological systems. Plausible models are constructed by determining the scope and level of detail, thus balancing predictive power and complexity while achieving the design goals (Aldridge et al., 2006). In this thesis, the network of interest is formalized as systems of ordinary differential equations after making appropriate assumptions.

#### 3.3.1 Steady State Model

The core event contained in Model 1, shown

$$AKT + E_1 \underset{a_1}{\overset{d_1}{\leftrightarrows}} AKT{:}E_1 \xrightarrow{k_1} pAKT + E_1$$

$$pAKT + E_2 \underset{a_2}{\overset{d_2}{\leftrightarrows}} pAKT{:}E_2 \xrightarrow{k_2} AKT + E_2$$

Figure 12, is the phosphorylation and dephosphorylation cycle (PdPC) of AKT ⇆ pAKT:

$$AKT + E_1 \underset{a_1}{\overset{d_1}{\leftrightarrows}} AKT{:}E_1 \xrightarrow{k_1} pAKT + E_1$$

$$pAKT + E_2 \underset{a_2}{\overset{d_2}{\leftrightarrows}} pAKT{:}E_2 \xrightarrow{k_2} AKT + E_2$$

Michaelis-Menten kinetics is assumed for PdPC mediated by enzymes $E_1$ and $E_2$. The nonlinear dynamical modeling equations are summarized in Table 11.

Table 11. Mathematical representation of Model 1

| | |
|---|---|
| Differential equations describing the Michaelis Menten Kinetics of the PdPC: | |
| $\frac{d[AKT]}{dt} = -a_1[AKT][E_1] + d_1[AKT:E_1] + k_2[pAKT:E_2]$ | (1) |
| $\frac{d[AKT:E_1]}{dt} = a_1[AKT][E_1] - (d_1 + k_1)[AKT:E_1]$ | (2) |
| $\frac{d[pAKT]}{dt} = -a_2[pAKT][E_2] + d_2[pAKT:E_2] + k_1[AKT:E_1]$ | (3) |
| $\frac{d[pAKT:E_2]}{dt} = a_2[pAKT][E_2] - (d_2 + k_2)[pAKT:E_2]$ | (4) |
| Kinetics of pIRS1, negative and positive feedback: | |
| $\frac{d[pIRS1]}{dt} = \gamma + (\Phi - \varepsilon \Psi)[pAKT] - \delta [pIRS1]$ | (5) |
| Conservation equations: | |
| $X_T = [AKT] + [pAKT]$ | (6) |
| $E_{1T} = [E_1] + [AKT:E_1]$ | (7) |
| $E_{2T} = [E_2] + [pAKT:E_2]$ | (8) |
| Describing the edge pIRS1→$E_1$ | |
| $E_{1T} = \beta[pIRS1]$ | (9) |

Feedback is represented by the term $(\boldsymbol{\Phi} - \boldsymbol{\varepsilon \Psi})[\boldsymbol{pAKT}]$ where the strength of the positive feedback pAKT → pIRS1 is represented with Φ and negative feedback loop mediated by mTOR is simplified as$(\boldsymbol{\varepsilon \Psi})[\boldsymbol{pAKT}]$. This simplification is justified by derivation of mTOR activation, given in Appendix A, which demonstrates that mTOR

activation is proportional to pAKT and the level of nutrients (Ψ). Negative feedback loop strength is represented with **ε**.

At steady state, equations (1)-(9) reduce to a third order polynomial of *x*, the percentage of the activated AKT in the steady state. A third order polynomial G is derived as equation 10 in Table 12 with new parameters which are derived from the previous ones.

Table 12. Model 1 Steady State Equation

| Steady state equation : | |
|---|---|
| $\mathrm{G}\,(x, \lambda, \theta, \mathrm{K}_1, \mathrm{K}_2) = 0$ | |
| $\mathrm{G} = \theta\, x^3 + \big((\mathrm{K}_2 - 1)\theta + \lambda - 1\big)x^2 + (\mathrm{K}_1 + 1 + (\mathrm{K}_2 - 1)\lambda - \mathrm{K}_2\theta)x - \mathrm{K}_2\lambda$ | (10) |
| Parameters | |
| $x = [pAKT]/x_T$ | |
| $\theta = (\Phi - \varepsilon\, \Psi\,)\beta\, k_1 X_T/(\delta k_2 E_{2T})$ | |
| $\lambda = \gamma\beta k_1/(\delta k_2 E_{2T})$ | |
| $K_1 = (d_1 + k_1)/(a_1 X_T)$ | |
| $K_2 = (d_2 + k_2)/a_2$ | |

### 3.3.2 Derivation of the bistable dynamic model

The variables which appear in the set of ODEs presented in Table 11 are redefined as:

$\tilde{x}_i = x_i/X_T \qquad i = 1{:}5$

and

$\tilde{\mathrm{E}}_{2\mathrm{T}} = E_{2T}/X_T$

where

$$x_1 = [AKT] \qquad x_2 = [AKT{:}\,E_1] \qquad x_3 = [pAKT] \qquad x_4 = [pAKT{:}\,E_2] \qquad x_5 = [pIRS1]$$

Dropping "~" for convenience, one gets

$$\frac{dx_1}{dt} = -a_1 x_1 X_T(\beta\, x_5 - x_2) + d_1 x_2 + k_2 x_4$$
$$\frac{dx_2}{dt} = a_1 x_1 X_T\,(\beta\, x_5 - x_2) - (d_1 + k_1) x_2$$
$$\frac{dx_3}{dt} = -a_2 x_3 X_T(\mathrm{E}_{2T} - x_4) + d_2 x_4 + k_1 x_2$$
$$\frac{dx_4}{dt} = a_2 x_3 X_T(E_{2T} - x_4) - (d_2 + k_2) x_4$$
$$\frac{dx_5}{dt} = \gamma / X_T + (\Phi - \varepsilon\, \Psi\,) x_3 - \delta\, x_5$$

Assumptions:

1. that the following is true not only at steady state but for all times:

$$x_1 + x_3 = 1$$

   i.e. $[AKT] + [pAKT] = X_T$

$$\frac{dx_1}{dt} = -a_1 x_1 X_T(\beta\, x_5 - x_2) + d_1 x_2 + k_2 x_4$$
$$\frac{dx_2}{dt} = a_1 x_1 X_T\,(\beta\, x_5 - x_2) - (d_1 + k_1) x_2$$
$$\frac{dx_4}{dt} = a_2 (1 - x_1) X_T(\mathrm{E}_{2T} - x_4) - (d_2 + k_2) x_4$$
$$\frac{dx_5}{dt} = \gamma / X_T + (\Phi - \varepsilon\, \Psi\,)(1 - x_1) - \delta\, x_5$$

2. that pseudo steady-state holds for the AKT and pAKT complexes i.e.

$$\frac{dx_2}{dt} = 0$$

$$x_2 = \frac{a_1 X_T \beta\ x_5 x_1}{a_1 X_T x_1 + \ (d_1 + k_1)}$$

$$\frac{dx_4}{dt} = 0$$

$$x_4 = \frac{a_2 X_T \mathrm{E}_{2T}(1 - x_1)}{a_2 X_T (1 - x_1) + \ (d_2 + \ k_2)}$$

$$K_1 = \frac{d_1 + k_1}{a_1\, X_T}$$

$$K_2 = \frac{d_2 + k_2}{a_2\, X_T}$$

$$x_2 = \frac{\beta\ x_5 x_1}{x_1 + \ K_1}$$

$$x_4 = \frac{\mathrm{E}_{2T}(1 - x_1)}{(1 - x_1) + \ K_2}$$

Substituting these into the original model one gets a reduced order two-dimensional dynamic model shown in Table 13 below:

Table 13. Dynamic Model 1

$$\frac{dx_1}{dt'} = -\frac{1}{K_1}\,\beta\, x_1 x_5 + \frac{\beta\, x_5 x_1^2}{K_1^2 + K_1 x_1} + \frac{1}{1+\left(\frac{k_1}{d_1}\right)}\left(\frac{\beta\, x_5 x_1}{K_1 + x_1}\right) + \frac{\frac{k_2}{d_1}}{1+\left(\frac{k_1}{d_1}\right)}\,\frac{\mathrm{E}_{2T}(1-x_1)}{K_2 + (1-x_1)} \tag{11}$$

$$\frac{dx_5}{dt'} = \frac{\zeta\delta}{\beta}\left(\frac{k2}{k1}\right)\mathrm{E}_{2T}\lambda(t) + (\Phi - \varepsilon\Psi)\zeta(1-x_1) - \delta_I \zeta x_5 \tag{12}$$

where $\zeta = \frac{1}{d_1 + k_1}$ $\quad t' = \frac{t}{\zeta}$ $\quad \lambda = \frac{\gamma\beta k_1}{\delta\, k_2 E_{2T}}$

$$x_3 = 1 - x_1(t) \tag{13}$$

$$\frac{d\Psi}{dt} = -0.1\,\Psi(t) + (1-x_1) \tag{14}$$

Ψ in Equation (14) denotes the nutrient level in the cell and we assumed that it is proportional to the level of pAKT since pAKT enables glucose uptake.
Simulations are performed for the following nominal values of the parameters:

$$E_{2T} = 1;\ \ \frac{k_2}{k_1} = 1;\ \ \frac{k_2}{d_1} = 10;\ \ \frac{k_2}{d_2} = 10;\ \ \frac{k_1}{d_2} = 10;\ \ \frac{d_2}{d_1} = 1;\ \ K_1 = K_2 = 0.05;$$
$$\frac{\delta}{\beta} = 1;\ \ \beta = 1;\ \ \zeta = 1;\ (\Phi - \varepsilon\Psi) = 1$$

The dynamic model is simulated in SIMULINK/MATLAB. A PID controller is used to implement the insulin supply. This controller adjusts the insulin supply λ to keep the nutrient level Ψ at desired levels.

The above base Model 1 is expanded by refining the set of differential equations to include the interactions constrained by Models 2-4.

ODEs of Model 2 are presented in Table 14. NO, ANG II, ROS and ONOO are introduced into the dynamic model. Steady-state solutions of (15)-(20) are reduced to two equations (21) and (23). Note that we have switched from $t'$ to $t$.

Table 14. Dynamic Model 2

$$\frac{dx_1}{dt} = -\frac{(d_1 + k_1)}{K_1}\beta\, x_1 x_5 + \frac{(d_1 + k_1)\beta\, x_5 x_1^2}{K_1^2 + K_1 x_1} + d_1 \frac{\beta\, x_5 x_1}{x_1 + K_1} + k_2 \frac{E_{2T}(1 - x_1)}{(1 - x_1) + K_2} + k_3 x_9 \tag{15}$$

$$\frac{dx_5}{dt} = \frac{\delta}{\beta}\left(\frac{k2}{k1}\right) E_{2T}\lambda(t) + (\Phi - \varepsilon(1 + \mathrm{k}_7\, x_7)\Psi)(1 - x_1) - \delta_I x_5 \tag{16}$$

$$\frac{dx_6}{dt} = k_4(1 - x_1) - k_8 x_8\, x_6 - \delta_N x_6 \tag{17}$$

$$\frac{dx_7}{dt} = k_6\, x_6 - \delta_{ang} x_7 \tag{18}$$

$$\frac{dx_8}{dt} = k_5 x_7 - \delta_R x_8 \tag{19}$$

$$\frac{dx_9}{dt} = k_8 x_8\, x_6 - \delta_{ON} x_9 \tag{20}$$

where

$x_6 = [NO]$ $x_7 = [ANG\ II]$ $x_8 = [ROS]$ $x_9 = [ONOO]$

For the steady state analysis:

$$\frac{dx_1}{dt} = -\frac{(d_1 + k_1)}{K_1}\beta\, x_1 x_5 + \frac{(d_1 + k_1)\beta\, x_5 x_1^2}{K_1^2 + K_1 x_1} + d_1 \frac{\beta\, x_5 x_1}{x_1 + K_1} + k_2 \frac{E_{2T}(1 - x_1)}{(1 - x_1) + K_2} + \frac{k_3\, k_8\, k_5\, k_6}{\delta_R\, \delta_{ON} \delta_{ang}}\, {x_6}^2 = 0 \tag{21}$$

where

$$x_5 = \left(\frac{\delta}{\beta}\left(\frac{k2}{k1}\right) E_{2T}\lambda(t) + \left(\Phi - \varepsilon\left(1 + \mathrm{k}_7\, \mathrm{k}_6\, x_6/\delta_{ang}\right)\Psi\right)(1 - x_1)\right)/(\delta_I) \tag{22}$$

$$\frac{dx_6}{dt} = k_4(1 - x_1) - \frac{k_8\, k_5\, k_6}{\delta_R \delta_{ang}} {x_6}^2 - \delta_N x_6 = 0 \tag{23}$$

Dynamic model 3 is shown in Table 15. In Model 3 pERK interactions are introduced. An external stimulus to ANG II is modeled as a disturbance u(t). New parameters which appear in (32) are derived from the existing ones and defined in Appendix C.

Table 15. Dynamic Model 3

$$\frac{dx_1}{dt} = -\frac{(d_1 + k_1)}{K_1}\beta\, x_1 x_5 + \frac{(d_1 + k_1)\beta\, x_5 x_1^2}{K_1^2 + K_1 x_1} + d_1 \frac{\beta\, x_5 x_1}{x_1 + K_1} + k_2 \frac{E_{2T}(1 - x_1)}{(1 - x_1) + K_2} + k_3\, x_9 \tag{24}$$

$$\frac{dx_5}{dt} = \frac{\delta}{\beta}\left(\frac{k2}{k1}\right) E_{2T}\lambda(t) + \left(\Phi - \varepsilon\Psi \mathrm{k_{e\_19}\, x_{10}}(1 + \mathrm{k_7\, x_7}\,)\right)(1 - x_1) - k_{e\_13}\, x_{10} - k_{e\_18}\, x_7 - \delta_I x_5 \tag{25}$$

$$\frac{dx_6}{dt} = k_4(1 - x_1) - k_8\, x_8 x_6 - \delta_N x_6 \tag{26}$$

$$\frac{dx_7}{dt} = k_6 x_6 + u(t) - \delta_{ang} x_7 \tag{27}$$

$$\frac{dx_8}{dt} = k_5 x_7 - \delta_R x_8 \tag{28}$$

$$\frac{dx_9}{dt} = k_8 x_8\, x_6 - \delta_{ON} x_9 \tag{29}$$

$$\frac{dx_{10}}{dt} = k_{e\_16} x_7 + k_{e\_15} x_7 x_5 + k_{e_{14}} x_5 + k_{e\_17}\, x_9 - k_{e\_20}(1 - x_1) - \delta_{ERK} x_{10} \tag{30}$$

where

$x_{10} = [pERK]$

For the steady state analysis:

$$\frac{dx_1}{dt} = -\frac{1}{K_1}\beta\, x_1 x_5 + \frac{\beta\, x_5 x_1^2}{K_1^2 + K_1 x_1} + \frac{d_1}{d_1 + k_1}\left(\frac{\beta\, x_5 x_1}{K_1 + x_1}\right) + \frac{k_2}{d_1 + k_1}\frac{E_{2T}(1 - x_1)}{K_2 + (1 - x_1)} + \frac{k_3 k_8 k_5 k_6}{\delta_{ON}\delta_R\delta_{ang}}\, {x_6}^2 + \frac{k_3 k_8 k_5}{\delta_{ON}\delta_R\delta_{ang}} u(t) = 0 \quad (31)$$

where

$$\begin{aligned} x_5 = {} & \left(\frac{\delta}{\beta}\left(\frac{k_2}{k_1}\right) E_{2T}\lambda(t) + (\Phi(1 - x_1) - (p_1\, x_6(1 - x_1) + p_3 u(t)(1 - x_1) + p_8(1 - x_1)\, {x_6}^2 \right. \\ & + p_{10}(1 - x_1)u(t)x_6 - p_{12}(1 - x_1)^2 + p_{13}x_6^2(1 - x_1) + p_{15}x_6 u(t)(1 - x_1) \\ & + p_{20}{x_6}^3(1 - x_1) + p_{22}u(t)x_6^2(1 - x_1) - p_{24}(1 - x_1)^2 x_6 \\ & + p_{37}(1 - x_1)\, x_6 u(t) + p_{39}(1 - x_1)u(t)^2 + p_{44}\,(1 - x_1){x_6}^2 u(t) \\ & + p_{46}(1 - x_1)u(t)^2 x_6 - p_{48}(1 - x_1)^2\, u(t))) \\ & - \left(p_{49}\, x_6 + p_{51}u(t) + p_{56}\, {x_6}^2 + p_{58}u(t)x_6 - p_{60}(1 - x_1)\right) \\ & \left. - \left(p_{61}\, x_6 + p_{63}u(t)\right)\right)/(\, p_4\, x_6(1 - x_1) + p_6 u(t)(1 - x_1) + \, p_7(1 - x_1) \\ & + \, p_{16}\, x_6^2\, (1 - x_1) + p_{18}u(t)x_6(1 - x_1) + \, p_{19}x_6(1 - x_1) \\ & + \, p_{40}\, (1 - x_1)x_6 u(t) + p_{42}(1 - x_1)u(t)^2 + \, p_{43}(1 - x_1)u(t) + \, p_{52}\, x_6 \\ & + p_{54}u(t) + \, p_{55} + \delta_I) \end{aligned} \quad (32)$$

$$\frac{dx_6}{dt} = \, k_4(1 - x_1) - \frac{k_8 k_5 k_6}{\delta_R\delta_{ang}}\, {x_6}^2 - \frac{k_8 k_5}{\delta_R\delta_{ang}} u(t)x_6 - \delta_N x_6 = 0 \quad (33)$$

Derivation of equation (32) and definition of the parameters p's can be found in Appendix C. Model 4 is given in

Table **16** which includes hyperglycemia effects. [G] is the blood glucose level, that is assumed to be effective when pAKT falls below 0.2. When the system is persistently at low pAKT level, glucose cannot be taken into the cell and blood glucose level rises.

Therefore [G] is modeled as a function that is proportional to blood glucose level when pAKT is below 0.2. Derivation of steady state equations (41)-(43) is given in Appendix B.

Table 16. Dynamic Model 4

$$\frac{dx_1}{dt} = -\frac{(d_1 + k_1)}{K_1}\beta\, x_1 x_5 + \frac{(d_1 + k_1)\beta\, x_5 x_1^2}{K_1^2 + K_1 x_1} + d_1 \frac{\beta\, x_5 x_1}{x_1 + K_1} + k_2 \frac{E_{2T}(1 - x_1)}{(1 - x_1) + K_2} + k_3\, x_9 \tag{34}$$

$$\frac{dx_5}{dt} = \frac{\delta}{\beta}\left(\frac{k2}{k1}\right)\tilde{E}_{2T}\lambda(t) + \left(\Phi - \varepsilon\Psi \mathrm{k_{e\_19}\, x_{10}}\left(1 + \mathrm{k_7\, x_7} + \mathrm{k_{G\_12}[G]}\right)\right)(1 - x_1) - k_{e\_13}\, x_{10} - k_{e\_18}\, x_7 - \delta_I x_5 \tag{35}$$

$$\frac{dx_6}{dt} = k_4(1 - x_1) - k_8\, x_8 x_6 + k_{G\_9}[G] - \delta_N x_6 \tag{36}$$

$$\frac{dx_7}{dt} = k_6 x_6 + k_{G\_10}[G] + u(t) - \delta_{ang} x_7 \tag{37}$$

$$\frac{dx_8}{dt} = k_5 x_7 + k_{G\_11}[G] - \delta_R x_8 \tag{38}$$

$$\frac{dx_9}{dt} = k_8 x_8\, x_6 - \delta_{ON} x_9 \tag{39}$$

$$\frac{dx_{10}}{dt} = k_{e\_16} x_7 + k_{e\_15} x_7 x_5 + k_{e_{14}} x_5 + k_{e\_17}\, x_9 - k_{e\_20}(1 - x_1) - \delta_{ERK} x_{10} \tag{40}$$

$$\frac{dG}{dt} = \left[\frac{1}{1 + e\text{^}(200\big((1 - x_1) - 0.2\big)}\right][0.2 - (1 - x_1)] - \delta_G G$$

For the steady state analysis:

$$\frac{dx_1}{dt} = -\frac{1}{K_1}\,\beta\, x_1 x_5 + \frac{\beta\, x_5 x_1^2}{K_1^2 + K_1 x_1} + \frac{d_1}{d_1 + k_1}\left(\frac{\beta\, x_5 x_1}{K_1 + x_1}\right) + \frac{k_2}{d_1 + k_1}\frac{E_{2T}(1 - x_1)}{K_2 + (1 - x_1)} + \frac{k_3 k_8 k_5 k_6}{\delta_{ON}\delta_R\delta_{ang}}\, {x_6}^2 + \left(\frac{k_3 k_8 k_5 k_{G\_10}}{\delta_{ON}\delta_R\delta_{ang}} + \frac{k_3 k_8 k_{G\_11}}{\delta_{ON}\delta_R}\right)[G]x_6 + \frac{k_3 k_8 k_5}{\delta_{ON}\delta_R\delta_{ang}}u(t) \tag{41}$$

where

$$\begin{aligned} x_5 = {} & \left(\frac{\delta}{\beta}\left(\frac{k_2}{k_1}\right) E_{2T}\lambda(t) + (\Phi(1 - x_1) - (p_1\, x_6(1 - x_1) + p_2[G](1 - x_1) + p_3 u(t)(1 - x_1)\right. \\ & + p_8(1 - x_1)\, {x_6}^2 + p_9(1 - x_1)[G]x_6 + p_{10}(1 - x_1)u(t)x_6 \\ & + p_{11}(1 - x_1)[G]x_6 - p_{12}(1 - x_1)^2 + p_{13}x_6^2(1 - x_1) + p_{14}[G]x_6(1 - x_1) \\ & + p_{15}x_6 u(t)(1 - x_1) + p_{20}{x_6}^3(1 - x_1) + p_{21}[G]x_6^2(1 - x_1) \\ & + p_{22}u(t)x_6^2(1 - x_1) + p_{23}[G]x_6^2(1 - x_1) - p_{24}(1 - x_1)^2 x_6 \\ & + p_{25}\, x_6[G](1 - x_1) + p_{26}(1 - x_1)[G]^2 + p_{27}(1 - x_1)u(t)[G] \\ & + p_{32}\,(1 - x_1)[G]{x_6}^2 + p_{33}(1 - x_1)[G]^2 x_6 + p_{34}(1 - x_1)[G]u(t)x_6 \\ & + p_{35}(1 - x_1)[G]^2 x_6 - p_{36}[G](1 - x_1)^2 + p_{37}(1 - x_1)\, x_6 u(t) \\ & + p_{38}(1 - x_1)[G]u(t) + p_{39}(1 - x_1)u(t)^2 + p_{44}\,(1 - x_1){x_6}^2 u(t) \\ & + p_{45}(1 - x_1)[G]x_6 u(t) + p_{46}(1 - x_1)u(t)^2 x_6 + p_{47}(1 - x_1)[G]x_6 u(t) \\ & \left. - p_{48}(1 - x_1)^2\, u(t))\right) \\ & - \left(p_{49}\, x_6 + p_{50}[G] + p_{51}u(t) + p_{56}\, {x_6}^2 + p_{57}[G]x_6 + p_{58}u(t)x_6\right. \\ & \left. + p_{59}[G]x_6 - p_{60}(1 - x_1)\right) \\ & - \left(p_{61}\, x_6 + p_{62}[G] + p_{63}u(t)\right))/(\, p_4\, x_6(1 - x_1) + p_5[G](1 - x_1) \\ & + p_6 u(t)(1 - x_1) + p_7(1 - x_1) + p_{16}\, x_6^2\,(1 - x_1) + p_{17}x_6[G](1 - x_1) \\ & + p_{18}u(t)x_6(1 - x_1) + p_{19}x_6(1 - x_1) + p_{28}\,(1 - x_1)x_6[G] \\ & + p_{29}(1 - x_1)[G]^2 + p_{30}(1 - x_1)[G]u(t) + p_{31}(1 - x_1)[G] \\ & + p_{40}\,(1 - x_1)x_6 u(t) + p_{41}(1 - x_1)[G]u(t) + p_{42}(1 - x_1)u(t)^2 \\ & + p_{43}(1 - x_1)u(t) + p_{52}\, x_6 + p_{53}[G] + p_{54}u(t) + p_{55} + \delta_I) \end{aligned} \tag{42}$$

$$\frac{dx_6}{dt} = k_4(1 - x_1) - \frac{k_8 k_5 k_6}{\delta_R\delta_{ang}}\, {x_6}^2 + (k_{G\_9} - (\frac{k_8 k_5 k_{G\_10}}{\delta_R\delta_{ang}} + \frac{k_8 k_{G\_11}}{\delta_R})x_6)[G] - \frac{k_8 k_5}{\delta_R\delta_{ang}}u(t)x_6 - \delta_N x_6 \tag{43}$$

(45)

### 3.3.3 Detection of Multistability: An Open Loop Approach

(Angeli et al., 2004) proposed an analysis technique to detect multistability in feedback systems where they analyze the behavior of the system by breaking the feedback loop. In this thesis, open-loop approach is applied to Model 1 and to a subnetwork of Model 2, where Ang II and its interactions are omitted and ROS is assumed to be externally stimulated. As shown in Figure 24 the loop is opened at the interaction where pIRS1 activates pAKT so that positive and negative feedbacks are blocked.

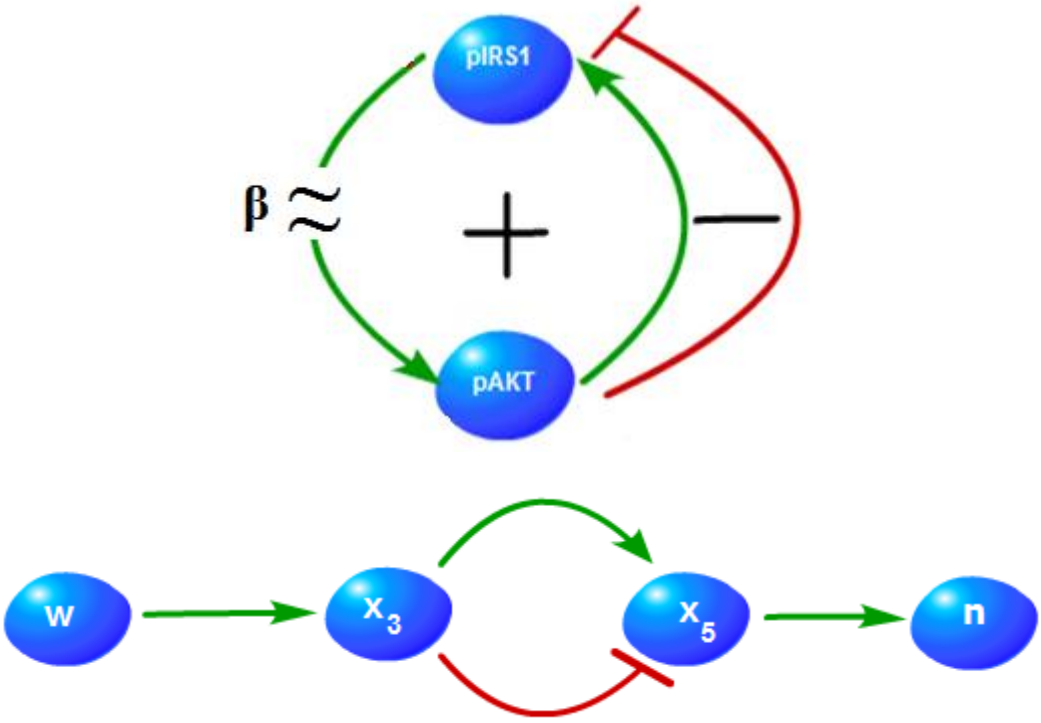


Figure 24. Model 1 breaking the loop

The effect of pIRS1 ($x_5$) on pAKT ($x_3$) is viewed as an input signal w which can be manipulated. The output n is analyzed as a function of input w and then the loop is reclosed letting w = n.

In Table 17 equation (11) is rewritten by letting $w = \beta x_5$

Table 17. Model 1 Open Loop Approach

$$\frac{dx_1}{dt'} = -\frac{1}{K_1}\ x_1\, w + \frac{w\, x_1^2}{K_1^2 + K_1 x_1} + \frac{d_1}{d_1 + k_1}\left(\frac{w\, x_1}{K_1 + x_1}\right) + \frac{k_2}{d_1 + k_1}\frac{E_{2T}(1 - x_1)}{K_2 + (1 - x_1)} \tag{46}$$

$$\frac{dx_5}{dt'} = \frac{\zeta\delta}{\beta}\left(\frac{k2}{k1}\right) E_{2T}\lambda(t) + (\Phi - \varepsilon\Psi)\zeta(1 - x_1) - \delta_I \zeta x_5 \tag{12}$$

Equations (46) and (12) are solved for steady-state and $x_5$ is plotted as a function of w. Then the bifurcation diagram, $x_5$ as a function of the strength β, is plotted which shows the bistability region for β. The plots are shown in results section.

The subnetwork of Model 2 includes the following events: pAKT enables NO production. Reactive oxygen species (ROS), super oxide, is generated and enters the system as an independent stimulus. NO and ROS react to form ONOO. ONOO directly inhibits pAKT. In Model 2, the loop is opened at the same interaction shown in Figure 25. Bifurcation diagram is plotted using equations given in Table 18.

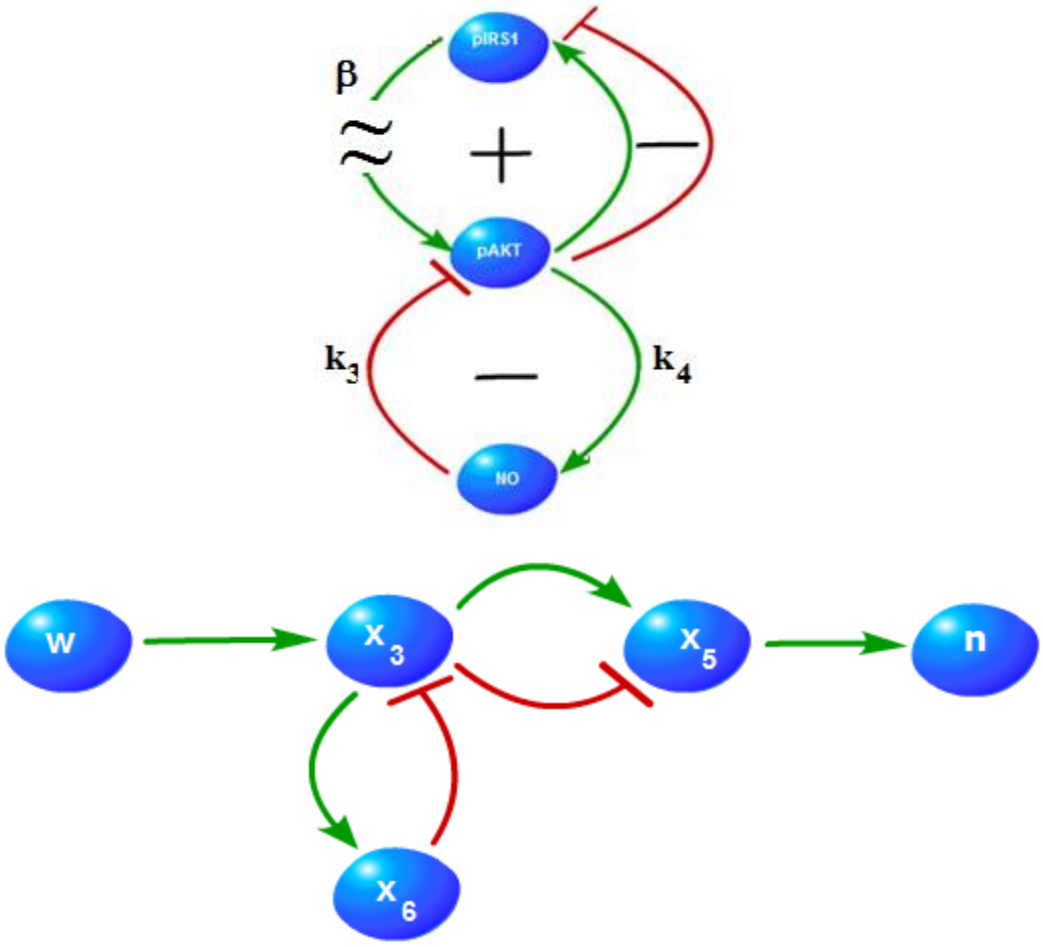


Figure 25. Subnetwork of Model 2 by breaking the loop

Table 18. Subnetwork of Model 2 Open Loop Approach

$$\frac{dx_1}{dt} = -\frac{1}{K_1}\ x_1\, w + \frac{w\, x_1^2}{K_1^2 + K_1 x_1} + \frac{d_1}{d_1 + k_1}\left(\frac{w\, x_1}{K_1 + x_1}\right) + \frac{k_2}{d_1 + k_1}\frac{E_{2T}(1 - x_1)}{K_2 + (1 - x_1)} + \frac{k_3 k_8 k_4 (1 - x_1) x_8}{\delta_{ON}(k_8 x_8 + \delta_{NO})} \quad (47)$$

$$\frac{dx5}{dt} = \frac{\zeta\delta}{w}\left(\frac{k2}{k1}\right) E_{2T}\lambda(t) x_5 + (\Phi - \varepsilon\Psi)\zeta(1 - x_1) - \delta_I \zeta x_5$$

# Chapter 4

# RESULTS AND DISCUSSION

## 4.1 Steady State Analysis of Model 1

Steady state analysis of Model 1 is carried out to generate response curves for pAKT activation to varying insulin supply. In Model 1 there are no significant disturbances due to cross-talking. Glucose uptake process, translocation of GLUT4 stimulated by pAKT, has all-or-none characteristics (Giri et al., 2004). pAKT is also responsible for cell proliferation which is also an on-off type process, below a threshold the system is unresponsive and once the threshold is exceeded the system fully responds. Thus the normal operation should have a toggle switch response curve where the system can switch from low to high pAKT values and vice versa. Steady state equation (10) is solved for various θ, K1 and K2 is set to 0.05. The response curves shown in Figure 26 are obtained. Critical parameter θ is proportional to $(\Phi - \varepsilon \Psi)$, the feedback strength. For positive values of θ, the response curve is switch like. Thus the normal operation of insulin signaling requires the positive feedback to be greater than the negative feedback. Furthermore, positive and negative feedback strengths should be balanced to yield a toggle switch, e.g. Blue curve θ = 1, so that the system is responsive to a small change in the insulin level and is able to fully switch both ways between high and low pAKT values.

**Cancer**

Coupling of positive and negative feedbacks play a significant role in the physiology of the system. Positive and negative feedback strengths should be balanced for a normal healthy operation. When positive feedback strength is increased to a higher level than its normal value due to a disturbance or when the negative feedback is decreased, $\theta$ increases and the response curve becomes a one way switch, e.g. in Figure 26 black curve $\theta = 2$. The system can switch from low pAKT to high pAKT level, however once it reaches the high pAKT state, it stays there even if all insulin is removed. It cannot be controlled by insulin since it would require insulin to be negative which is not realistic. Thus the system remains in high pAKT level which drives uncontrolled cell proliferation, defined as cancer state.

This can help explain why anticancer drugs that target mTOR inhibition are less successful than expected. mTOR inhibition lessens the effects leading to cancer through other pathways. However, as far as the insulin signaling pathway is concerned, mTOR inhibition weakens the mTOR mediated negative feedback to pIRS1, increase $\theta$ and account for persistent pAKT activation.

**Diabetes**

When $\theta$ falls to negative values, e.g. red curve $\theta = -3$, the system remains in low pAKT state even if large quantities of insulin are supplied. This is defined as the insulin resistant state where the glucose uptake is impaired due to persistent low pAKT activity. Disturbances that strengthen the negative feedback can cause the diabetes progression.

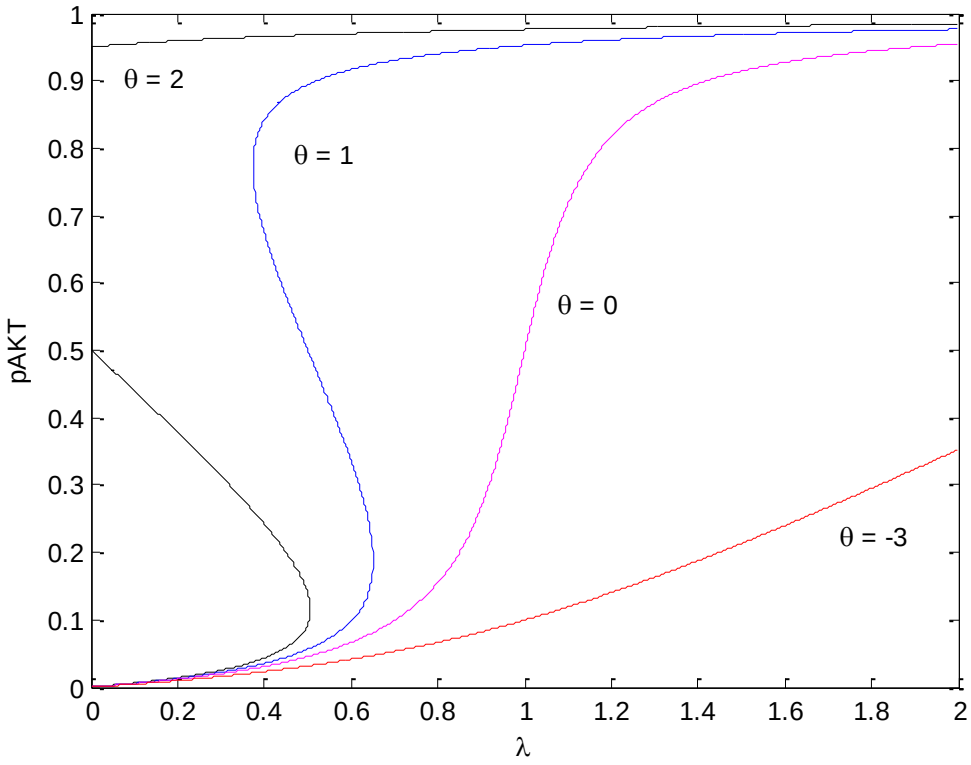


Figure 26. Response curve pAKT(insulin). Black curve θ = 2 one way switch. Blue curve θ = 1 toggle switch. Magenta curve θ = 0 monotone type with high sensitivity. Red curve θ = -3 monotone type with low sensitivity.

### 4.2 Normal Operation of Insulin Signaling

Parameters of the insulin signaling pathway are fixed such that there is bistability and necessary sensitivity to insulin. Scenario 1 demonstrates the normal insulin cycle dynamics.

Scenario 1: Normal Insulin Cycle

Under normal conditions the system can switch between the following two steady states

Steady State A:

$\lambda = 0.5$ pAKT = 0.05594 $\Psi = 0.5594$

Steady State B:

$\lambda = 0.6712$ pAKT = 0.915 $\Psi = 9.15$

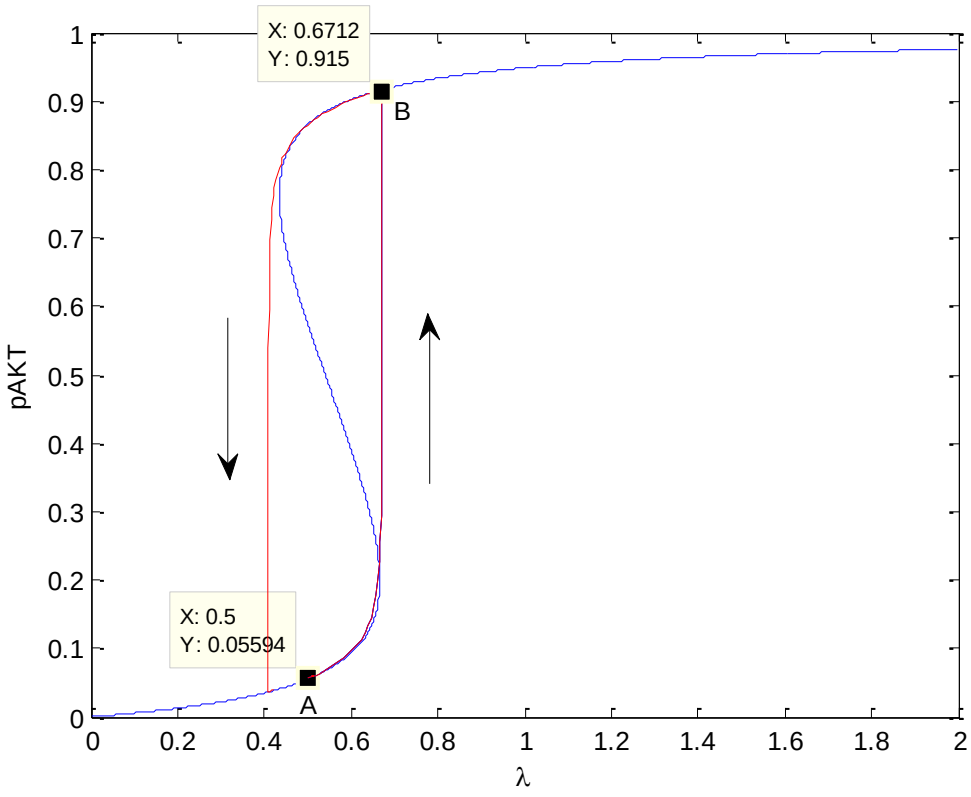


Figure 27. Normal Insulin Cycle

In Figure 27 the blue curve shows the steady state solution for a normal operating system and the red curves belong to the dynamic response. State A, the cell has low nutrient level and requires glucose uptake. By stimulating insulin, the system switches to

State B, where pAKT is activated and glucose is taken into the cell. Withdrawing insulin enables the switch back to low pAKT.

**Applying Open Loop Approach to Model 1**

Figure 28 represents steady state characteristic curve $x_5$ as a function of $w = \beta x_5$. Lines represent unitary feedback. Above and below the dashed black lines the system is monostable, in between, e.g. red line, there are three steady states, two being stable (I, III) and one unstable (II) and there are β values corresponding to these regions.

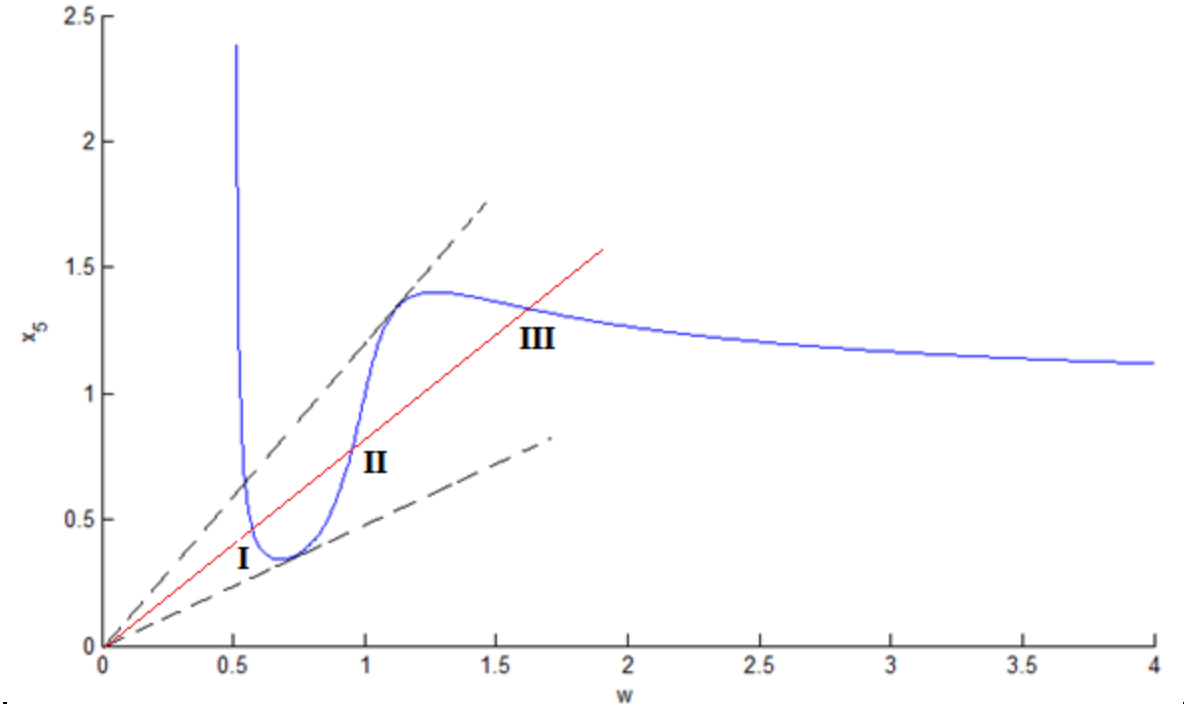


Figure 28. Steady State curve ($x_5$ as a function of w) for model 1 λ = 0.5

In Figure 29 $x_5$ is plotted as a function of the strength β. The system exhibits bistability for values of β between 0.84 and 2.07. Figure 30 shows the steady state curves

of Model 1 for various β. For λ = 0.5, response curves with β between 0.84 and 2.07, e.g. blue curve β = 1, there are three intersection points. For β > 2.07, the system has one steady state, high pAKT, and constant high level pAKT state is characterized as cancer.

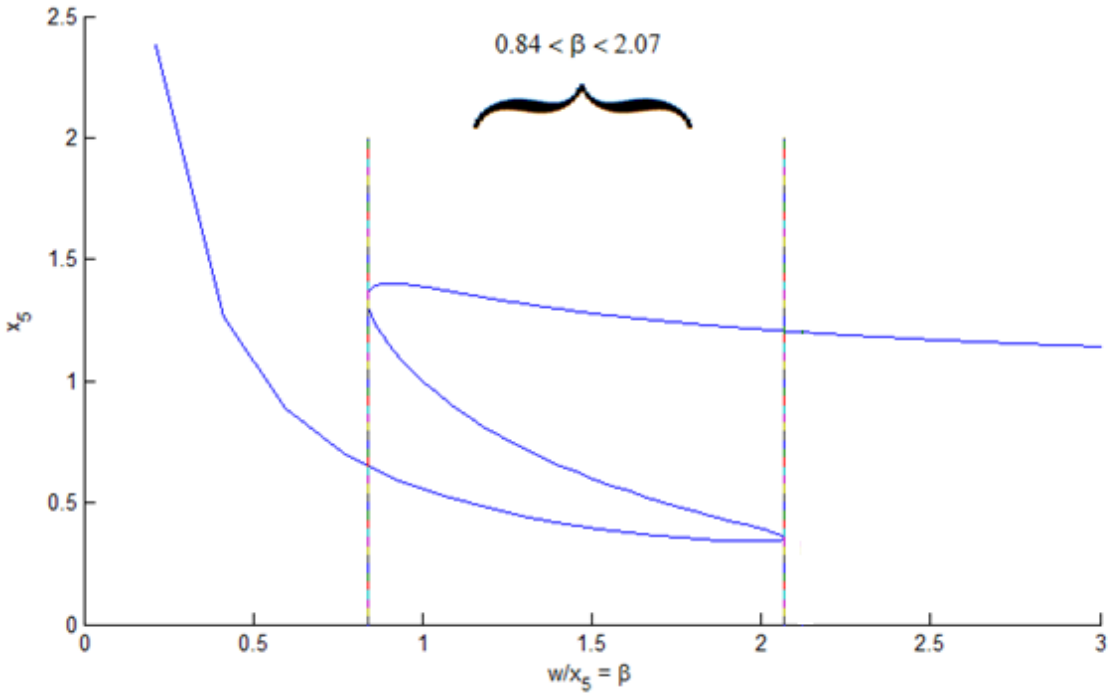


Figure 29. Bifurcation diagram showing bistability when β is between 0.84 and 2.07 for model 1 λ = 0.5

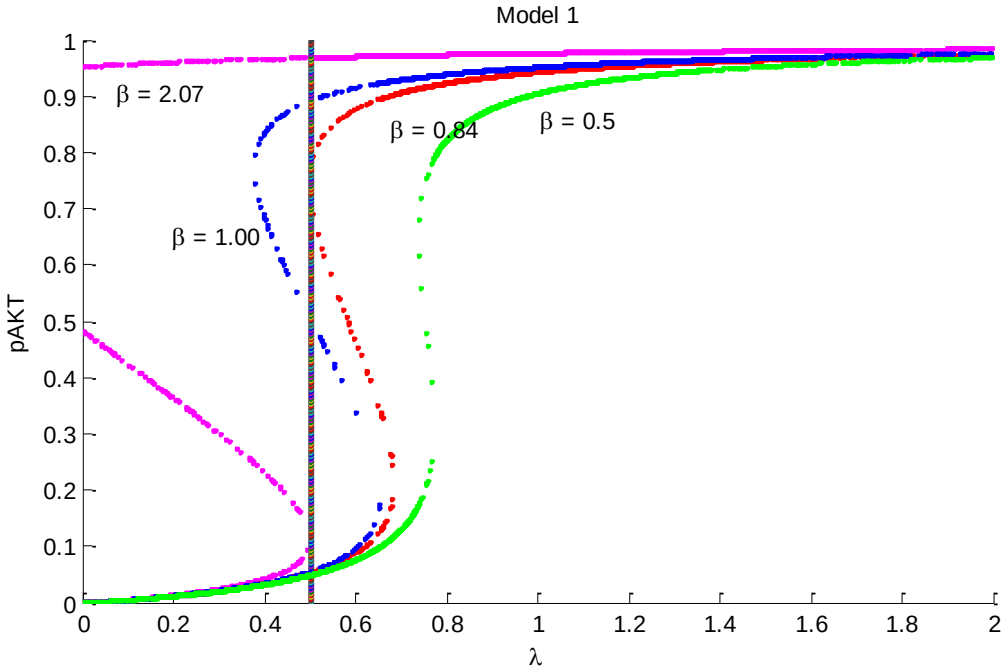


Figure 30. Steady State curve (pAKT as a function of λ) for Model 1. Black line for λ = 0.5. When β is 0.84(red) or 2.07(magenta) there are 2 solutions at λ = 0.5. For 0.84 < β < 2.07 there are 3 solutions like blue curve (β=1). For β > 2.07 or β < 0.84 there exists only 1 solution like green curve (β=0.5).

By breaking the loop at the interaction where pIRS1 activates pAKT, the limits of the strength of this interaction (β) that ensures bistability are found. For values of β outside this region the system looses bistability. For high values of β the steady state curve has S-Shape but the system cannot switch from high to low values of pAKT and constant high level pAKT state is characterized as cancer.

**Applying Open Loop Approach to the Subnetwork of Model 2**

The subnetwork of Model 2 under study in this section includes an additional negative feedback formed by the inhibition of pAKT by ONOO. pAKT enables NO production. Reactive oxygen species (ROS), super oxide, is generated and enters the system as an independent stimulus. NO and ROS react to form ONOO. ONOO directly

inhibits pAKT. Figure 31 shows the bistability limits of β for different $k_3$ values, where $k_3$ denotes the strength of pAKT inhibition by NO. As $k_3$ increases the range of β shifts to a higher region because increase in β can compensate the inhibitory action of ONOO by activating pAKT more. Figure 32 and Figure 33 shows the steady state curves of this system when k3 is 1 and 2, respectively. In Figure 32, for β>3.23 there exist only 1 solution. However, in Figure 33, for β slightly higher than 3.36 the system will be bistable. That is, changing the strength of the negative feedback to pAKT changes the limits of β that produces bistability. This suggest that for systems where there is disturbance that enhances insulin mediated activation of pAKT, enforcing the negative feedback to pAKT would recover the system back to bistability and prevent persistent activated pAKT state (cancer). Conversely, if β values are normal, addition of this negative feedback causes the system to lose its bistability characteristics. The system may reside in low pAKT state and thus develop insulin resistance.

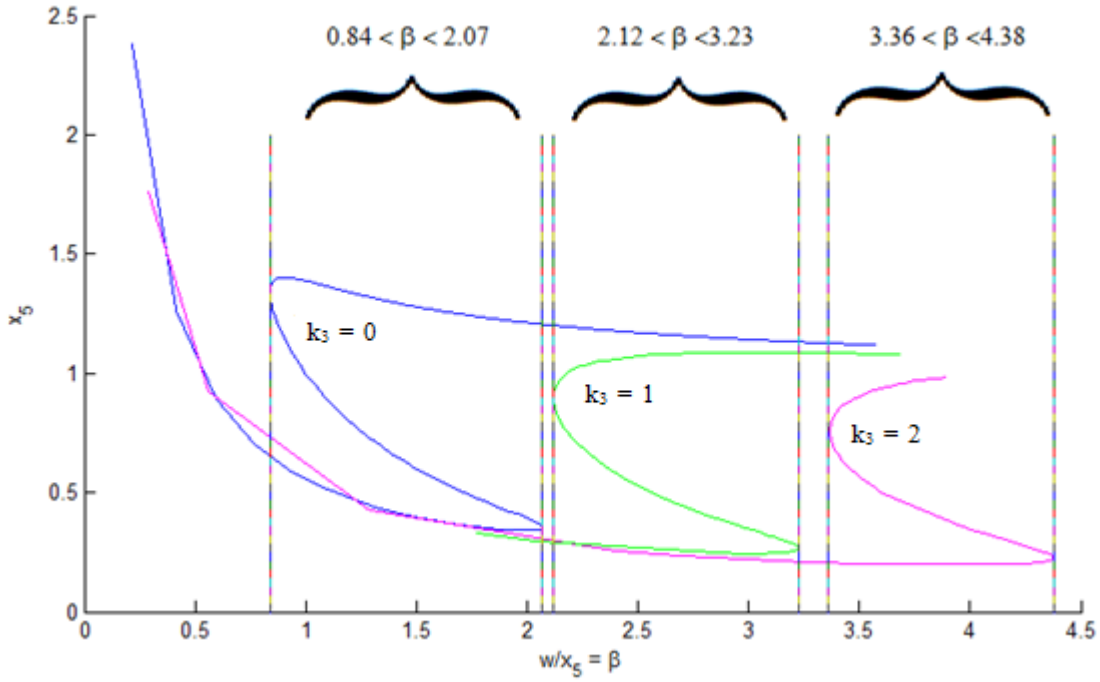


Figure 31. Bifurcation diagram showing bistability limits for β at different $k_3$ values for model 2 λ = 0.5

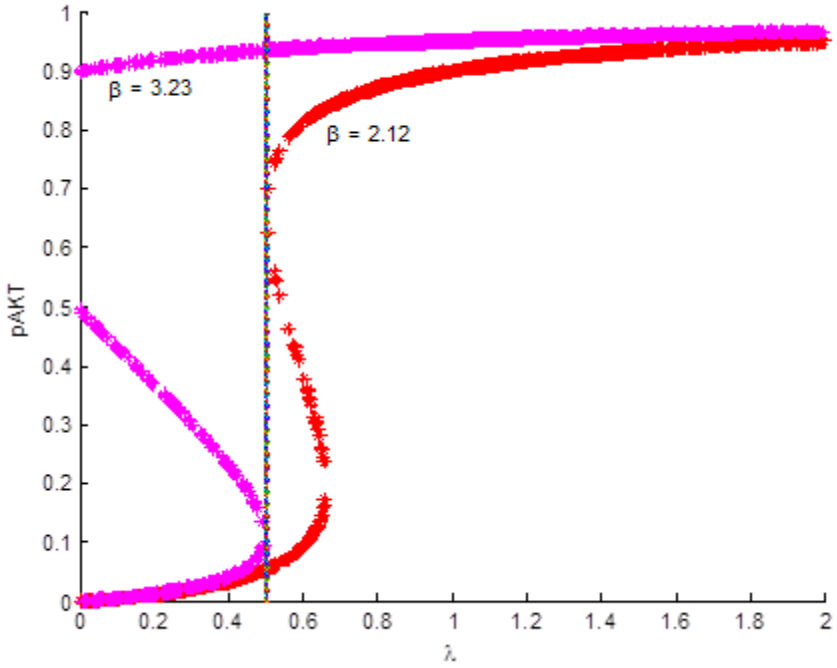


Figure 32. Steady State curve (pAKT as a function of λ) for Model 2 $k_3 = 1$. Black line for λ = 0.5. When β is 2.12(red) or 3.23(magenta) there are 2 solutions at λ = 0.5. For 2.12 < β < 3.23 there are 3 solutions. For β > 3.23 or β < 2.12 there exists only 1 solution.

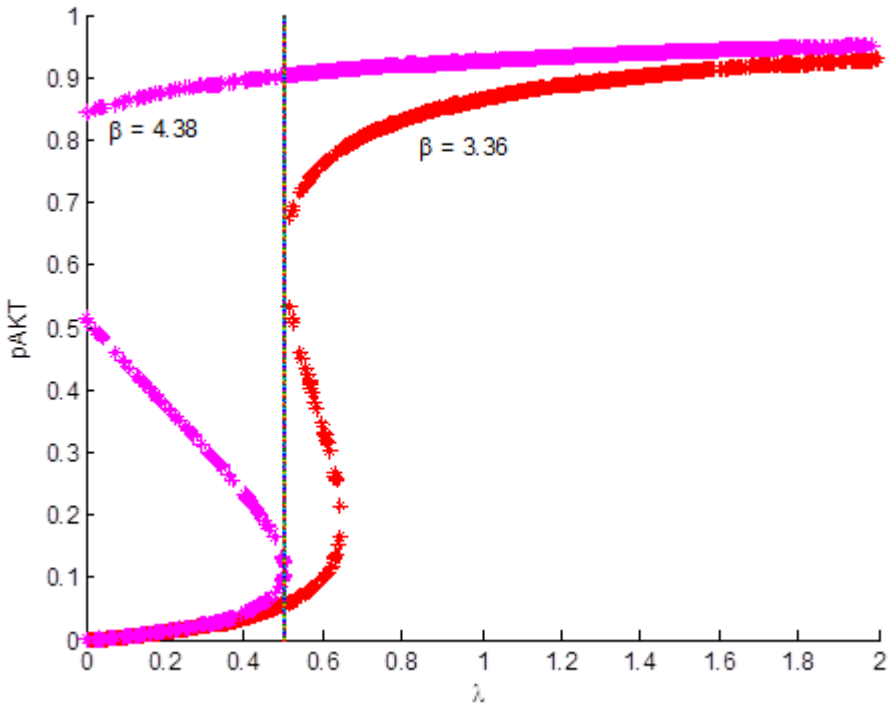


Figure 33. Steady State curve (pAKT as a function of λ) for Model 2 $k_3$ = 2. Black line for λ = 0.5. When β is 3.36(red) or 4.38(magenta) there are 2 solutions at λ = 0.5. For 3.36 < β < 4.38 there are 3 solutions. For β > 4.38 or β < 3.36 there exists only 1 solution.

### 4.3 Analysis of Model 2

Model 2 includes the crosstalk with Ang II. There are 5 negative loops and 1 positive loop as listed in Table 7. For steady state analysis Equation (21) & (23) are solved for $x_1$ by changing $x_6$. Both are plotted in the same diagram and the intersection points are identified as the steady state points.

Scenario M2.1: Model 2 Base Case

Bistability holds for the following set of parameters:

Table 19. Model 2 Parameter Set M2

| | | | |
|---|---|---|---|
| $E_{2T} = 1$ | $K_1 = 0.05$ | $K_2 = 0.05$ | |
| $\beta = 1$ | $\Phi = 1$ | $\varepsilon = 0.01$ | $\Psi = 0.559$ |
| $\delta = 1$ | $\delta_N = 0.01$ | $\delta_{ON} = 0.01$ | $\delta_{ang} = 1$ |
| $d_1 = 1/11$ | $d_2 = 1/11$ | | |
| $k_1 = 10/11$ | $k_2 = 10/11$ | $k_3 = 0.1$ | $k_4 = 0.01$ |
| $k_5 = 0.1$ | $k_6 = 10$ | $k_7 = 0.1$ | $k_8 = 0.1$ |

In Figure 34 blue and black curves are solutions of Equation (21) and (23) respectively, parameter values listed in

Table **19** are used and λ is set to 0.5. The curves intersect at three points, steady states $S_1$, $S_2$, and $S_3$. Dynamic simulations are carried out starting from initial points, $I_1$, $I_2$, $I_3$, and $I_4$. Steady State $S_3$ is reached when the dynamic simulation starts from $I_1$ and $I_3$. Steady State $S_1$ is reached when the dynamic simulation starts from $I_2$ and $I_4$. Figure 34 shows that steady states $S_1$ and $S_3$ are stable, whereas $S_2$ is unstable. When the simulation starts from an initial state above $S_2$, it reaches $S_3$, high pAKT stable steady state. And when it starts below $S_2$, it reaches $S_1$, low pAKT stable steady state. Model 2 is bistable for the set of parameters given in

Table **19.**

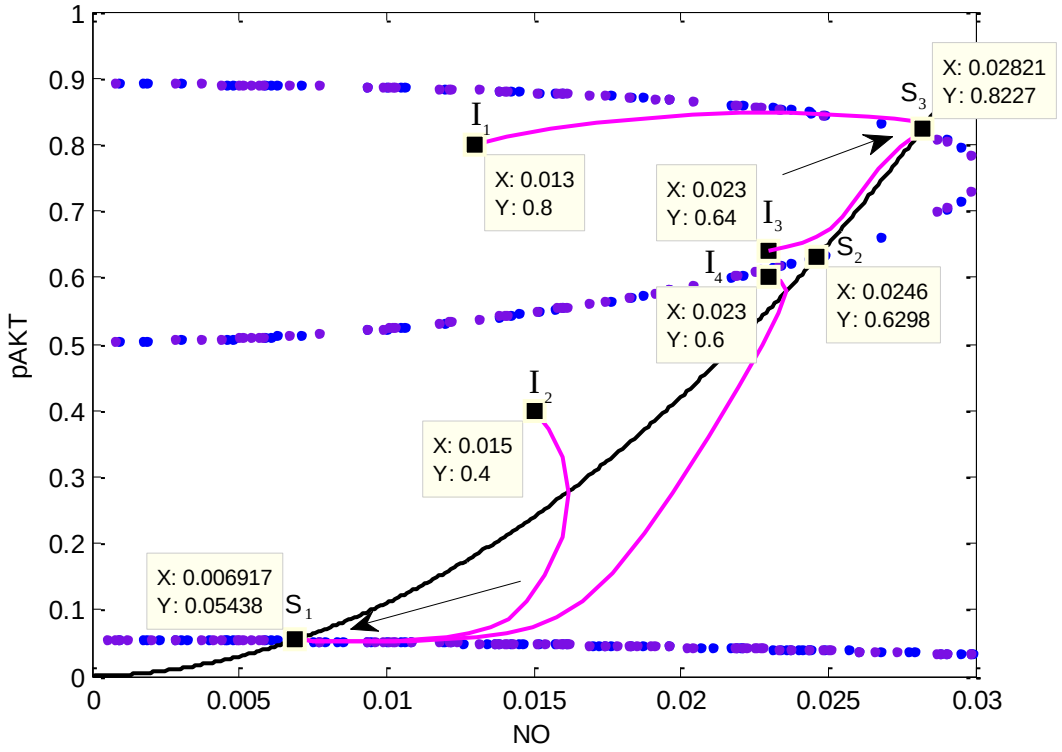


Figure 34. Model 2 Base Case Scenario: Scenario 1

Equation (21) is solved using the same parameter set M2 (Table 19) for various λ and plotted in Figure 35. The intersection points with black curve (solution of Equation (23)) are recorded as steady state pAKT and NO values and plotted against λ in Figure 36. Since NO production depends on activation of pAKT, NO switches as pAKT switches.

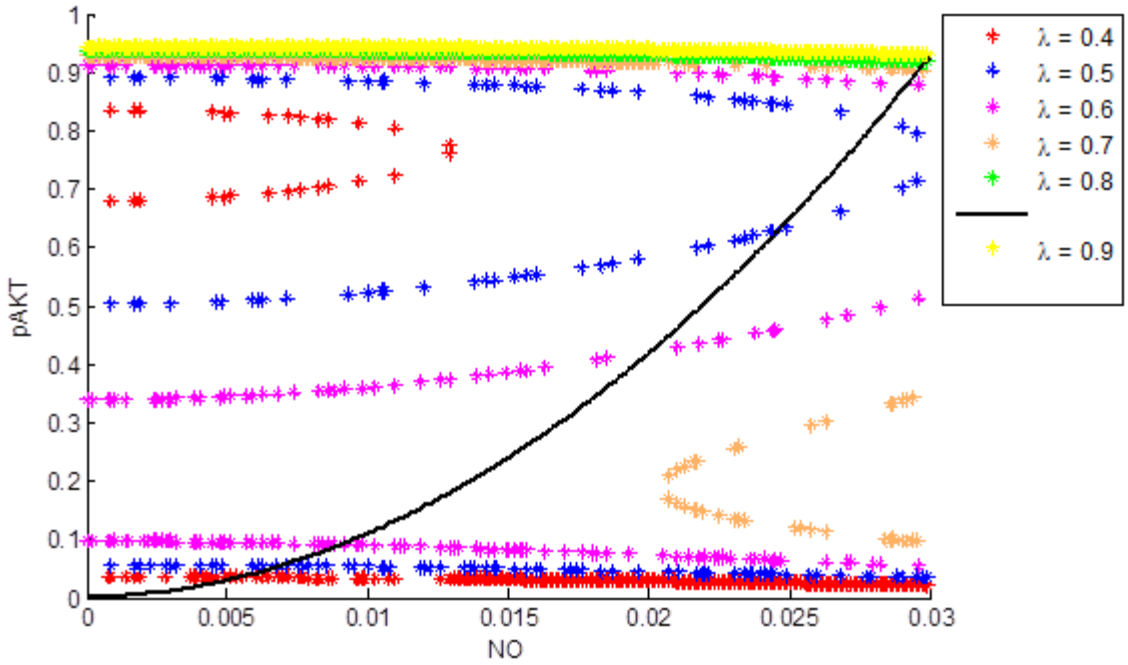


Figure 35. Steady state solutions of Equation (21) and (23) for various λ. (Parameter Set M2)

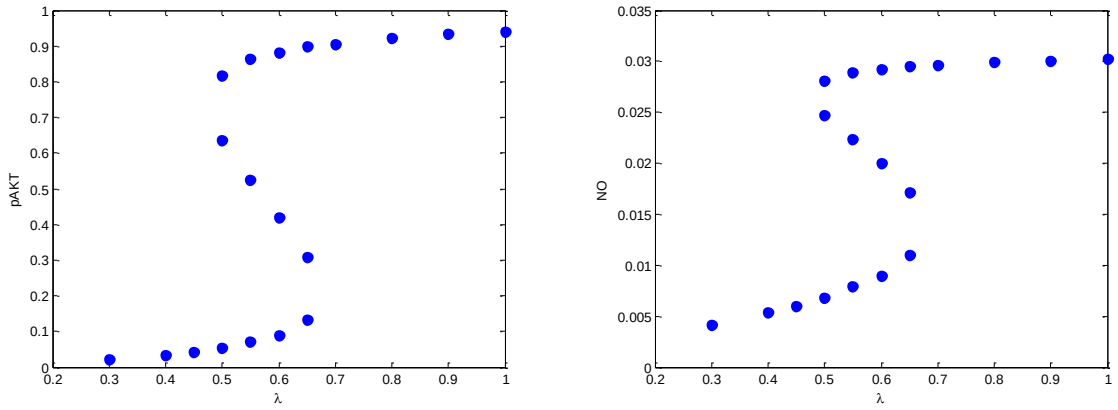


Figure 36. Scenario 1 Bistable Curves λ vs. pAKT and λ vs NO

Scenario M2.2: $k_3$ is increased from 0.1 to 1

In Figure 37, the red curve shows the solution of Equation (21) when the same parameters (Parameter set M2) except $k_3$ are used. $k_3$ is increased from 0.1 to 1. Equation (23) does not depend on $k_3$. Comparing with the previous solution (blue curve), steady states $S_2$ and $S_3$ are lost. Dynamic simulation starting from $I_1$ goes to $S_1$ instead of $S_3$. As the strength of inhibition to pAKT, $k_3$, is increased the system loses bistability and becomes monostable.

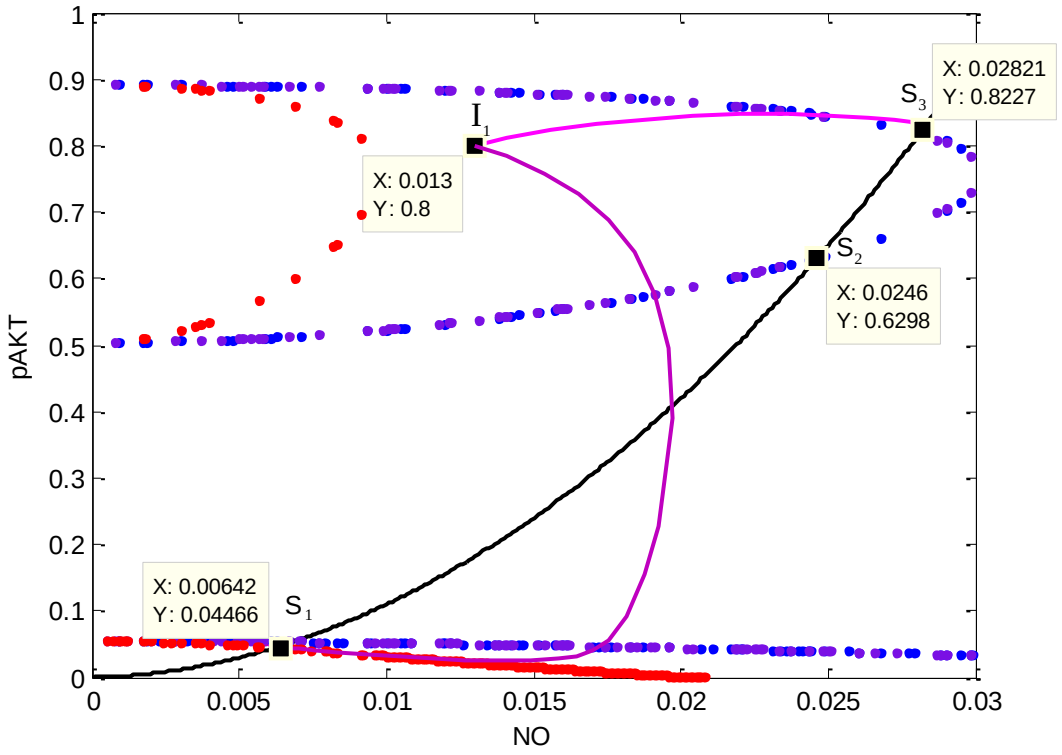


Figure 37. Model 2 comparison of Scenario 2 ($k_3$ = 1.0) with Scenario 1 ($k_3$ = 0.1).

In Figure 38 for each colored curve there is only one intersection with the black curve. That means for any λ there exists only one steady state and the system is not

bistable. Steady state points are plotted in in Figure 30, pAKT(λ) and NO(λ) curves are monotonically increasing.

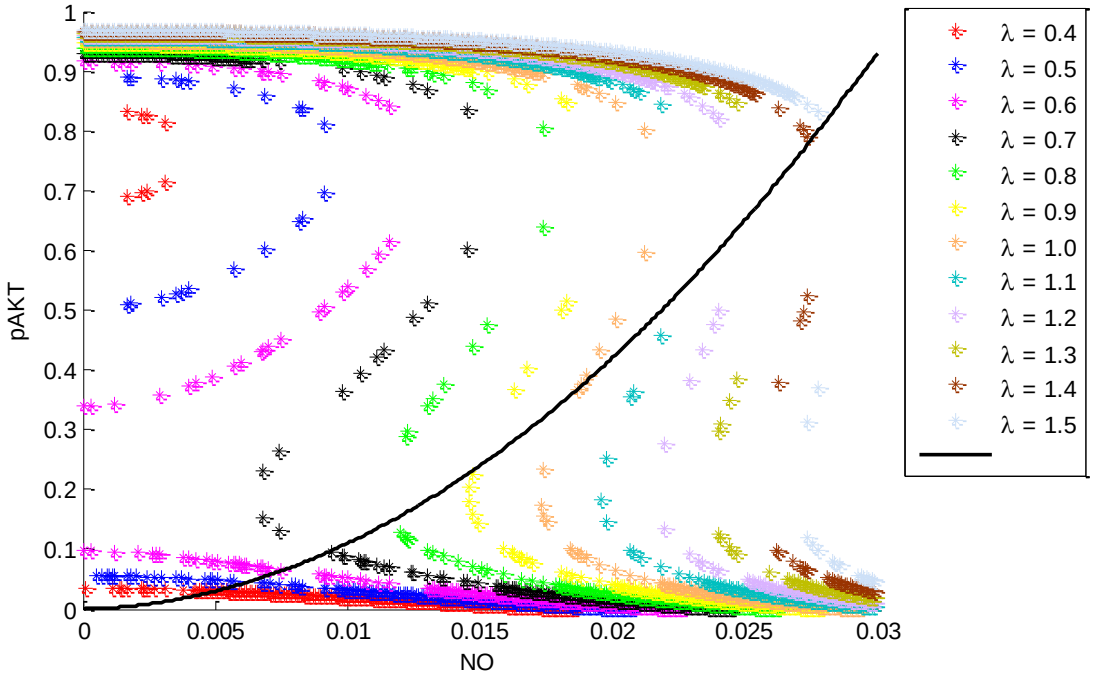


Figure 38. Steady state solutions of Equation (21) and (23) for various λ. (Parameter Set M2 except $k_3$, $k_3$ = 1.0)

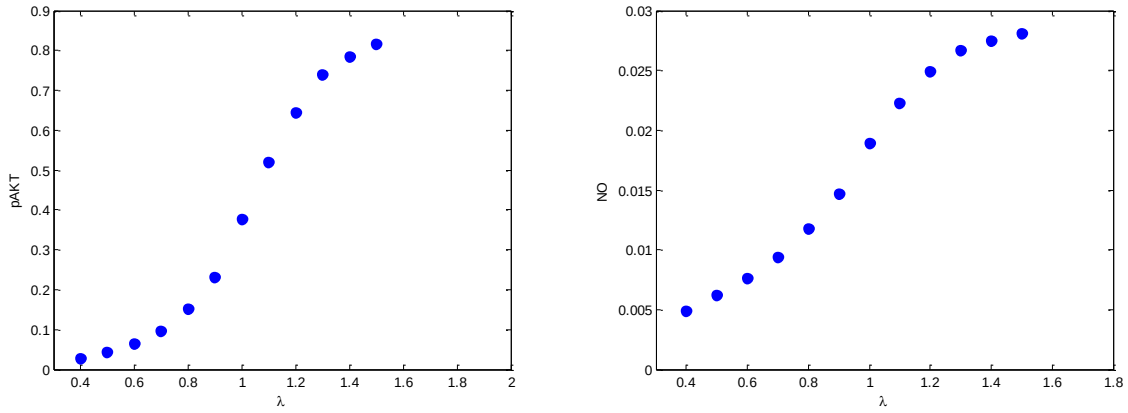


Figure 39. Scenario 2 Curves λ vs. pAKT and λ vs NO

Scenario M2.3: $k_7$ is increased from 0.1 to 100

In Figure 40, the red curve shows the solution of Equation (21) when the same parameters (Parameter set M2) except $k_7$ are used. $k_7$ is increased from 0.1 to 100. Again compared with solutions of Scenario 1, the system loses bistability. Increasing the strength of $k_7$ illustrates the effects of Ang II to interfere with the insulin signaling through mTOR.

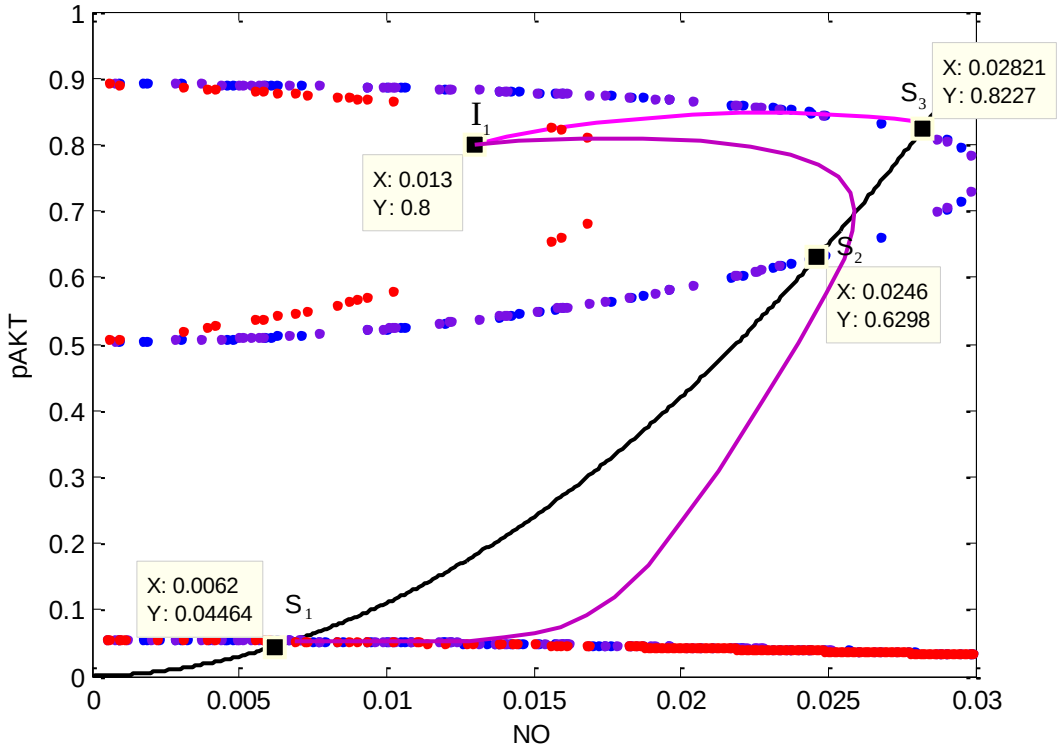


Figure 40. Model 2 comparison of Scenario 3 ($k_7$ = 0.1) with Scenario 1 ($k_7$ = 100).

Scenario M2.4: $k_4$ is increased from 0.01 to 0.015

In this Scenario, $k_4$ is increased from 0.01 to 0.015. Figure 41 shows the comparison with Scenario 1, Equation (21) doesn't depend on $k_4$ but Equation (23) depends on $k_4$. The dotted black curve shows the solution of Equation (23) as $k_4$ is increased from 0.01 to 0.015. Again compared with solutions of Scenario 1, the system loses bistability. Increasing $k_4$, more NO is produced. Elevated NO levels leads to activation of Ang II and production of ONOO which in turn impairs insulin signaling as shown in Scenario M2.2 and M2.3.

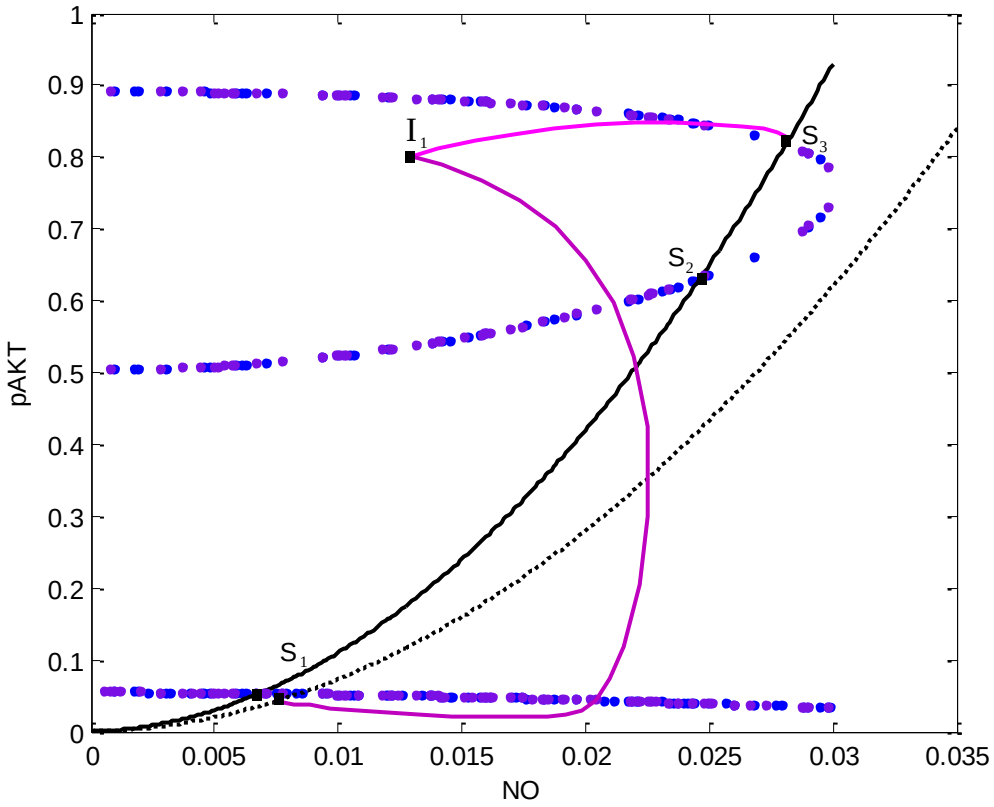


Figure 41. Model 2 comparison of Scenario 4 ($k_4$ = 0.015) with Scenario 1 ($k_4$ = 0.01).

### 4.4 Analysis of Model 3

Model 3 includes interactions related to pERK. For the parameter set M3 given in Table 20, the system is bistable. λ vs pERK steady state curve is S-Shaped and it is found that pERK switches in this system. As pERK is responsible for cell growth mechanisms, the on-off activation characteristics were expected.

Scenario M3.1: Model 3 Base Case

Bistability holds for the following set of parameters:

Table 20. Model 3 Parameter Set M3

| | | | |
|---|---|---|---|
| $E_{2T} = 1$ | $K_1 = 0.05$ | $K_2 = 0.05$ | |
| $\beta = 1$ | $\Phi = 1$ | $\varepsilon = 0.01$ | $\Psi = 0.559$ |
| $\delta = 1$ | $\delta_N = 0.01$ | $\delta_{ON} = 0.01$ | $\delta_{ang} = 1$ |
| $d_1 = 1/11$ | $d_2 = 1/11$ | $u = 0$ | |
| $k_1 = 10/11$ | $k_2 = 10/11$ | $k_3 = 0.1$ | $k_4 = 0.01$ |
| $k_5 = 0.1$ | $k_6 = 10$ | $k_7 = 0.1$ | $k_8 = 0.1$ |
| $k_{e\_13} = 0.01$ | $k_{e\_14} = 0.01$ | $k_{e\_15} = 0.01$ | $k_{e\_16} = 0.01$ |
| $k_{e\_17} = 0.01$ | $k_{e\_18} = 0.01$ | $k_{e\_19} = 0.01$ | $k_{e\_20} = 0.01$ |

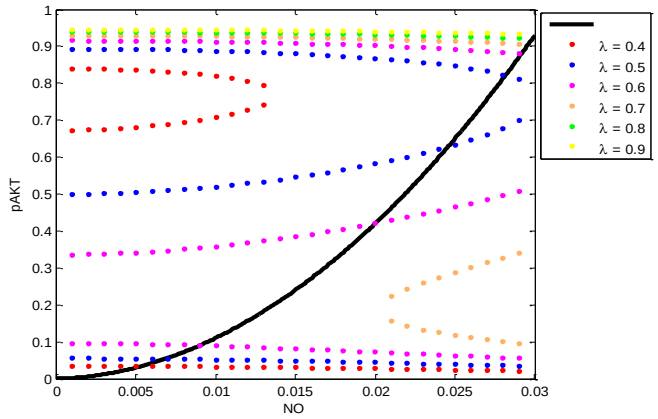


Figure 42. Steady state solutions of Equation (31) and (33) for various λ. (Parameter Set M3)

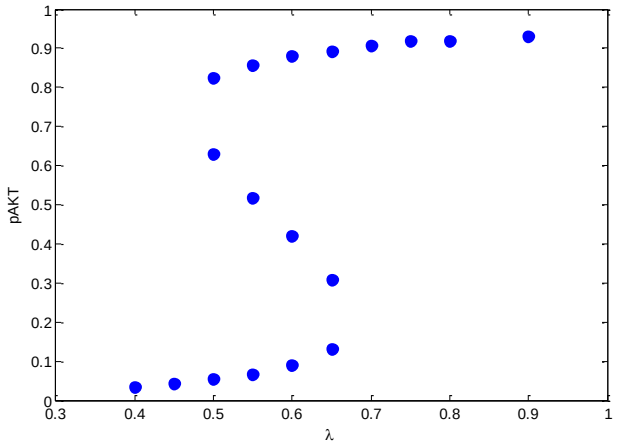


Figure 43 Scenario M3.1 Bistable Curve λ vs. pAKT

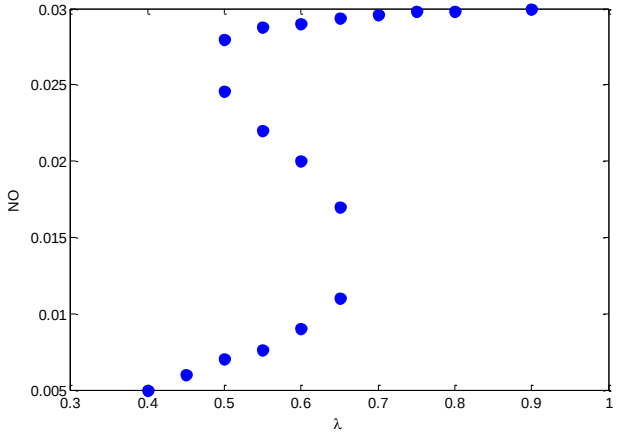


Figure 44. Scenario M3.1 Bistable Curve λ vs. NO

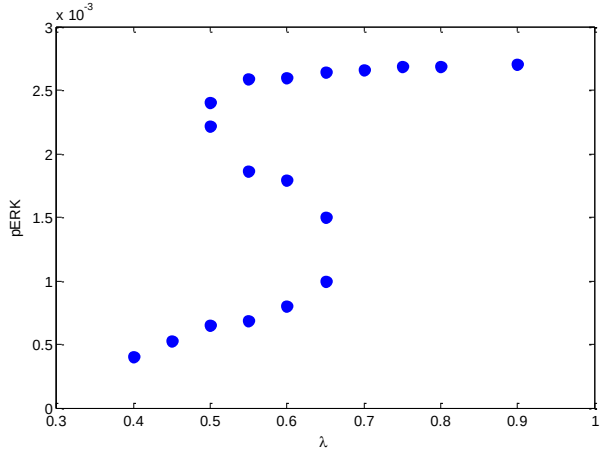


Figure 45. Scenario M3.1 Bistable Curve λ vs. pERK

Scenario M3.2: $k_{e13}$ is increased from 0.01 to 100

Parameters M3 are kept except $k_{e13}$. Results of increasing $k_{e13}$ shows that inhibition of pIRS1 by pERK results in loss of bistability in λ vs pAKT, NO, and pERK curves. NO and pERK bistability is lost because their actication depend directly and indirectly to pAKT respectively. Since NO is produced by direct activation of pAKT as pAKT cannot switch to high levels NO cannot as well. pERK gets activated through ONOO and Ang II and their activation depend on NO. As NO is a monotonically increasing function of lambda, pERK has the same characteristics as well.

In Figure 42, dynamic simulations of Scenario M3.1 and M3.2 are shown starting from initial state $I_1$. Scenario M3.1 goes to high pAKT state whereas Scenario M3.2 goes to low pAKT state. In Figures 43-45, the steady state curves loses S-Shape characteristics and becomes monotonically increasing.

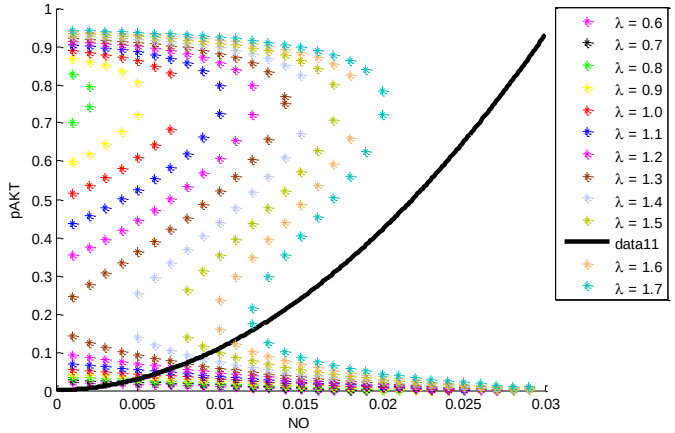


Figure 46. Steady state solutions of Equation (31) and (33) for various λ. (Parameter Set M3 except $k_{e\_13}$, $k_{e\_13}$ = 100)

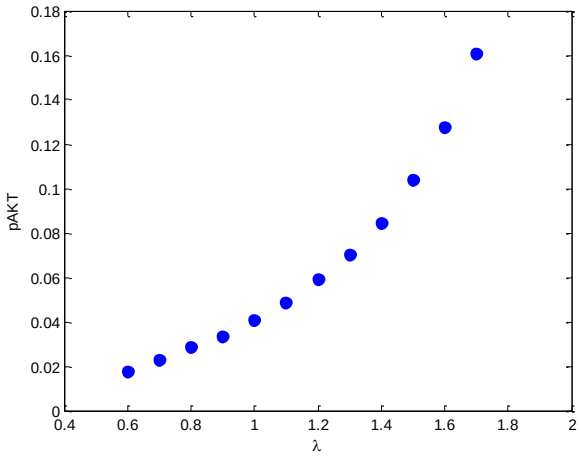


Figure 47 Scenario M3.2 Curves λ vs. pAKT (bistability is lost)

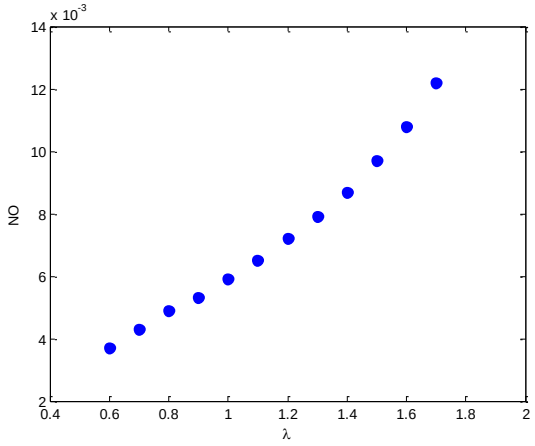


Figure 48. Scenario M3.2 Curves λ vs. NO (bistability is lost)

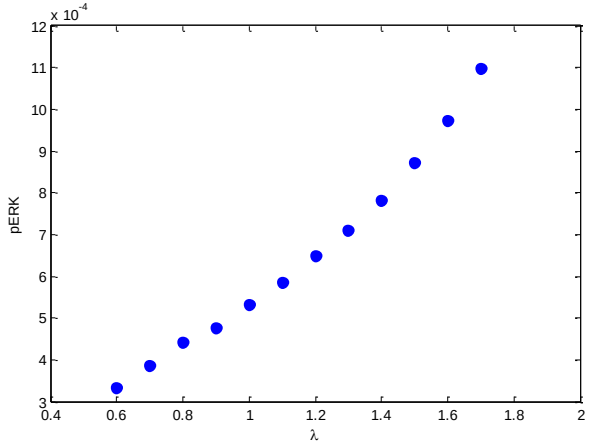


Figure 49. Scenario M3.2 Curves λ vs. pERK (bistability is lost)

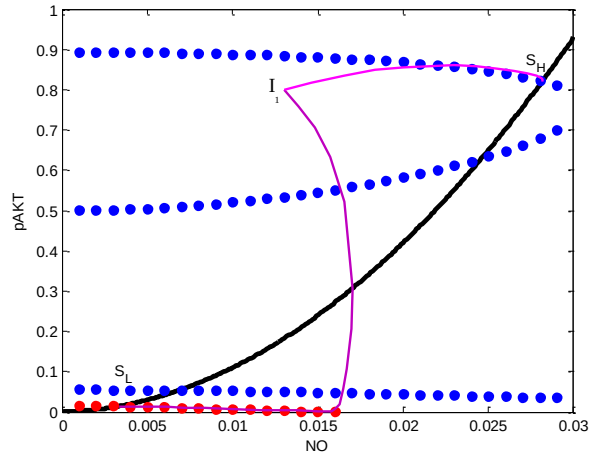


Figure 50 Model 3 comparison of Scenario M3.2 ($k_{e\_13}$ = 100) with Scenario M3.1 ($k_{e\_13}$ = 0.01)

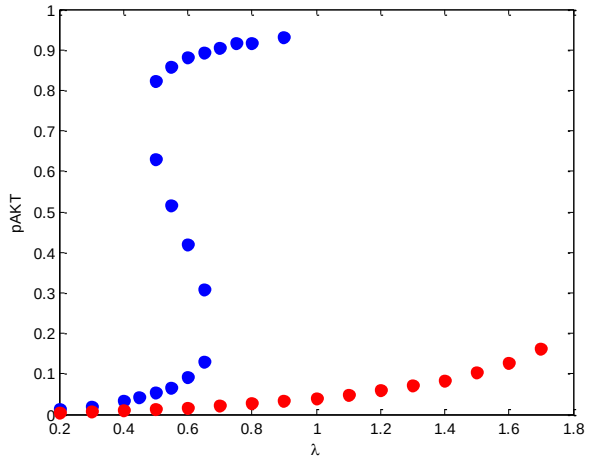


Figure 51 Steady state curve λ vs pAKT Scenario M3.2 (red) with Scenario M3.1 (blue)

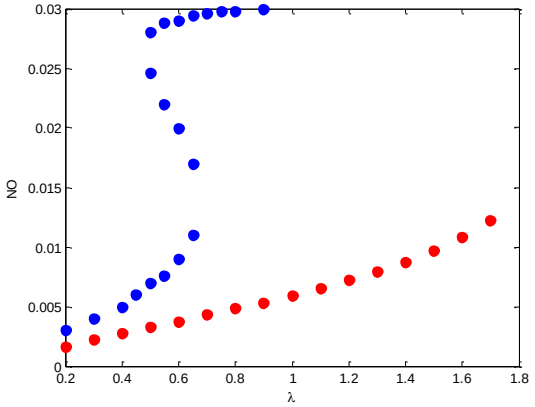


Figure 52 Steady state curve λ vs NO Scenario M3.2 (red) with Scenario M3.1 (blue)

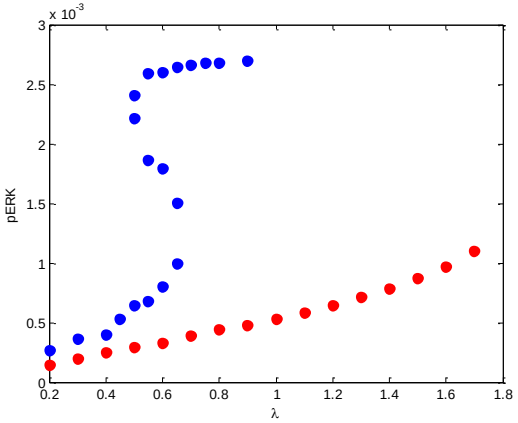


Figure 53 Steady state curve λ vs pERK Scenario M3.2 (red) with Scenario M3.1 (blue)

Scenario M3.3: Model 3 $k_{e13}$ is increased from 0.01 to 100 and $k_{e20}$ is increased from 0.01 to 0.035

In Scenario M3.2, pERK induces insulin resistance through inhibiting pIRS1. In Scenario M3.3 $k_{e20}$ is increased as well. Figure 54 presents that when the strength of inhibition of pERK by AKT increases, it can recover the inhibitory effect of pERK to pIRS1. Thus the double inhibitory effect results in a positive effect to restore bistability.

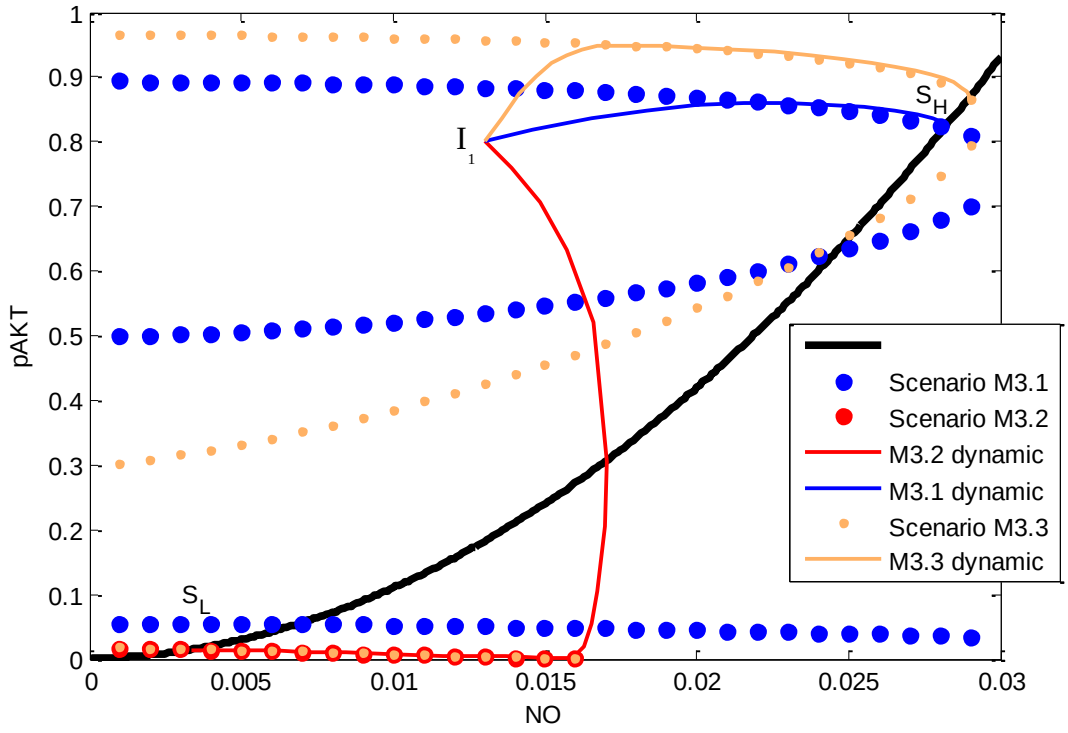


Figure 54 Model 3 comparison of Scenario M3.3, M3.2 and M3.1

Scenario M3.4: Model 3 Effects of $k_{e13}$ $k_{e14}$ $k_{e15}$ $k_{e16}$ $k_{e17}$ $k_{e18}$ $k_{e19}$

Scenario M3.4 summarizes the contributions of other system parameters to the bistability nature of the system. As the strength of these parameters are increased, bistability can be lost.

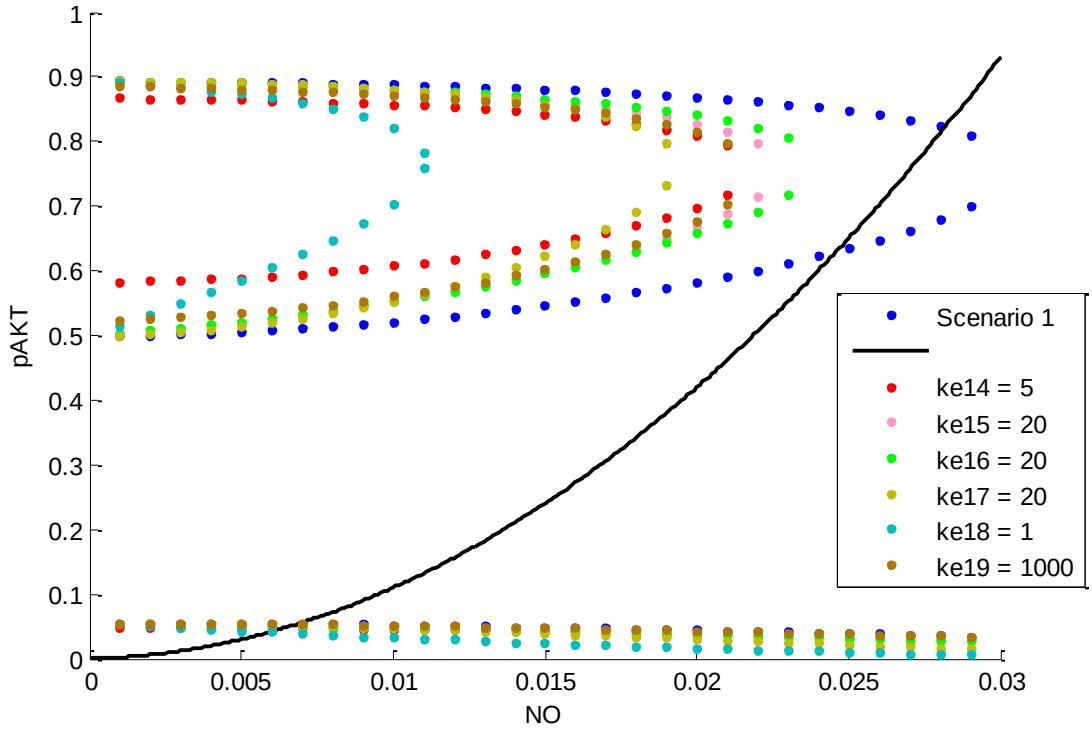


Figure 55. Scenario M3.4

### 4.5 Analysis of Model 4

Model 4 covers the hyperglycemia effects. When the system stays in low pAKT level for a period of time hyperglycemia may develop due to impaired glucose uptake.

Scenario M4.1: Model 4

Parameter Set M4 is an arbitrary set of the systems parameters that ensures insulin resistance, the case when pAKT persistently stays below 0.2.

Table 21. Model 4 Parameter Set M4

| | | | |
|---|---|---|---|
| $E_{2T} = 1$ | $K_1 = 0.05$ | $K_2 = 0.05$ | |
| $\beta = 1$ | $\Phi = 1$ | $\varepsilon = 0.01$ | $\Psi = 0.559$ |
| $\delta = 1$ | $\delta_N = 0.01$ | $\delta_{ON} = 0.01$ | $\delta_{ang} = 1$ |
| $d_1 = 1/11$ | $d_2 = 1/11$ | $u = 0$ | $\delta_{erk} = 1$ |
| $k_1 = 10/11$ | $k_2 = 10/11$ | $k_3 = 0.2$ | $k_4 = 0.02$ |
| $k_5 = 0.2$ | $k_6 = 10$ | $k_7 = 10$ | $k_8 = 0.2$ |
| $k_{e\_13} = 2$ | $k_{e\_14} = 0.02$ | $k_{e\_15} = 0.02$ | $k_{e\_16} = 0.02$ |
| $k_{e\_17} = 0.02$ | $k_{e\_18} = 0.02$ | $k_{e\_19} = 0.02$ | $k_{e\_20} = 0.01$ |
| $k_{G\_9} = 0.001$ | $k_{G\_10} = 0.001$ | $k_{G\_11} = 0.001$ | $k_{G\_12} = 0.001$ |

The solutions of Equations (41) and (43) are plotted in Figure 56. As $k_{G10}$, $k_{G11}$, and $k_{G12}$ are increasing Equation (41) curve shifts down but this doesn't have a significant effect on the system because pAKT is already low and the system is in the insulin resistant state. Nonetheless it can be argued that hyperglycemia strengthen the onset of insulin resistance.

The increase in $k_{G9}$ shifts the Equation (43) curve to the right, system moves to higher NO region. This represents the GPR91 mediated activation of NO. The increase in NO can explain the presence of glomerular hyperfiltration observed in diabetic patients. On the other hand, the increases in $k_{G10}$ and $k_{G11}$ shifts the Equation (43) curve to the left, meaning that their effect decrease NO. This is evident from Equations (37) and (38), hyperglycemia stimulates Ang II and ROS production which in turn decrease NO by converting it to ONOO and also by impairing insulin signaling. As NO decreases, vasodilation is impaired. At the same time production of Ang II increases blood pressure and thus hyperglycemia contributes to hypertension development.

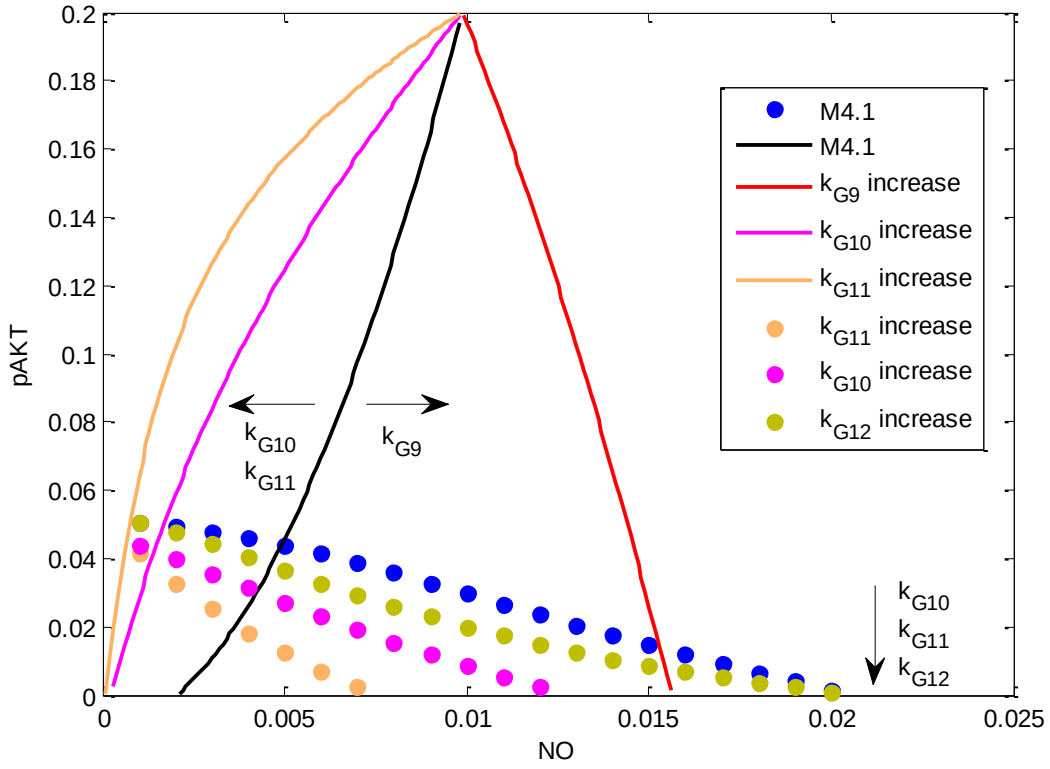


Figure 56. Model 4 Hyperglycemia Effects

### 4.6 Coupling Model 4 with Blood Pressure Control

In Model 4, Ang II disturbance is included as u(t), but in scenarios so far it was 0. When Ang II gets stimulated because of reasons explained in literature review, the strengths of inhibitions covered in previous scenarios increases and insulin resistance develops as illustrated in

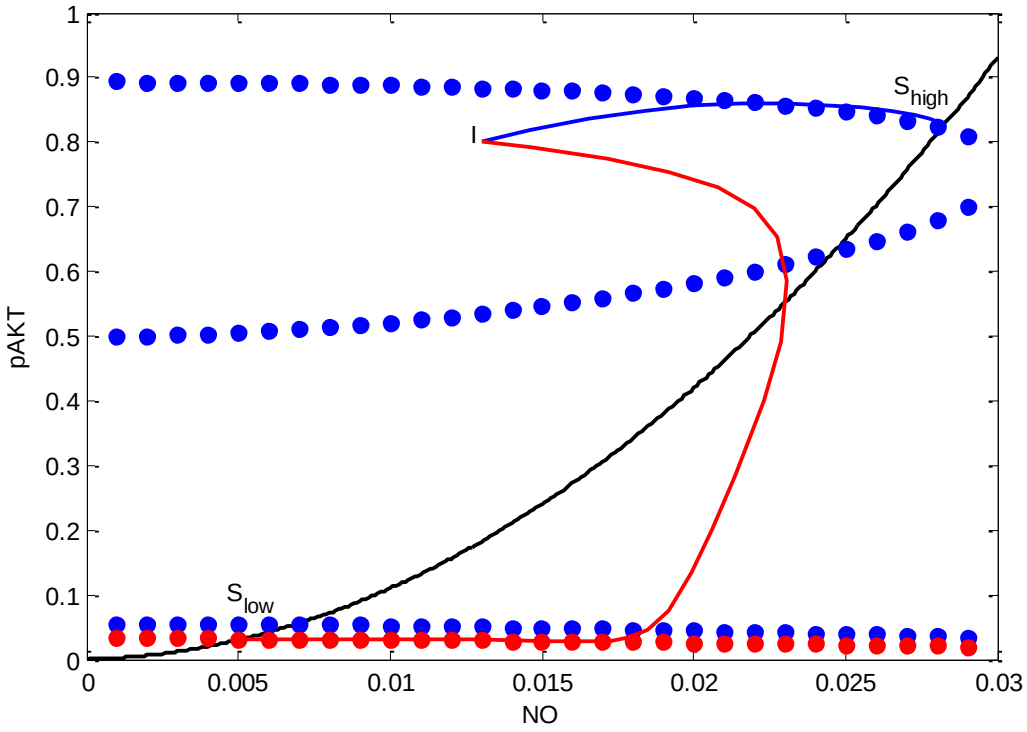


Figure 57. Steady State. Model 4 u(t) = 0.05

Overactivation of Ang II enters Blood Pressure Control System as disturbance through two ways as show in Figure 58 which summarizes the method employed to simulate the blood pressure control system. The change in the extracellular fluid volume (EFV) is sensed and longterm blood pressure and aldosterone controllers act to bring EFV back to its normal value. Longterm blood pressure controller changes the pressure following the events of renal-body fluid mechanism. Blood Pressure directly affects Glomerular filtration rate (GFR). GFR is controlled by afferent and efferent arterioles. Ang

II and NO may have regulatory as well as disturbance effects on the resistances of afferent and efferent arterioles.

Aldosterone controller manipulates reabsorption and Ang II can increase reabsorption through production of aldosterone. Urinary Volume Output (UO) is modeled as the difference between GFR and reabsorption. EFV is the difference between Urinary Volume Load and Urinary Volume Output.

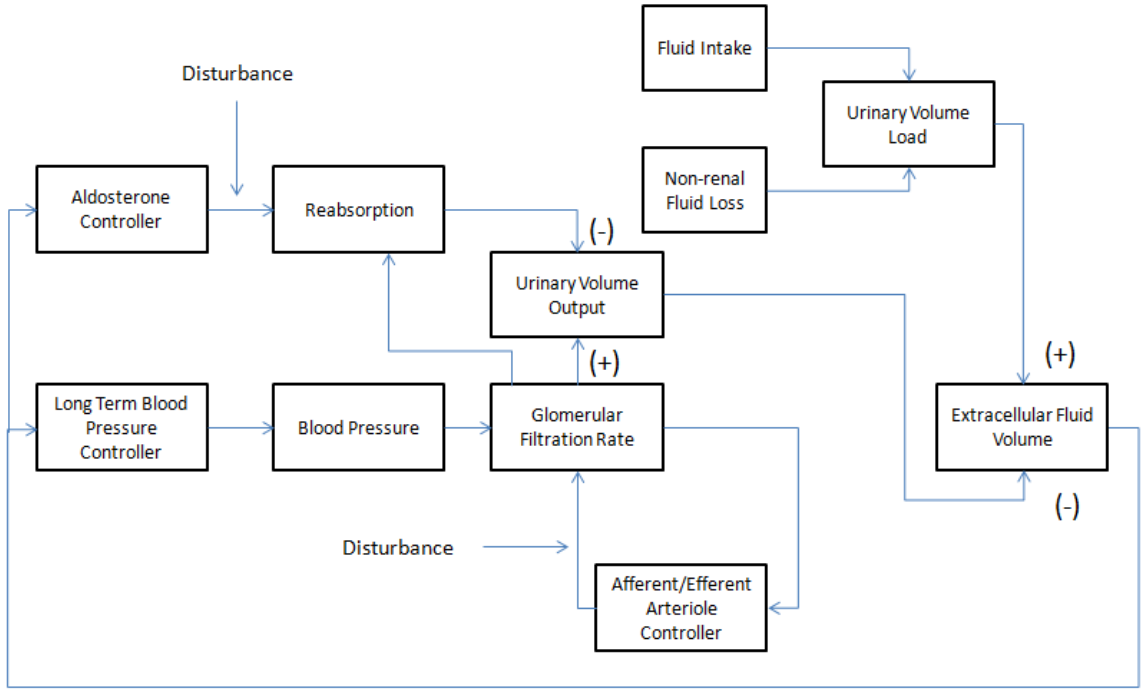


Figure 58. Schematic representation of Simulink Model constracted for Blood Pressure Control System

Renal-body fluid volume feedback mechanism: Normal Response

### BP Model Simulation 1. Fluid Load Step Change Initial:1000 Final:1005

As the fluid load is increased, the normal steady state BP level must change as well. The renal function curve in Figure 3 is very steep, therefore the change in BP is very small.

Extracellular fluid volume is regulated within narrow limits as shown in Figure 60. Urinary Output is increased.

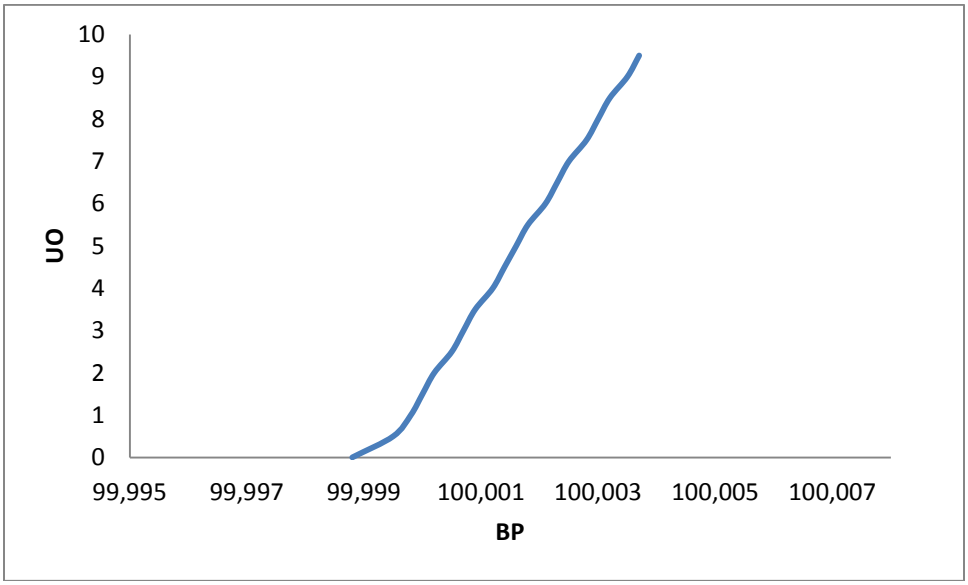


Figure 59. Renal function curve for normal condition obtained from our model. Steady state Blood Pressure Level changes with the volume load change. The change is small due to the high sensitivity of urinary output to blood pressure. The curve is very steep.

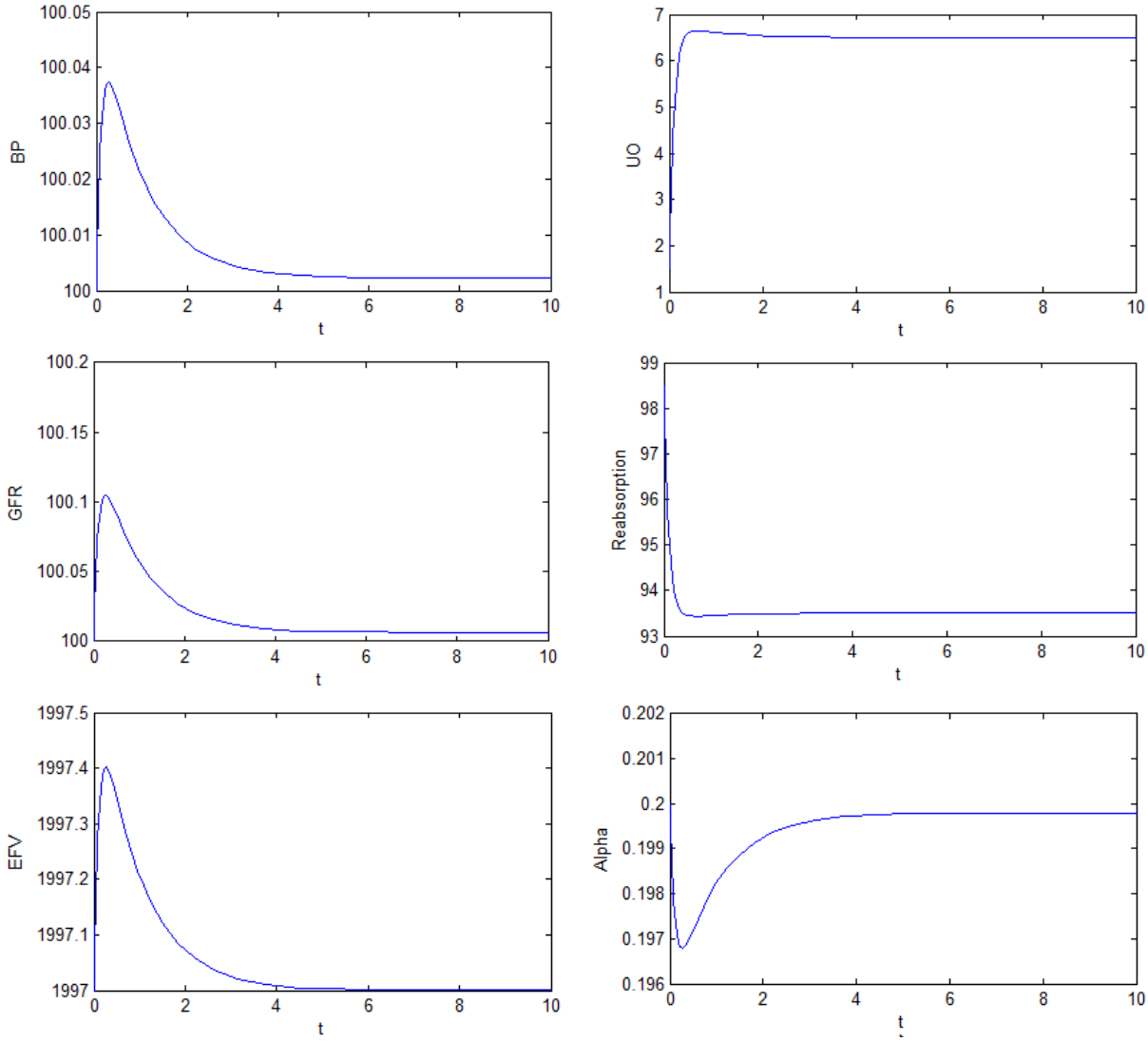

Figure 60. Simulation 1 blood pressure control dynamics

### BP Model Simulation 2. Initial condition for EFV integrator 1/s is set to 1950 (Steady State: 1997)

Initial condition for EFV integrator 1/s is set to 1950. This case may represent a circumstance such as bleeding, loss of blood volume corresponding to an initial decrease in

blood pressure. The negative feedback mechanism act to bring EFV and BP to their normal levels.

As blood pressure decreases initially, GFR decreases as well. GFR is regulated by manipulating efferent and afferent resistances. Efferent arteriole is constriction and afferent arteriole relaxation increases α to bring GFR back to normal. As GFR returns to its normal value so does α.

The system responses to the decrease in pressure by increasing reabsorption. Aldosterone production is increased more fluid is reabsorbed and thus UO is decreased. As EFV reaches its steady state value aldosterone production is decreased.

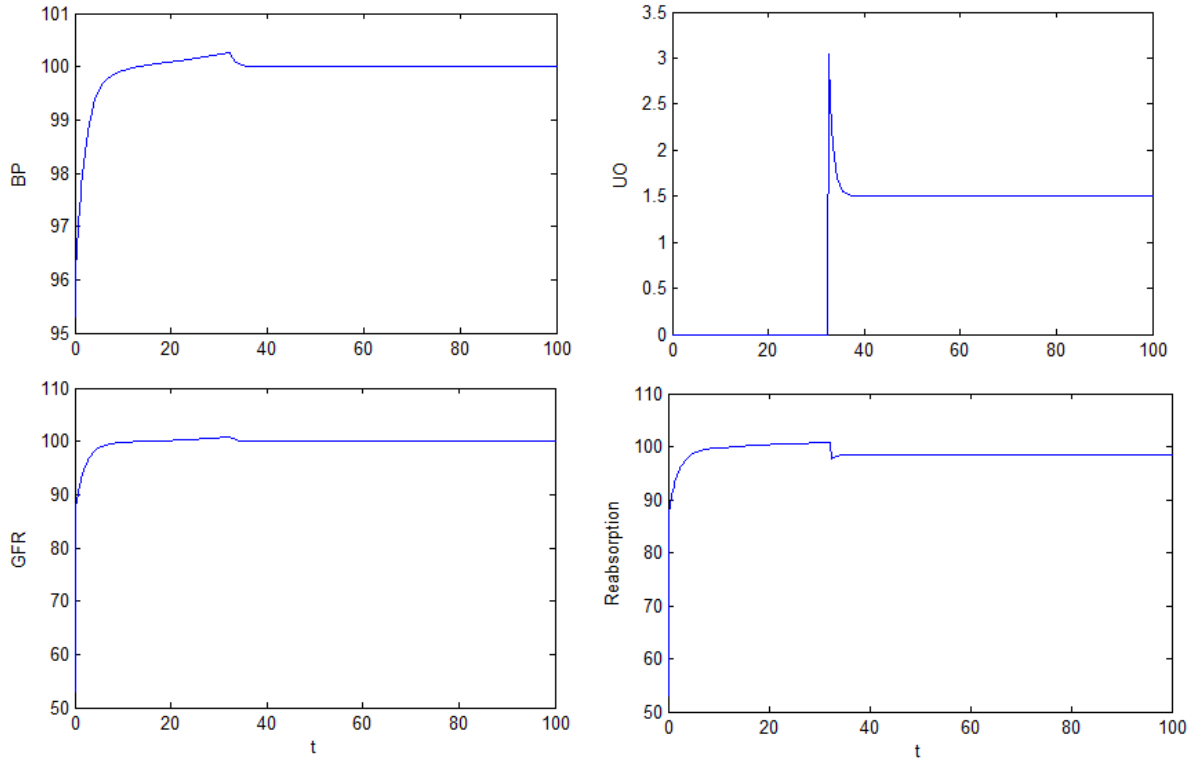

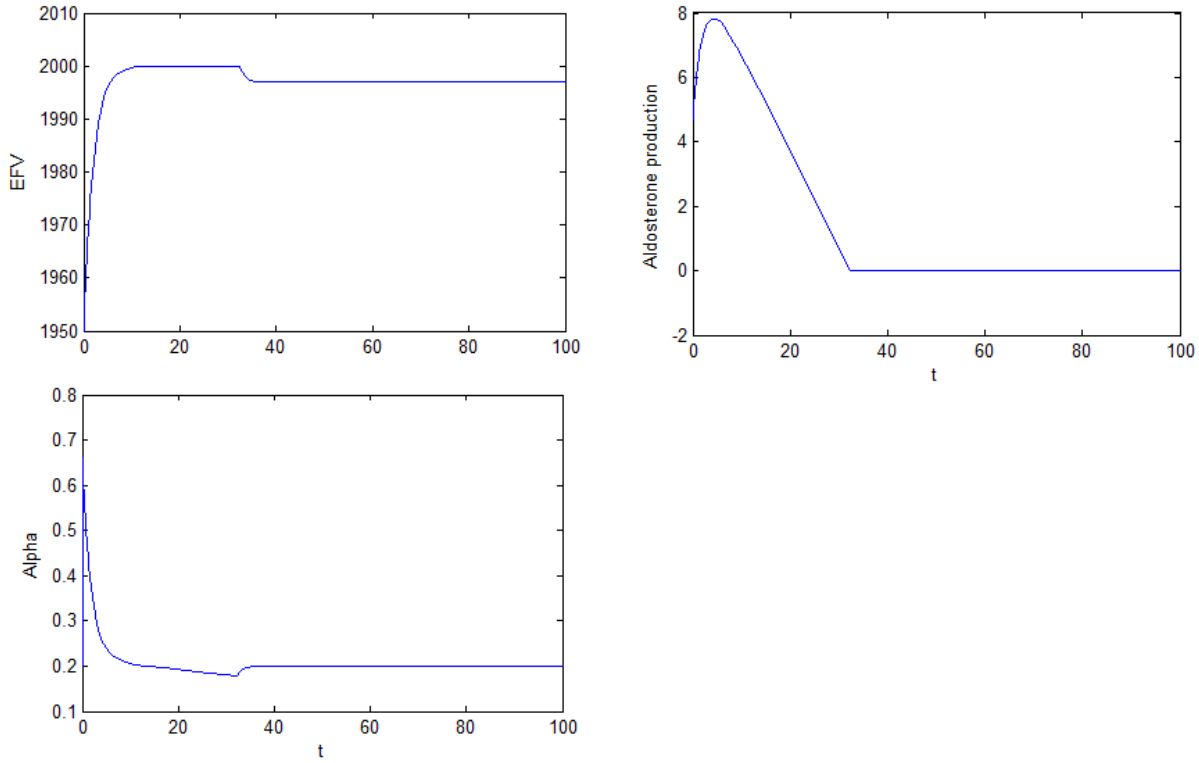

Figure 61. Simulation 2 Blood pressure control dynamics

## BP Model Simulation 3. Abnormal cases

Ang II stimulate aldosterone production and increases reabsorption

When reabsorption is stimulated due to production of aldosterone as a result of overactiovation of Ang II (disturbance represented by u(t) in Model 4) the blood pressure rises to a new setpoint for the same urinary volume output level. EFV is controlled. GFR increase as well, hyperfiltration. So presence of high levels of Ang II induces insulin resistance as shown in Scenario Model4 and causes high blood pressure by stimulating reabsorption.

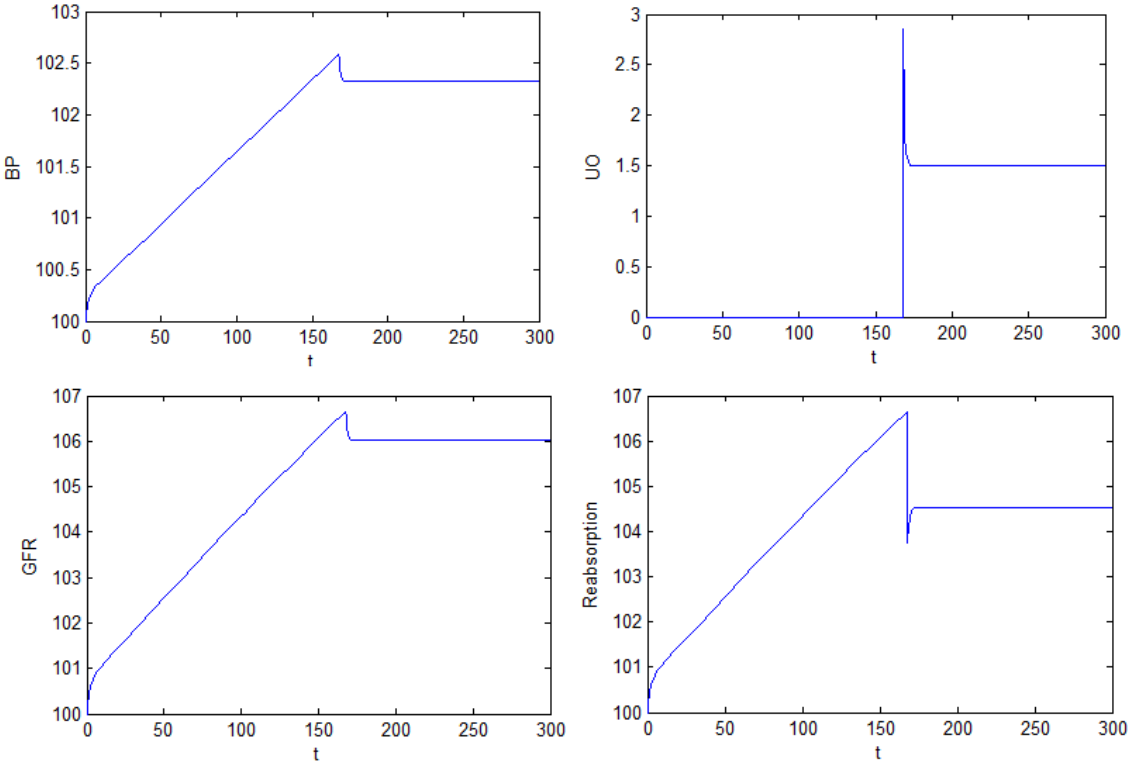
BP
t
UO
t
GFR
t
Reabsorption
t

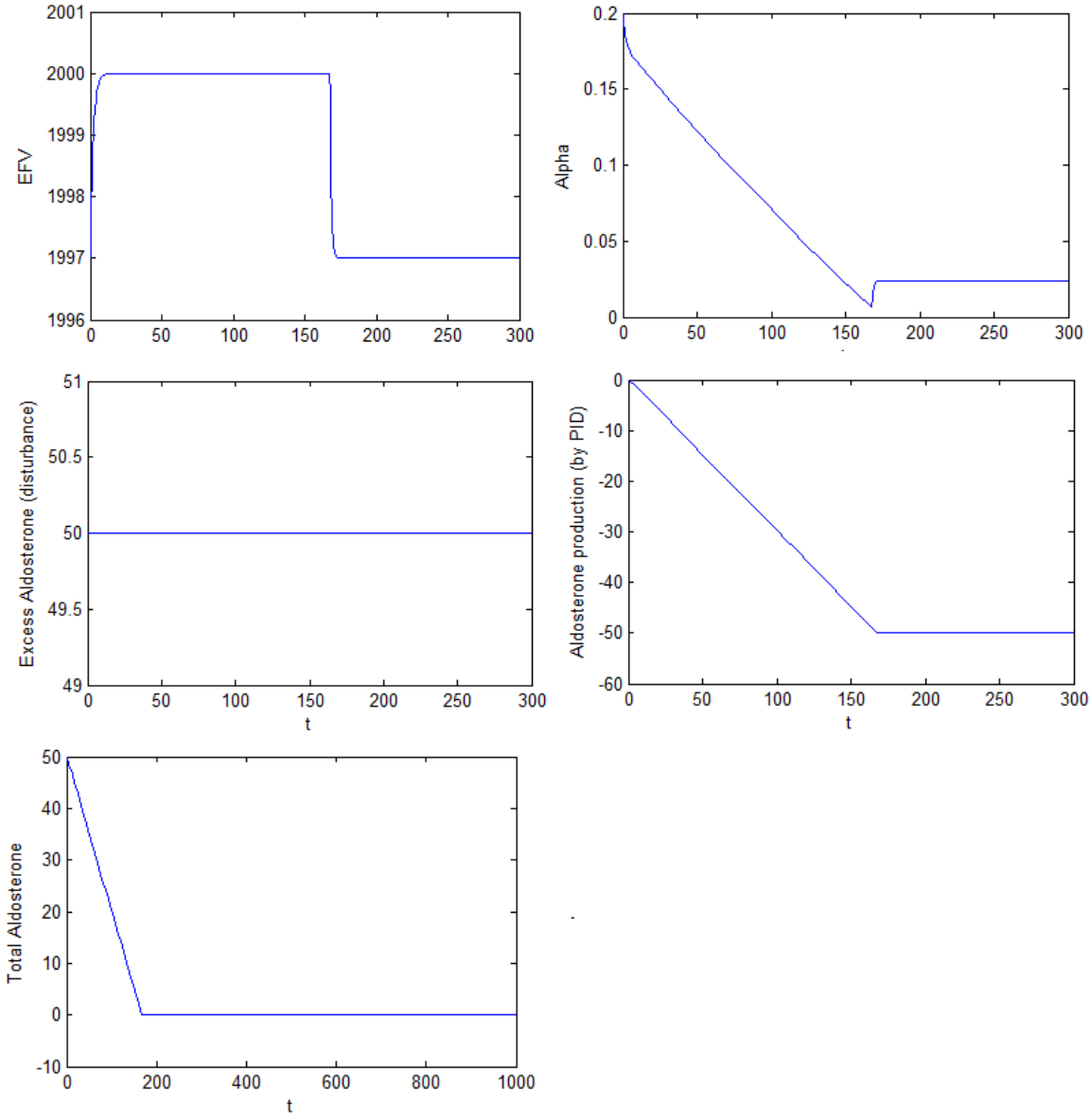

Figure 62. Simulation 2 Blood pressure control dynamics

Ang II overstimulation effect on afferent arteriole

As a normal regulatory role, when GFR is decreased Ang II is produced to constrict efferent arteriole to increase glomerular hydrostatic pressure and GFR. It is important to note that this occurs in situations such as decreased arterial pressure or volume depletion to help prevent the decrease in GFR.

However, angiotensin also constricts the afferent arteriole. This disturbance effect of angiotensin is compensated by NO, a vasodilator agent that reduces blood pressure, as NO relaxes afferent arterioles and increase GFR (hyperfiltration). The effects of ANG II afferent constriction and NO hyperfiltration cancel each other and the total effect to the blood pressure level is not significant.

Constriction of afferent arteriole:

When Ang II is overstimulated and NO is absent, afferent arteriole constriction increases blood pressure.

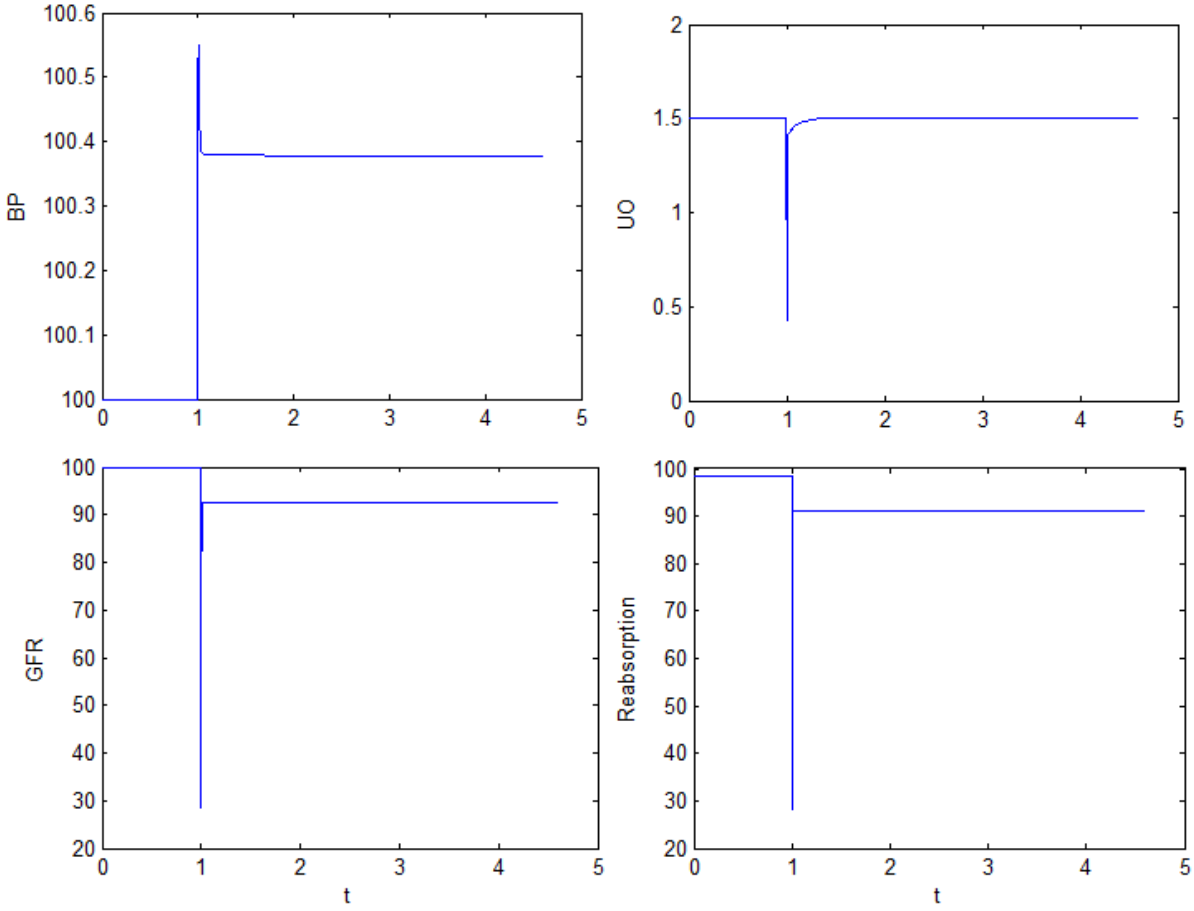
BP
UO
GFR
Reabsorption
t
t

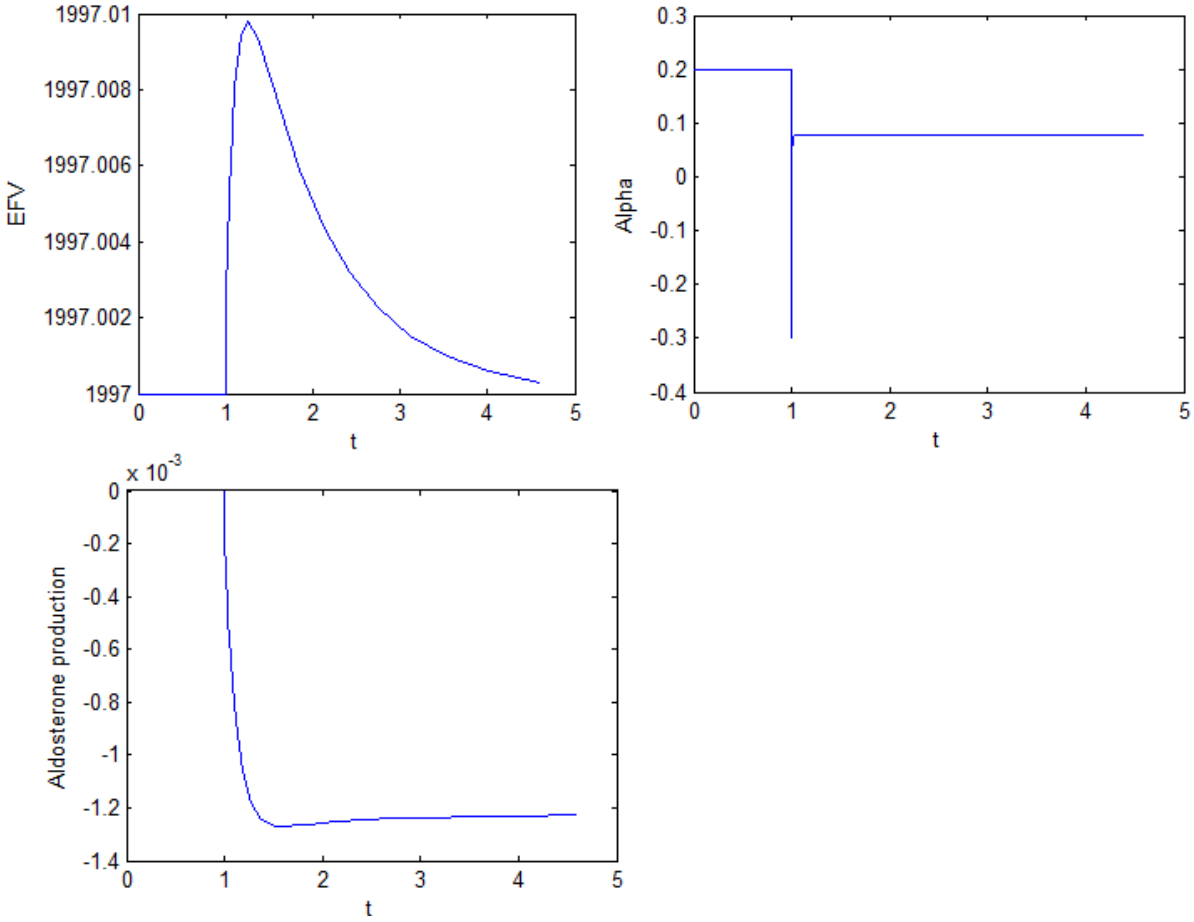

Figure 63. Simulation 4 Blood pressure control dynamics

Relaxation of afferent arteriole:

NO can induce hyperfiltration and reduce blood pressure.

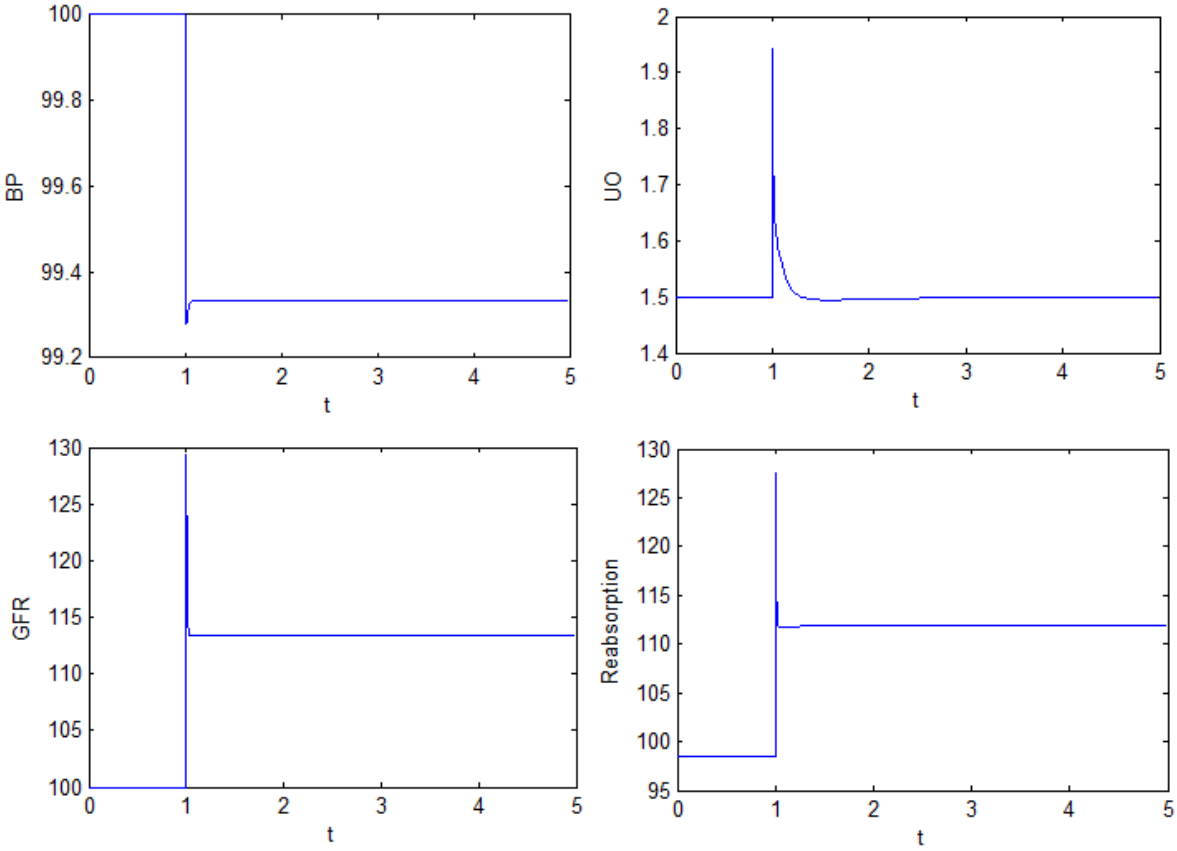
BP
100
99.8
99.6
99.4
99.2
0
1
2
3
4
5
t
UO
2
1.9
1.8
1.7
1.6
1.5
1.4
0
1
2
3
4
5
t
GFR
130
125
120
115
110
105
100
0
1
2
3
4
5
t
Reabsorption
130
125
120
115
110
105
100
95
0
1
2
3
4
5
t

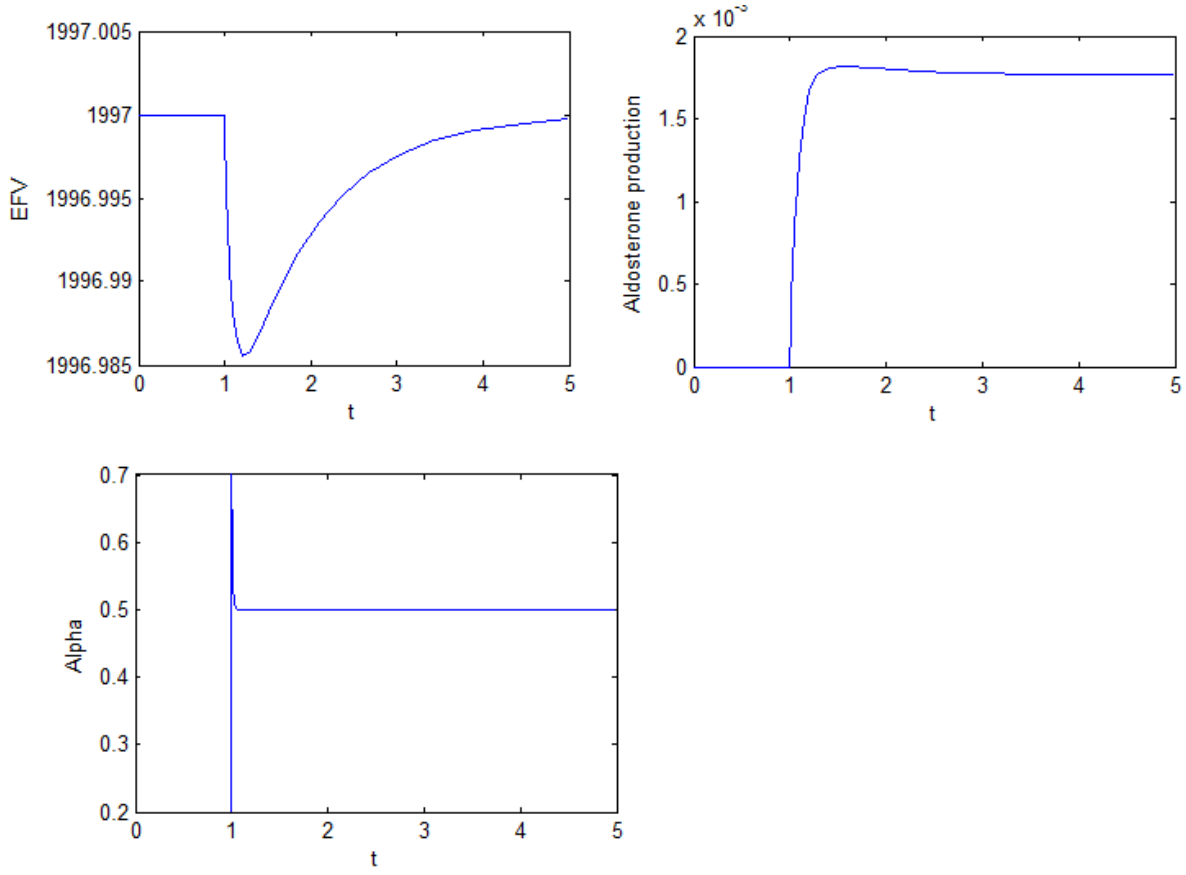


Figure 64. Simulation 5 Blood pressure control dynamics

# Chapter 5

# CONCLUSION

In this thesis, we reviewed available knowledge about regulatory mechanisms of glucose homeostasis, cell proliferation, blood pressure and identified components and their interactions that play significant role in the progression of diseases such as diabetes and hypertension. We proposed mathematical models for the crosstalk of insulin and Ang II signaling pathways. We developed a novel blood pressure regulation model which includes a long term blood pressure controller, an absorption controller, and a glomerular filtration rate controller. Our contribution to existing literature of steady state analysis of insulin signaling pathways, were to couple the system with Ang II signaling and develop dynamic models to show both the steady state and the dynamic behavior of the crosstalk. Furthermore, by combining the crosstalk system with blood pressure model we simulated Ang II effects on blood pressure dynamics and showed the mutual occurrence of insulin resistance and high blood pressure for the first time.

The normal regulatory response of insulin signaling is identified to be bistable so that AKT can switch between low and high levels. It is shown that the interaction parameters in the model, the balance of positive and negative feedback strengths are important in maintaining bistability. pAKT regulates pIRS1 both positively and negatively. For a normal bistable response, the effect of positive feedback should be greater than the negative feedback. When the difference between the feedback strengths is negative, the system loses bistability and a large amount of insulin needs to be supplied to activate pAKT. In severe insulin resistant cases the system settles in low pAKT state and glucose uptake is impaired, thus characterized as diabetes. Ang II and pERK can impair insulin signaling through several mechanisms: by direct inhibition of pAKT by ONOO, by directly

inhibiting pIRS1 or by increasing the negative feedback to pIRS1 via activating mTOR. Ang II and pERK are involved in both physiological and pathological blood pressure and cell proliferation respectively. Systems with over activated Ang II and pERK as a result of a disfunction (e.g diseased kidneys can stimulate Ang II) can induce diabetes through these mechanisms.

pIRS1 activates pERK to mediate cell growth. Activation of pERK by IRS1 is required for a normal regulatory mechanism to carry out insulin induced cell survival or differentiation mechanisms, but in turn pERK has inhibitory actions on pIRS1. Activation of pERK by pIRS1 and inhibition of pERK by pIRS1 forms a negative feedback loop. Insulin also mediates vasodilation by stimulating NO production. NO in turn activates Ang II and Ang II inhibits pIRS1 as explained earlier. The events following stimulation of NO by pIRS1, activation of Ang II by NO and inhibition of pIRS1 by Ang II forms a negative feedback loop. We also found that pERK and NO has also bistable characteristics and switches in the system like pAKT.

On the other hand, when pAKT is over activated (e.g. through enhanced activation of pAKT by pIRS1), uncontrolled cell proliferation appears and the persistent high pAKT level is characterized as cancer. In a cancer state, therapeutic actions to decrease pAKT can be taken. Here we suggest that inhibitory actions of Ang II and pERK on insulin signaling can drive a normal system to diabetes but if the system is in cancer state these actions may be beneficial as they decrease pAKT.

A positive feedback loop with double negative interaction is identified as pIRS1 activates pAKT; pAKT inhibits pERK and in turn pERK inhibits pIRS1. We conclude that pAKT may recover the inhibitory actions of pERK on pIRS1 by inhibiting pERK.

Activation of pAKT is also significant for vasodilator actions of insulin as pAKT stimulates NO production. When insulin signaling is impaired, vasodilation is impaired as well. To maintain blood pressure within narrow limits NO and Ang II should be balanced.

NO activates Ang II and Ang II leads to consumption of NO to produce ONOO. ONOO and Ang II in turn impair insulin signaling and lead to further decrease in NO. The effects should be balanced to keep NO and Ang II at desired levels to maintain blood pressure.

Hyperglycemia is a consequence of diabetes. High blood sugar enhances Ang II activation. Over stimulated Ang II causes high blood pressure and leads to hypertension through increasing reabsorption, through having disturbance effect on the afferent and efferent control of GFR.

Investigating the regulatory and diseased mechanism at system level provides a valuable understanding of complex interacting pathways. A fine balance of interactions between the signaling agents should be maintained to avoid diseases. As there are redundant mechanisms that can induce diabetes, hypertension or cancer, multiple targeting should be aimed as therapeutic strategies.

# APPENDIX A

Nutrient availability is sensed and regulatory signals are transmitted through mTOR complex. Akt activates mTor (mammalian Target of Rapamycin) by phosphorylating the tuberous sclerosis complex (TSC), heterodimer of hamartin (TSC1) and tuberin (TSC2). The TSC1/2 complex controls the balance between two forms of a small GTPase called Rheb. Rheb-GDP is the inactive form whereas Rheb-GTP directly activates mTor. AKT-dependent phosphorylation of TSC2 inactivates the TSC complex and thus the conversion to the inactive Rheb-GDP form is inhibited (Nayak et al., 2011). ERK phosphorylates a distinct site on TSC2 leading to a greater inhibition of Rheb-GDP (Winter et al., 2011). In Winter the two effects are linearly additive. We have also considered a multiplicative effect which could be due to interdependent pAKT-PERK phosphorilation of TSC complex. Ang II also promotes activation of mTOR (Pulakat et al., 2011).

Since active Rheb-GTP form is favored, mTOR becomes activated as illustrated in Figure 65. Reactions for this activation process are listed in Table 22. Inactivated form of mTOR is defined as TOR and since the mechanism for the activation by ANG II is unknown, it is assumed that nutrients and ANG II promote the association of R-GTP with TOR. Differential equation model is given in Table 23. mTOR mediated feedback is incorporated in Model 1 equations as a function of pAKT and the level of nutrients. In expanded models

ANG II and pERK activations are also added and these are justified with the derivation given in Table 24.

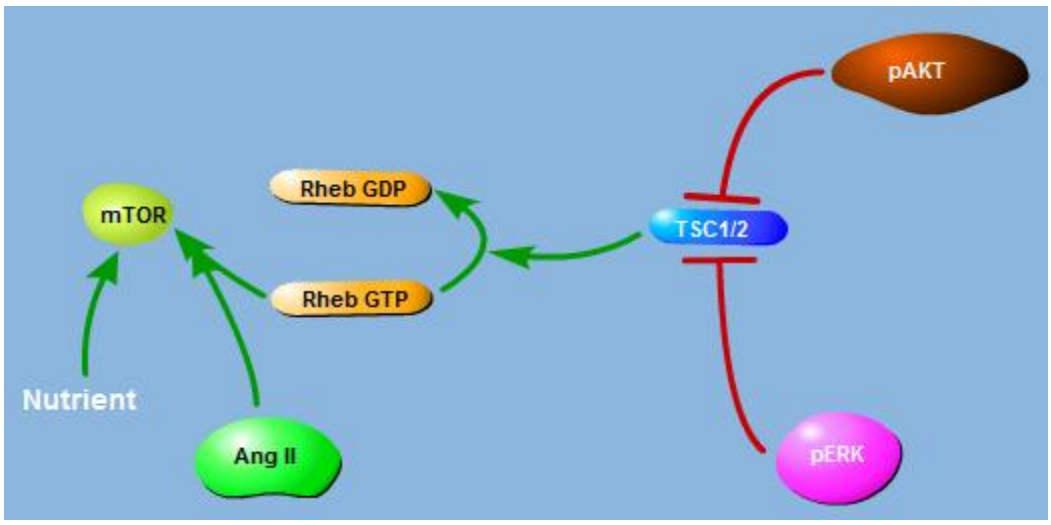


Figure 65. Activation of mTOR

Table 22. mTOR activation reactions.

| Activation of mTOR by pAKT. Adapted from (Nayak et al., 2011) | |
|---|---|
| $TSC1 + TSC2 \underset{k_1}{\overset{k_{-1}}{\leftrightarrows}} TSC1\text{-}TSC2$ | (r_A.1) |
| $Rheb + GDP \underset{k_2}{\overset{k_{-2}}{\leftrightarrows}} R\text{-}GDP$ | (r_A.2) |
| $Rheb + GTP \underset{k_3}{\overset{k_{-3}}{\leftrightarrows}} R\text{-}GTP$ | (r_A.3) |
| $TSC1\text{-}TSC2 + pAKT \underset{k_4}{\overset{k_{-4}}{\leftrightarrows}} TSC1\text{-}TSC2\text{-}pAKT$ | (r_A.4) |
| $TSC1\text{-}TSC2\text{-}pAKT \xrightarrow{k_5} TSC1\text{-}TSC2\text{-}P + pAKT$ | (r_A.5) |
| $R\text{-}GTP + TSC1\text{-}TSC2 \underset{k_6}{\overset{k_{-6}}{\leftrightarrows}} R\text{-}GTP\text{-}TSC1\text{-}TSC2$ | (r_A.6) |
| $R\text{-}GTP\text{-}TSC1\text{-}TSC2 \underset{k_7}{\overset{k_{-7}}{\leftrightarrows}} R\text{-}GDP + TSC1\text{-}TSC2$ | (r_A.7) |
| $R\text{-}GTP + TOR \underset{k_8}{\overset{k_{-8}}{\leftrightarrows}} R\text{-}GTP\text{-}TOR$ | (r_A.8) |
| $R\text{-}GTP\text{-}TOR \xrightarrow{k_9} R\text{-}GTP + mTOR$ | (r_A.9) |
| $mTOR \xrightarrow{k_{10}} TOR$ | (r_A.10) |

| Nutrient level and Angiotensin II affects r_A.8 |
|---|
| $\text{R-GTP} + \text{TOR} \underset{\Psi,ang}{\overset{k_{-8}}{\underset{k_8}{\leftrightarrows}}} \text{R-GTP-TOR}$ (modified r_A.8) |
| pERK phosphorylates TSC1/2 complex (parallel with TSC1/2 complex phosphorylation by pAKT) |
| $\text{TSC1-TSC2} + \text{pERK} \overset{k_{-11}}{\underset{k_{11}}{\leftrightarrows}} \text{TSC1-TSC2-pERK}$ (r_A.11)<br>$\text{TSC1-TSC2-pERK} \overset{k_{12}}{\rightarrow} \text{TSC1-TSC2-P} + \text{pERK}$ (r_A.12) |
| pERK and pAKT interdependentlyphosphorylateTSC1/2 complex |
| $\text{TSC1-TSC2} + \text{pAKT} + \text{pERK} \overset{k_{-13}}{\underset{k_{13}}{\leftrightarrows}} \text{TSC1-TSC2-pAKT-pERK}$ (r_A.13)<br>$\text{TSC1-TSC2-pAKT-pERK} \overset{k_{14}}{\rightarrow} \text{TSC1-TSC2-P} + \text{pAKT} + \text{pERK}$ (r_A.14) |

Table 23. Differential Equations for Modeling mTOR activation (pAKT and pERK activation parallel)

$$\frac{d[mTOR]}{dt} = -k_{10}\,[mTOR] + k_9\,[R-GTP-TOR] \quad \text{(A.1)}$$

$$\frac{d[R-GTP-TOR]}{dt} = k_8\,[R-GTP][TOR]\Psi(1+\,(ANG)) - \,(k_{-8}+k_9)[R-GTP-TOR] \quad \text{(A.2)}$$

$$\frac{d[R-GTP]}{dt} = k_3[Rheb][GTP] - k_{-3}[R-GTP] - k_6[R-GTP][TSC1-TSC2] + k_{-6}[R-GTP-TSC1-TSC2] + \,(k_{-8}+k_9)[R-GTP-TOR]\, - k_8[R-GTP][TOR]\,\Psi\,(1+\,(ANG)) \quad \text{(A.3)}$$

$$\frac{d[R-GTP-TSC1-TSC2]}{dt} = k_6[R-GTP][TSC1-TSC2] - (k_{-6}+k_7)[R-GTP-TSC1-TSC2] + k_{-7}[R-GDP][TSC1-TSC2] \quad \text{(A.4)}$$

$$\frac{d[TSC1-TSC2]}{dt} = k_1[TSC1][TSC2] - k_{-1}[TSC1-TSC2] - k_4[TSC1-TSC2][pAKT] + k_{-4}[TSC1-TSC2-pAKT] - k\ [TSC1-TSC2][pERK] + k_{-11}[TSC1-TSC2-pERK] + (k_7+k_{-6})[R-GTP-TSC1-TSC2] - k_6[R-GTP][TSC1-TSC2] - k_{-7}[R-GDP][TSC1-TSC2] \quad \text{(A.5)}$$

$$\frac{d[R-GDP]}{dt} = k_2[Rheb][GTP] - k_{-2}[R-GDP] + k_7[R-GTP-TSC1-TSC2] - k_{-7}[R-GDP][TSC1-TSC2] \quad \text{(A.6)}$$

$$\frac{d[TSC1-TSC2-pAKT]}{dt} = k_4[\text{TSC1}-\text{TSC2}][\text{pAKT}] - (\text{k}_{-4}+\text{k}_5)\,[TSC1-TSC2-pAKT] \quad \text{(A.7)}$$

$$\frac{d[TSC1-TSC2-pERK]}{dt} = k_{11}[\text{TSC1}-\text{TSC2}][\text{pERK}] - (\text{k}_{-11}+\text{k}_{12})\,[TSC1-TSC2-pERK] \quad \text{(A.8)}$$

Table 24. Derivation of mTOR activation

From A.2 at steady-state

$$[R-GTP-TOR] = \frac{k_8}{k\_8+k9}[R-GTP][TOR]\Psi\,(1+(ANG)) \quad \text{(A.9)}$$

From A.4

$$[R-GTP-TSC1-TSC2] = k_6/(k_{-6}+k_7)\,[R-GTP][TSC1-TSC2] + k_{-7}/(k_{-6}+k_7)\,[R-GDP][TSC1-TSC2] \quad \text{(A.10)}$$

From A.7

$$[TSC1-TSC2-pAKT] = \frac{k_4}{\text{k}_{-4}+\text{k}_5}\ [\text{TSC1-TSC2}][\text{pAKT}] \quad \text{(A.11)}$$

From A.8

$$[TSC1-TSC2-pERK] = k_{11}/(\text{k}_{-11}+\text{k}_{12})[\text{TSC1}-\text{TSC2}][\text{pERK}] \quad \text{(A.12)}$$

Insert A.11, A.12, A.10 into A.5

$$\frac{d[TSC1-TSC2]}{dt} = k_1[TSC1][TSC2] - k_{-1}[TSC1-TSC2] - k_4[TSC1-TSC2][pAKT] + k_{-4}\left(\frac{k_4}{\mathrm{k}_{-4}+\mathrm{k}_5}\,[\mathrm{TSC1-TSC2}][\mathrm{pAKT}]\right) - k\ \ [TSC1-TSC2][pERK] + k_{-11}\left(\frac{k_{11}}{\mathrm{k}_{-11}+\mathrm{k}_{12}}[\mathrm{TSC1-TSC2}][\mathrm{pERK}]\right) + (k_7+k_{-6})\left(\frac{k_6}{k_{-6}+k_7}\,[R-GTP][TSC1-TSC2] + \frac{k_{-7}}{(k_{-6}+k_7)}[R-GDP][TSC1-TSC2]\right) - k_6[R-GTP][TSC1-TSC2] - k_{-7}[R-GDP][TSC1-TSC2]$$

$$\frac{d[TSC1-TSC2]}{dt} = k_1[TSC1][TSC2] - k_{-1}[TSC1-TSC2] - k_4[TSC1-TSC2][pAKT] + k_{-4}\left(\frac{k_4}{\mathrm{k}_{-4}+\mathrm{k}_5}\,[\mathrm{TSC1-TSC2}][\mathrm{pAKT}]\right) - k\ \ [TSC1-TSC2][pERK] + k_{-11}\left(\frac{k_{11}}{\mathrm{k}_{-11}+\mathrm{k}_{12}}[\mathrm{TSC1-TSC2}][\mathrm{pERK}]\right) + (k_6[R-GTP][TSC1-TSC2] + k_{-7}[R-GDP][TSC1-TSC2]) - k_6[R-GTP][TSC1-TSC2] - k_{-7}[R-GDP][TSC1-TSC2]$$

$$\frac{d[TSC1-TSC2]}{dt} = k_1[TSC1][TSC2] - k_{-1}[TSC1-TSC2] - \left(\frac{k_4\mathrm{k}_5}{\mathrm{k}_{-4}+\mathrm{k}_5}\,[\mathrm{TSC1-TSC2}][\mathrm{pAKT}]\right) - \left(\frac{k_{11}k_{12}}{\mathrm{k}_{-11}+\mathrm{k}_{12}}[\mathrm{TSC1-TSC2}][\mathrm{pERK}]\right)$$

$$[TSC1-TSC2] = \frac{k_1[TSC1][TSC2]}{k_{-1} + \left(\frac{k_4\mathrm{k}_5}{\mathrm{k}_{-4}+\mathrm{k}_5}\,[\mathrm{pAKT}]\right) + \left(\frac{k_{11}k_{12}}{\mathrm{k}_{-11}+\mathrm{k}_{12}}[\mathrm{pERK}]\right)} \quad \text{(A.13)}$$

[pAKT] and [pERK] posphorylate $[TSC1-TSC2]$, thus $[TSC1-TSC2-P]$ forms. Therefore as [pAKT] and [pERK] are increased $[TSC1-TSC2]$ is decreased.

A.10 Into A.6

$$\frac{d[R-GDP]}{dt} = k_2[Rheb][GTP] - k_{-2}[R-GDP] + k_7\left[ k_6/(k_{-6}+k_7)\,[R-GTP][TSC1-TSC2] + k_{-7}/(k_{-6}+k_7)\,[R-GDP][TSC1-TSC2]\right] - k_{-7}[R-GDP][TSC1-TSC2]$$

$$[R-GDP] = \frac{k_2[Rheb][GTP] + \frac{k_7 k_6}{k_{-6}+k_7}[R-GTP][TSC1-TSC2]}{k_{-2} + \frac{k_{-7}k_{-6}}{k_{-6}+k_7}[TSC1-TSC2]} \quad \text{(A.14)}$$

A.9, A.10, A.14 Into A.3

$$\frac{d[R-GTP]}{dt} = k_3[Rheb][GTP] - k_{-3}[R-GTP] - k_6[R-GTP][TSC1-TSC2] + k_{-6}[R-GTP-TSC1-TSC2] + (k_{-8}+k_9)[R-GTP-TOR] - k_8[R-GTP][TOR]\,\Psi\,(1+(ANG))$$

$$[R-GTP] = \frac{k_{-2}k_3[Rheb][GTP] + \frac{k_3k_{-6}k_{-7} + k_2k_{-7}k_{-6}}{k_{-6}+k_7}[Rheb][GTP][TSC1-TSC2]}{k_{-2}k_{-3} + \frac{k_{-2}k_6k_7 + k_{-3}k_{-7}k_{-6}}{k_{-6}+k_7}[TSC1-TSC2]} \quad \text{(A.15)}$$

k = $[Rheb][GTP]$

a $= k_{-2}k_3$

b $= \frac{k_3k_{-6}k_{-7} + k_2k_{-7}k_{-6}}{k_{-6}+k_7}$

c $= k_{-2}k_{-3}$

d $= \frac{k_{-2}k_6k_7 + k_{-3}k_{-7}k_{-6}}{k_{-6}+k_7}$

$$[R-GTP] = k\frac{a + b[TSC1-TSC2]}{c + d\,[TSC1-TSC2]}$$

Taking the derivative

$$\frac{d[R-GTP]}{d[TSC1-TSC2]} = k\frac{bc-ad}{(c+d[TSC1-TSC2])^2}$$

$$(bc-ad) = \frac{k_{-2}(k_{-7}k_{-6}k_{-3}k_2 - k_{-2}k_3k_6k_7)}{k_{-6}+k_7}$$

(bc-ad) is negative if $k_{-7}k_{-6}k_{-3}k_2 < k_{-2}k_3k_6k_7$.

$k_7$ is the rate constant for the formation of the products $[R-GDP]\ and\ [TSC1-TSC2]\ from\ the\ [R-GTP-TSC1-TSC2]$ complex. $k_{-7}$ is the rate constant for the formation of the complex from these products. The complex is an intermediate and therefore the product formation reaction is much faster $k_7 \gg k_{-7}$ .

Reactions related to the formation of R-GDP and R-GTP, $k_{-2} < k_2$ and $k_{-3} < k_3$. But the two reactions are very similar and their rate constants are close. Therefore the following assumption is made $k_{-3}k_2 \cong k_{-2}k_3$.

$k_6$ is the rate constant for the formation of the $[R-GTP-TSC1-TSC2]$ complex from the reactants $[R-GTP]\ and\ [TSC1-TSC2]$ and $k_{-6}$ is the rate of the reverse reaction. The forward and the reverse reaction rates are on the same order. Therefore the following assumption is made $k_{-6} \cong k_6$.

With these assumptions, the term ( $k_{-7}k_{-6}k_{-3}k_2 < k_{-2}k_3k_6k_7$ ) simplifies to $k_{-7} < k_7$. And this holds according to the previous explanation.

$\frac{d[R-GTP]}{d[TSC1-TSC2]}$ is negative since (bc-ad) is negative. This is consistent with the explanation that TSC1/2 complex controls the balance between R-GTP and R-GDP. As the concentration of TSC1/2 complex increases the inactive form of Rheb protein, R-GDP, is formed and the concentration of R-GTP decreases.

$$[R-GTP] = k\frac{e + f\,[aAkt] + i\,[pERK]}{g + h\,[aAkt] + j\,[pERK]} \quad \text{(A.16)}$$

where

$$\mathrm{e} = k_{-_2}k_3k_{-1} + \frac{k_3k_{-6}k_{-7}\mathrm{k}_1 + \mathrm{k}_1\,k_2k_{-7}k_{-6}}{k_{-6} + k_7}\,[\mathrm{TSC1}][\mathrm{TSC2}]$$

$$\mathrm{f} = \frac{k_4k_5\,k_{-_2}k_3}{k_{\_-4} + k_5}$$

$$\mathrm{g} = k_{-2}k_{-_3}k_{-1} + \frac{k_{-2}k_6k_7k_1 + k_1k_{-3}k_{-7}k_{-6}}{k_{-6} + k_7}\,[\mathrm{TSC1}][\mathrm{TSC2}]$$

$$\mathrm{h} = \frac{k_4k_5k_{-2}k_{-_3}}{k_{\_-4} + k_5}$$

$$i = \frac{k_{11}k_{12}\;k_{-_2}k_3}{k_{\_-11} + k_{12}}$$

$$j = \frac{k_{11}k_{12}k_{-2}k_{-_3}}{k_{\_-11} + k_{12}}$$

$A.1\ and\ A.9$

$$[mTOR] = \frac{k_9}{k_{10}}\,(\frac{k_8}{k_{-8} + k9})[R-GTP][TOR]\Psi\,(1 + \,(ANG)) \quad \text{(A.17)}$$

(A.16) into (A.17)

$$[mTOR] = \,k_n\Psi\,(1 + \,(ANG))[TOR]\,\frac{e + f\,[pAKT] + i\,[pERK]}{g + h\,[pAKT] + j\,[pERK]} \quad \text{(A.18)}$$

$$\frac{d[mTOR]}{d[pAKT]} = k_n\Psi\,\big(1 + \,(ANG)\big)[TOR]\,\frac{(fg - eh) + (fj - hi)[pERK]}{(g + h\,[pAKT] + j\,[pERK])^2} \quad \text{(A.19)}$$

$$= k_n\Psi\,\big(1 + \,(ANG)\big)[TOR]\,\alpha_1$$

$$\frac{d[mTOR]}{d[pERK]} = k_n\Psi\,(1 + \,(ANG))[TOR]\,\frac{(i\,g - j\,e) + (h\,i\,\, - j\,f)[pAKT]}{(g + h\,[pAKT] + j\,[pERK])^2} \quad \text{(A.20)}$$

$$= k_n\Psi\,\big(1 + \,(ANG)\big)[TOR]\alpha_2$$

$$(fg - eh) = \frac{(k_{-2}k_1\,k_4k_5\,)(k_{-_2}k_3k_7k_6 - k_2k_{-7}k_{-6}k_{-_3})}{(k_{-6} + k_7)(k_{-4} + k_5)}$$

$$(fj - hi) = \frac{k_4 k_5 k_{-_2} k_3}{k_{-4} + k_5} \frac{k_{11} k_{12} k_{-2} k_{-_3}}{k_{-11} + k_{12}} - \frac{k_4 k_5 k_{-2} k_{-_3}}{k_{-4} + k_5} \frac{k_{11} k_{12}\ k_{-_2} k_3}{k_{-11} + k_{12}} = 0$$

$$(i\ g - j\ e) = \frac{(k_{-2} k_1\ k_{11} k_{12})(k_{-_2} k_3 k_7 k_6 - k_2 k_{-7} k_{-6} k_{-_3})}{(k_{-6} + k_7)(k_{-11} + k_{12})}$$

$$(h\ i\ - j\ f) = 0$$

$\alpha_1$ and $\alpha_2$ are positive since (fg – eh) and (ig-je) are positive. Therefore

$\frac{d[mTOR]}{d[pAKT]}$ *and* $\frac{d[mTOR]}{d[pERK]}$ are positive as well . This is consistent with the known fact that pAkt and pERK positively regulate, activate mTOR. Thus A.18 can be approximated by and expressed in linear form:

$$\begin{aligned}[mTOR] &= k_n \Psi(1 + k_7(ANG))[TOR]\alpha_1[pAKT] + \\ &\quad k_n \Psi(1 + k_7(ANG))[TOR]\alpha_2[pERK] \\ &= \varepsilon\Psi(1 + k_7(ANG))[pAKT] + \varepsilon\ \Psi(1 + k_7(ANG))k_{e-19}[pERK]\end{aligned} \qquad \text{A.21}$$

Equation (A.21) tells that mTOR mediated inhibition can become effective when pAKT or pERK gets activated. Their effects are additive and depend on the level of nutrients. When ANG is present both of these effects are enhanced.

The negative feedback term in Equation (16) is justified with (A.21) for [pERK] = 0, which is true for Model 2.

If the effects of pAKT and pERK on TSC1/2 complex are assumed to be multiplicative then equation (A.5) should be written as:

$$\frac{d[TSC1-TSC2]}{dt} = k_1[TSC1][TSC2] - k_{-1}[TSC1-TSC2] - k_{13}[TSC1-TSC2][pAKT][pERK] + k_{-13}[TSC1-TSC2 - pAKT-pERK] + (k_7+k_{-6})[R-GTP-TSC1-TSC2] - k_6[R-GTP][TSC1-TSC2] - k_{-7}[R-GDP][TSC1-TSC2] \quad \text{(A.22)}$$

$$\frac{d[TSC1-TSC2-pAKT-pERK]}{dt} = k_{13}[\mathrm{TSC1-TSC2}][\mathrm{pAKT}][\mathrm{pERK}] - (k_{-13}+k_{14})\,[TSC1-TSC2-pAKT-pERK] \quad \text{(A.23)}$$

When mTOR activation is derived based on (r_A.13) and (r_A.14), (A.24) is obtained.

| | |
|---|---|
| $[mTOR] = k_n\Psi\,(1 + k_7(ANG))[TOR]\,\frac{l + m\,[pAKT]\,[pERK]}{n + o\,[pAKT]\,[pERK]}$ | (A.24) |
| And [mTOR] given by A.18 can be approximated by | |
| $[mTOR] = (\varepsilon + \varepsilon\,k_7(ANG))\Psi\,[pAKT][pERK]$ | (A.25) |

$$[mTOR] = k_n\Psi(1+k_7(ANG))[TOR]\alpha_3[pAKT][pERK]$$
$$= \varepsilon_M\Psi(1+k_7(ANG))[pAKT]k_{e-19}[pERK]$$

From (A.25) Equation (25) can be corrected as:

$$\frac{dx_5}{dt} = \frac{\delta}{\beta}\left(\frac{k2}{k1}\right)E_{2T}\lambda(t) + (\Phi - \varepsilon\Psi(1+\mathrm{k_7\,x_7})\,\mathrm{k_{e\_19}x_{10}})(1-x_1) - k_{e\_13}\,x_{10} - k_{e\_18}\,x_7 - \delta_I x_5$$

## APPENDIX B

Table 25. Mathematical representation of Model 1

| | |
|---|---|
| Differential equations describing the Michaelis Menten Kinetics of the PdPC: | |
| $\frac{d[AKT]}{dt} = -a_1[AKT][E_1] + d_1[AKT{:}E_1] + k_2[pAKT{:}E_2]$ | (B.1) |
| $\frac{d[AKT{:}E_1]}{dt} = a_1[AKT][E_1] - (d_1 + k_1)[AKT{:}E_1]$ | (B.2) |
| $\frac{d[pAKT]}{dt} = -a_2[pAKT][E_2] + d_2[pAKT{:}E_2] + k_1[AKT{:}E_1]$ | (B.3) |
| $\frac{d[pAKT{:}E_2]}{dt} = a_2[pAKT][E_2] - (d_2 + k_2)[pAKT{:}E_2]$ | (B.4) |
| Kinetics of pIRS1, negative and positive feedback: | |
| $\frac{d[pIRS1]}{dt} = \gamma + (\Phi - \varepsilon\,\Psi)[pAKT] - \delta\,[pIRS1]$ | (B.5) |
| Conservation equations: | |
| $X_T = [AKT] + [pAKT]$ | (B.6) |
| $E_{1T} = [E_1] + [AKT{:}E_1]$ | (B.7) |
| $E_{2T} = [E_2] + [pAKT{:}E_2]$ | (B.8) |
| Describing the edge pIRS1→$E_1$ | |
| $E_{1T} = \beta[pIRS1]$ | (B.9) |

Table 26. Derivation of the steady state equation of Model 1

At steady state from equations B.2, B.6, and B.7:

$$\frac{d[AKT:E_1]}{dt} = 0$$

$$[AKT:E_1] = \frac{a_1[AKT][E_1]}{(d_1 + k_1)} = \frac{[AKT][E_1]}{K_{m1}} = \frac{E_{1T}(X_T - [pAKT])}{K_{m1} + X_T - [pAKT]} \quad \text{(B.10)}$$

where $K_{m1} = (d_1 + k_1)/a_1$

From equations B.4 and B.8:

$$\frac{d[pAKT:E_2]}{dt} = 0$$

$$[pAKT:E_2] = \frac{a_2[pAKT][E_2]}{(d_2 + k_2)} = \frac{[pAKT][E_2]}{K_{m2}} = \frac{E_{2T}[pAKT]}{K_{m2} + [pAKT]} \quad \text{(B.11)}$$

where $K_{m2} = (d_2 + k_2)/a_2$

The addition of B.1 and B.2:

$$k_1[AKT:E_1] = k_2[pAKT:E_2] \quad \text{(B.12)}$$

Substituting B.10 and B.11:

$$\frac{k_1E_{1T}(X_T - [pAKT])}{K_{m1} + X_T - [pAKT]} = \frac{k_2E_{2T}[pAKT]}{K_{m2} + [pAKT]} \quad \text{(B.13)}$$

From equations B.5 and B.9:

$$\frac{d[pIRS1]}{dt} = 0$$

$$\gamma + (\Phi - \varepsilon\,\Psi\,)[pAKT] - \frac{\delta}{\beta}\,E_{1T} = 0 \qquad \text{(B.14)}$$

$$E_{1T} = \frac{\beta}{\delta}(\gamma + (\Phi - \varepsilon\,\Psi\,)[pAKT])$$

$$E_{1T} = \frac{\beta}{\delta}\gamma + \frac{\beta}{\delta}(\Phi - \varepsilon\,\Psi\,)[pAKT]$$

Equation B.13 is rearranged:

$$K_{m2}k_1E_{1T}X_T - K_{m2}k_1E_{1T}[pAKT] + k_1E_{1T}X_T[pAKT] - k_1E_{1T}[pAKT]^2 = K_{m1}k_2E_{2T}[pAKT] + X_Tk_2E_{2T}[pAKT] - k_2E_{2T}[pAKT]^2$$

$E_{1T}$ is eliminated using B.14:

$$\frac{\beta}{\delta}\gamma\,K_{m2}k_1X_T - \frac{\beta}{\delta}\gamma\,K_{m2}k_1\,[pAKT] + \frac{\beta}{\delta}\gamma k_1X_T[pAKT] - \frac{\beta}{\delta}\gamma k_1[pAKT]^2 + K_{m2}k_1X_T\frac{\beta}{\delta}(\Phi - \varepsilon\,\Psi\,)[pAKT] - K_{m2}k_1\frac{\beta}{\delta}(\Phi - \varepsilon\,\Psi\,)[pAKT]^2 + k_1X_T\frac{\beta}{\delta}(\Phi - \varepsilon\,\Psi\,)[pAKT]^2 - k_1\frac{\beta}{\delta}(\Phi - \varepsilon\,\Psi\,)[pAKT]^3 = K_{m1}k_2E_{2T}[pAKT] + X_Tk_2E_{2T}[pAKT] - k_2E_{2T}[pAKT]^2$$

$$k_1\frac{\beta}{\delta}(\Phi - \varepsilon\,\Psi\,)[pAKT]^3 - k_2E_{2T}[pAKT]^2 + \frac{\beta}{\delta}\gamma k_1[pAKT]^2 + K_{m2}k_1\frac{\beta}{\delta}(\Phi - \varepsilon\,\Psi\,)[pAKT]^2 - k_1X_T\frac{\beta}{\delta}(\Phi - \varepsilon\,\Psi\,)[pAKT]^2 + K_{m1}k_2E_{2T}[pAKT] + X_Tk_2E_{2T}[pAKT] + \frac{\beta}{\delta}\gamma\,K_{m2}k_1\,[pAKT] - \frac{\beta}{\delta}\gamma k_1X_T[pAKT] - K_{m2}k_1X_T\frac{\beta}{\delta}(\Phi - \varepsilon\,\Psi\,)[pAKT] - \frac{\beta}{\delta}\gamma\,K_{m2}k_1X_T = 0$$

$$k_1\frac{\beta}{\delta}(\Phi-\varepsilon\,\Psi\,)[pAKT]^3+\left(-k_2E_{2T}+\frac{\beta}{\delta}\gamma k_1+K_{m2}k_1\frac{\beta}{\delta}(\Phi-\varepsilon\,\Psi\,)-k_1X_T\frac{\beta}{\delta}(\Phi-\varepsilon\,\Psi\,)\right)[pAKT]^2$$

$$+\ (K_{m1}k_2E_{2T}+X_Tk_2E_{2T}+\frac{\beta}{\delta}\gamma\,K_{m2}k_1\ -\frac{\beta}{\delta}\gamma k_1X_T-K_{m2}k_1X_T\frac{\beta}{\delta}(\Phi-\varepsilon\,\Psi\,))[pAKT]$$

$$-\frac{\beta}{\delta}\gamma\,K_{m2}k_1X_T=0$$

Divide by ( $k_2E_{2T}X_T^2$)

$$(\Phi-\varepsilon\,\Psi\,)\frac{\beta k_1}{\delta k_2E_{2T}X_T^2}[pAKT]^3$$

$$+\left(-\frac{1}{X_T^2}+\frac{\beta\gamma k_1}{\delta k_2E_{2T}X_T^2}+\frac{K_{m2}k_1\beta}{\delta k_2E_{2T}X_T^2}(\Phi-\varepsilon\,\Psi\,)-\frac{k_1X_T\beta}{\delta k_2E_{2T}X_T^2}(\Phi-\varepsilon\,\Psi\,)\right)[pAKT]^2+\ (K_{m1}/\,X_T^2$$

$$+1/X_T+\frac{\beta}{\delta\,k_2E_{2T}X_T^2}\,\gamma\,K_{m2}k_1-\frac{\beta k_1\gamma}{\delta\,k_2E_{2T}X_T}-\frac{\beta\,K_{m2}k_1}{\delta\,k_2E_{2T}X_T}(\Phi-\varepsilon\,\Psi\,))[pAKT]-\frac{\beta\,K_{m2}k_1\gamma}{\delta\,k_2E_{2T}X_T}=0$$

Cubic equation of x is obtained:

$$(\Phi-\varepsilon\,\Psi\,)\frac{\beta k_1X_T}{\delta k_2E_{2T}}x^3+\left(-1+\frac{\beta\gamma k_1}{\delta k_2E_{2T}}+\frac{K_2k_1\beta X_T}{\delta k_2E_{2T}}(\Phi-\varepsilon\,\Psi\,)-\frac{k_1X_T\beta}{\delta k_2E_{2T}}(\Phi-\varepsilon\,\Psi\,)\right)x^2+\ (K_1+1$$

$$+\frac{\beta}{\delta\,k_2E_{2T}}\,\gamma\,K_2k_1-\frac{\beta k_1\gamma}{\delta\,k_2E_{2T}}-\frac{\beta\,K_2k_1X_T}{\delta\,k_2E_{2T}}(\Phi-\varepsilon\,\Psi\,))x-\frac{\beta\,K_2k_1\gamma}{\delta\,k_2E_{2T}}=0$$

Where

$x=[pAKT]/X_T$

$$K_1=\frac{K_{m1}}{X_T}\qquad\qquad K_2=\frac{K_{m2}}{X_T}$$

$$\theta x^3 + ((K_2 - 1)\theta + \lambda - 1)x^2 + (K_1 + 1 + (K_2 - 1)\lambda - K_2\theta)x - K_2\lambda = 0$$

where

$$\theta = (\Phi - \varepsilon\,\Psi)\frac{\beta k_1 X_T}{\delta k_2 E_{2T}} \qquad \lambda = \frac{\beta\gamma k_1}{\delta k_2 E_{2T}}$$

Table 27. Model 1 Steady State Equation

| Steady state equation : | |
|---|---|
| $G(x, \lambda, \theta, K_1, K_2) = 0$ | |
| $G = \theta x^3 + \left((K_2 - 1)\theta + \lambda - 1\right)x^2 + (K_1 + 1 + (K_2 - 1)\lambda - K_2\theta)x - K_2\lambda$ | |
| Parameters | |
| $x = [pAKT]/x_T$ | |
| $\theta = (\Phi - \varepsilon\,\Psi)\beta\, k_1 X_T/(\delta k_2 E_{2T})$ | |
| $\lambda = \gamma\beta k_1/(\delta k_2 E_{2T})$ | |
| $K_1 = (d_1 + k_1)/(a_1 X_T)$ | |
| $K_2 = (d_2 + k_2)/a_2$ | |

## APPENDIX C

$$\frac{dx_1}{dt} = -\frac{(d_1 + k_1)}{K_1}\beta\, x_1 x_5 + \frac{(d_1 + k_1)\beta\, x_5 x_1^2}{K_1^2 + K_1 x_1} + d_1 \frac{\beta\, x_5 x_1}{x_1 + K_1} + k_2 \frac{\tilde{E}_{2T}(1 - x_1)}{(1 - x_1) + K_2} + k_3\, x_9 \tag{34}$$

$$\frac{dx_5}{dt} = \frac{\delta}{\beta}\left(\frac{k2}{k1}\right)\tilde{E}_{2T}\lambda(t) + \left(\Phi - \varepsilon\Psi \mathrm{k_{e\_19}\, x_{10}}\left(1 + \mathrm{k_7\, x_7} + \mathrm{k_{G\_12}[G]}\right)\right)(1 - x_1) - k_{e\_13}\, x_{10} - k_{e\_18}\, x_7 - \delta_I x_5 \tag{35}$$

$$\frac{dx_6}{dt} = k_4(1 - x_1) - k_8\, x_8 x_6 + k_{G\_9}[G] - \delta_N x_6 \tag{36}$$

$$\frac{dx_7}{dt} = k_6 x_6 + k_{G\_10}[G] + u(t) - \delta_{ang} x_7 \tag{37}$$

$$\frac{dx_8}{dt} = k_5 x_7 + k_{G\_11}[G] - \delta_R x_8 \tag{38}$$

$$\frac{dx_9}{dt} = k_8 x_8\, x_6 - \delta_{ON} x_9 \tag{39}$$

$$\frac{dx_{10}}{dt} = k_{e\_16} x_7 + k_{e\_15} x_7 x_5 + k_{e_{14}} x_5 + k_{e\_17}\, x_9 - k_{e\_20}(1 - x_1) - \delta_{ERK} x_{10} \tag{40}$$

$$\frac{dG}{dt} = \left[\frac{1}{1 + e\text{^}(200\left((1 - x_1) - 0.2\right)}\right][0.2 - (1 - x_1)] - \delta_G G$$

$$x_7 = \frac{k_6}{\delta_{ang}}\ x_6 + \frac{k_{G\_10}}{\delta_{ang}}[G] + \frac{1}{\delta_{ang}}u(t)$$

$$x_8 = \frac{k_5 k_6}{\delta_R \delta_{ang}}\ x_6 + \frac{k_5 k_{G\_10}}{\delta_R \delta_{ang}}[G] + \frac{k_5}{\delta_R \delta_{ang}}u(t) + \frac{k_{G\_11}}{\delta_R}[G]$$

$$x_9 = \frac{k_8 k_5 k_6}{\delta_{ON} \delta_R \delta_{ang}}\ {x_6}^2 + \left(\frac{k_8 k_5 k_{G\_10}}{\delta_{ON} \delta_R \delta_{ang}} + \frac{k_8 k_{G\_11}}{\delta_{ON} \delta_R}\right)[G]\ x_6 + \frac{k_8 k_5}{\delta_{ON} \delta_R \delta_{ang}}u(t)$$

$$\begin{aligned} x_{10} = {} & \frac{k_{e\_16}\ k_6}{\delta_{ERK} \delta_{ang}}\ x_6 + \frac{k_{e\_16}\ k_{G\_10}}{\delta_{ERK} \delta_{ang}}[G] + \frac{k_{e\_16}}{\delta_{ERK} \delta_{ang}}u(t) + \frac{k_{e\_15} k_6}{\delta_{ERK} \delta_{ang}}\ x_6[x5] + \frac{k_{e\_15}\ k_{G\_10}}{\delta_{ERK} \delta_{ang}}[G][x5] \\ & + \frac{k_{e\_15}}{\delta_{ERK} \delta_{ang}}u(t)[x5] + \frac{k_{e\_14}}{\delta_{ERK}}[x_5] + \frac{k_8 k_{e\_17} k_5 k_6}{\delta_{ERK} \delta_{ON} \delta_R \delta_{ang}}\ {x_6}^2 + \frac{k_8 k_{e\_17} k_5 k_{G\_10}}{\delta_{ERK} \delta_{ON} \delta_R \delta_{ang}}[G] x_6 \\ & + \frac{k_8 k_{e\_17} k_5}{\delta_{ERK} \delta_{ON} \delta_R \delta_{ang}}u(t) x_6 + \frac{k_8 k_{e\_17} k_{G\_11}}{\delta_{ERK} \delta_{ON} \delta_R}[G] x_6 - \frac{k_{e\_20}}{\delta_{ERK}}(1 - x_1) \end{aligned}$$

$$\frac{dx_5}{dt} = \frac{\delta}{\beta}\left(\frac{k2}{k1}\right)\tilde{E}_{27}\lambda(t)$$
$$+\left(\Phi - \varepsilon\Psi k_{e_{19}}\left(\frac{k_{e\_16}\ k_6}{\delta_{ERK}\delta_{ang}}\ x_6 + \frac{k_{e\_16}\ k_{G\_10}}{\delta_{ERK}\delta_{ang}}[G] + \frac{k_{e\_16}}{\delta_{ERK}\delta_{ang}}u(t) + \frac{k_{e\_15}k_6}{\delta_{ERK}\delta_{ang}}\ x_6[x5]\right.\right.$$
$$+\frac{k_{e\_15}\ k_{G\_10}}{\delta_{ERK}\delta_{ang}}[G][x5] + \frac{k_{e\_15}}{\delta_{ERK}\delta_{ang}}u(t)[x5] + \frac{k_{e\_14}}{\delta_{ERK}}[x_5] + \frac{k_8 k_{e\_17}k_5k_6}{\delta_{ERK}\delta_{ON}\delta_R\delta_{ang}}\ {x_6}^2$$
$$+\frac{k_8 k_{e\_17}k_5k_{G\_10}}{\delta_{ERK}\delta_{ON}\delta_R\delta_{ang}}[G]x_6 + \frac{k_8 k_{e\_17}k_5}{\delta_{ERK}\delta_{ON}\delta_R\delta_{ang}}u(t)x_6 + \frac{k_8 k_{e\_17}k_{G\_11}}{\delta_{ERK}\delta_{ON}\delta_R}[G]x_6$$
$$\left.\left.-\frac{k_{e\_20}}{\delta_{ERK}}(1-x_1)\right)\left(1 + k_7\left(\frac{k_6}{\delta_{ang}}\ x_6 + \frac{k_{G\_10}}{\delta_{ang}}[G] + \frac{1}{\delta_{ang}}u(t)\right) + k_{G\_12}[G]\right)\right)(1-x_1)$$
$$-k_{e\_13}\left(\frac{k_{e\_16}\ k_6}{\delta_{ERK}\delta_{ang}}\ x_6 + \frac{k_{e\_16}\ k_{G\_10}}{\delta_{ERK}\delta_{ang}}[G] + \frac{k_{e\_16}}{\delta_{ERK}\delta_{ang}}u(t) + \frac{k_{e\_15}k_6}{\delta_{ERK}\delta_{ang}}\ x_6[x5]\right.$$
$$+\frac{k_{e\_15}\ k_{G\_10}}{\delta_{ERK}\delta_{ang}}[G][x5] + \frac{k_{e\_15}}{\delta_{ERK}\delta_{ang}}u(t)[x5] + \frac{k_{e\_14}}{\delta_{ERK}}[x_5] + \frac{k_8 k_{e\_17}k_5k_6}{\delta_{ERK}\delta_{ON}\delta_R\delta_{ang}}\ {x_6}^2$$
$$\left.+\frac{k_8 k_{e\_17}k_5k_{G\_10}}{\delta_{ERK}\delta_{ON}\delta_R\delta_{ang}}[G]x_6 + \frac{k_8 k_{e\_17}k_5}{\delta_{ERK}\delta_{ON}\delta_R\delta_{ang}}u(t)x_6 + \frac{k_8 k_{e\_17}k_{G\_11}}{\delta_{ERK}\delta_{ON}\delta_R}[G]x_6 - \frac{k_{e\_20}}{\delta_{ERK}}(1-x_1)\right)$$
$$-k_{e\_18}\left(\frac{k_6}{\delta_{ang}}\ x_6 + \frac{k_{G\_10}}{\delta_{ang}}[G] + \frac{1}{\delta_{ang}}u(t)\right) - \delta_i x_5$$

$$
\begin{aligned}
x_5 = (\frac{\delta}{\beta}\left(\frac{k_2}{k_1}\right) E_{2T}\lambda(t) + (\Phi(1-x_1) - (p_1\, x_6(1-x_1) + p_2[G](1-x_1) + p_3 u(t)(1-x_1) \\
&+ p_8(1-x_1)\, {x_6}^2 + p_9(1-x_1)[G]x_6 + p_{10}(1-x_1)u(t)x_6 \\
&+ p_{11}(1-x_1)[G]x_6 - p_{12}(1-x_1)^2 + p_{13}x_6^2(1-x_1) + p_{14}[G]x_6(1-x_1) \\
&+ p_{15}x_6u(t)(1-x_1) + p_{20}{x_6}^3(1-x_1) + p_{21}[G]x_6^2(1-x_1) \\
&+ p_{22}u(t)x_6^2(1-x_1) + p_{23}[G]x_6^2(1-x_1) - p_{24}(1-x_1)^2x_6 \\
&+ p_{25}\, x_6[G](1-x_1) + p_{26}(1-x_1)[G]^2 + p_{27}(1-x_1)u(t)[G] \\
&+ p_{32}\,(1-x_1)[G]{x_6}^2 + p_{33}(1-x_1)[G]^2x_6 + p_{34}(1-x_1)[G]u(t)x_6 \\
&+ p_{35}(1-x_1)[G]^2x_6 - p_{36}[G](1-x_1)^2 + p_{37}(1-x_1)\, x_6u(t) \\
&+ p_{38}(1-x_1)[G]u(t) + p_{39}(1-x_1)u(t)^2 + p_{44}\,(1-x_1){x_6}^2u(t) \\
&+ p_{45}(1-x_1)[G]x_6u(t) + p_{46}(1-x_1)u(t)^2x_6 + p_{47}(1-x_1)[G]x_6u(t) \\
&- p_{48}(1-x_1)^2\, u(t))) \\
&- \left(p_{49}\, x_6 + p_{50}[G] + p_{51}u(t) + p_{56}\, {x_6}^2 + p_{57}[G]x_6 + p_{58}u(t)x_6\right. \\
&+ \left. p_{59}[G]x_6 - p_{60}(1-x_1)\right) \\
&- \left(p_{61}\, x_6 + p_{62}[G] + p_{63}u(t)\right))/(\, p_4\, x_6(1-x_1) + p_5[G](1-x_1) \\
&+ p_6u(t)(1-x_1) + p_7(1-x_1) + p_{16}\, x_6^2\,(1-x_1) + p_{17}x_6[G](1-x_1) \\
&+ p_{18}u(t)x_6(1-x_1) + p_{19}x_6(1-x_1) + p_{28}\,(1-x_1)x_6[G] \\
&+ p_{29}(1-x_1)[G]^2 + p_{30}(1-x_1)[G]u(t) + p_{31}(1-x_1)[G] \\
&+ p_{40}\,(1-x_1)x_6u(t) + p_{41}(1-x_1)[G]u(t) + p_{42}(1-x_1)u(t)^2 \\
&+ p_{43}(1-x_1)u(t) + p_{52}\, x_6 + p_{53}[G] + p_{54}u(t) + p_{55} + \delta_I)
\end{aligned}
$$

$$p_1 = \frac{\varepsilon\Psi k_{e_{19}} k_{e_{16}}\, k_6}{\delta_{ERK}\delta_{ang}}$$

$$p_2 = \frac{\varepsilon\Psi k_{e_{19}} k_{e_{16}}\, k_{G_{10}}}{\delta_{ERK}\delta_{ang}}$$

$$p_3 = \frac{\varepsilon\Psi k_{e_{19}} k_{e_{16}}}{\delta_{ERK}\delta_{ang}}$$

$$p_4 = \frac{\varepsilon\Psi k_{e_{19}} k_{e_{15}} k_6}{\delta_{ERK}\delta_{ang}}$$

$$p_5 = \frac{\varepsilon\Psi k_{e_{19}} k_{e_{15}}\, k_{G_{10}}}{\delta_{ERK}\delta_{ang}}$$

$$p_6 = \frac{\varepsilon\Psi k_{e_{19}} k_{e_{15}}}{\delta_{ERK}\delta_{ang}}$$

$$p_7 = \frac{\varepsilon\Psi k_{e_{19}} k_{e_{14}}}{\delta_{ERK}}$$

$$p_8 = \frac{\varepsilon\Psi k_{e_{19}} k_8 k_{e_{17}} k_5 k_6}{\delta_{ERK}\delta_{ON}\delta_R\delta_{ang}}$$

$$p_9 = \frac{\varepsilon\Psi k_{e_{19}} k_8 k_{e_{17}} k_5 k_{G_{10}}}{\delta_{ERK}\delta_{ON}\delta_R\delta_{ang}}$$

$$p_{10} = \frac{\varepsilon\Psi k_{e_{19}} k_8 k_{e_{17}} k_5}{\delta_{ERK}\delta_{ON}\delta_R\delta_{ang}}$$

$$p_{11} = \frac{\varepsilon\Psi k_{e_{19}} k_8 k_{e_{17}} k_{G_{11}}}{\delta_{ERK}\delta_{ON}\delta_R}$$

$$p_{12} = \frac{\varepsilon\Psi k_{e_{19}} k_{e_{20}}}{\delta_{ERK}}$$

$$p_{13} = \frac{\varepsilon\Psi k_{e_{19}} k_{e_{16}}\, k_7 k_6^2}{\delta_{ERK}\delta_{ang}^2}$$

$$p_{14} = \frac{\varepsilon\Psi k_{e_{19}} k_{e_{16}}\, k_{G_{10}} k_7 k_6}{\delta_{ERK}\delta_{ang}^2}$$

$$p_{15} = \frac{\varepsilon\Psi k_{e_{19}} k_{e_{16}} k_7 k_6}{\delta_{ERK}\delta_{ang}^2}$$

$$p_{16} = \frac{\varepsilon\Psi k_{e_{19}} k_{e_{15}} k_7 k_6^2}{\delta_{ERK}\delta_{ang}^2}$$

$$p_{17} = \frac{\varepsilon\Psi k_{e_{19}} k_{e_{15}} k_{G_{10}} k_7 k_6}{\delta_{ERK}\delta_{ang}^2}$$

$$p_{18} = \frac{\varepsilon\Psi k_{e_{19}} k_{e_{15}} k_7 k_6}{\delta_{ERK}\delta_{ang}^2}$$

$$p_{19} = \frac{\varepsilon\Psi k_{e_{19}} k_{e_{14}} k_7 k_6}{\delta_{ERK}\delta_{ang}}$$

$$p_{20} = \frac{\varepsilon\Psi k_{e_{19}} k_8 k_{e_{17}} k_5 k_7 k_6^2}{\delta_{ERK}\delta_{ON}\delta_R\delta_{ang}^2}$$

$$p_{21} = \frac{\varepsilon\Psi k_{e_{19}} k_8 k_{e_{17}} k_5 k_{G_{10}} k_7 k_6}{\delta_{ERK}\delta_{ON}\delta_R\delta_{ang}^2}$$

$$p_{22} = \frac{\varepsilon\Psi k_{e_{19}} k_8 k_{e_{17}} k_5 k_7 k_6}{\delta_{ERK}\delta_{ON}\delta_R\delta_{ang}^2}$$

$$p_{23} = \frac{\varepsilon\Psi k_{e_{19}} k_8 k_{e_{17}} k_{G_{11}} k_7 k_6}{\delta_{ERK}\delta_{ON}\delta_R\delta_{ang}}$$

$$p_{24} = \frac{\varepsilon\Psi k_{e_{19}} k_{e_{20}} k_7 k_6}{\delta_{ERK}\delta_{ang}}$$

$$p_{25} = \frac{\varepsilon\Psi k_{e_{19}} k_{e_{16}}\, k_6 (k_7 k_{G_{10}} + \delta_{ang}\, k_{G_{12}})}{\delta_{ERK}\delta_{ang}^2}$$

$$p_{26} = \frac{\varepsilon\Psi k_{e_{19}} k_{e_{16}}\, k_{G_{10}} (k_7 k_{G_{10}} + \delta_{ang}\, k_{G_{12}})}{\delta_{ERK}\delta_{ang}^2}$$

$$p_{27} = \frac{\varepsilon\Psi k_{e_{19}} k_{e_{16}} (k_7 k_{G_{10}} + \delta_{ang}\, k_{G_{12}})}{\delta_{ERK}\delta_{ang}^2}$$

$$p_{28} = \frac{\varepsilon\Psi k_{e_{19}} k_{e_{15}} k_6 (k_7 k_{G_{10}} + \delta_{ang}\, k_{G_{12}})}{\delta_{ERK}\delta_{ang}^2}$$

$$p_{29} = \frac{\varepsilon\Psi \mathrm{k}_{e_{19}} k_{e_{15}} k_{G_{10}} (\mathrm{k}_7 k_{G_{10}} + \delta_{ang}\, \mathrm{k}_{G_{12}})}{\delta_{ERK}\delta_{ang}^2}$$

$$p_{30} = \frac{\varepsilon\Psi \mathrm{k}_{e_{19}} k_{e_{15}} (\mathrm{k}_7 k_{G_{10}} + \delta_{ang}\, \mathrm{k}_{G_{12}})}{\delta_{ERK}\delta_{ang}^2}$$

$$p_{31} = \frac{\varepsilon\Psi \mathrm{k}_{e_{19}} k_{e_{14}} (\mathrm{k}_7 k_{G_{10}} + \delta_{ang}\, \mathrm{k}_{G_{12}})}{\delta_{ERK}\delta_{ang}}$$

$$p_{32} = \frac{\varepsilon\Psi \mathrm{k}_{e_{19}} k_8 k_{e_{17}} k_5 k_6 (\mathrm{k}_7 k_{G_{10}} + \delta_{ang}\, \mathrm{k}_{G_{12}})}{\delta_{ERK}\delta_{ON}\delta_R\delta_{ang}^2}$$

$$p_{33} = \frac{\varepsilon\Psi \mathrm{k}_{e_{19}} k_8 k_{e_{17}} k_5 k_{G_{10}} (\mathrm{k}_7 k_{G_{10}} + \delta_{ang}\, \mathrm{k}_{G_{12}})}{\delta_{ERK}\delta_{ON}\delta_R\delta_{ang}^2}$$

$$p_{34} = \frac{\varepsilon\Psi \mathrm{k}_{e_{19}} k_8 k_{e_{17}} k_5 (\mathrm{k}_7 k_{G_{10}} + \delta_{ang}\, \mathrm{k}_{G_{12}})}{\delta_{ERK}\delta_{ON}\delta_R\delta_{ang}^2}$$

$$p_{35} = \frac{\varepsilon\Psi \mathrm{k}_{e_{19}} k_8 k_{e_{17}} k_{G_{11}} (\mathrm{k}_7 k_{G_{10}} + \delta_{ang}\, \mathrm{k}_{G_{12}})}{\delta_{ERK}\delta_{ON}\delta_R\delta_{ang}}$$

$$p_{36} = \frac{\varepsilon\Psi \mathrm{k}_{e_{19}} k_{e_{20}} (\mathrm{k}_7 k_{G_{10}} + \delta_{ang}\, \mathrm{k}_{G_{12}})}{\delta_{ERK}\delta_{ang}}$$

$$p_{37} = \frac{\varepsilon\Psi \mathrm{k}_{e_{19}} k_{e_{16}} k_6 \mathrm{k}_7}{\delta_{ERK}\delta_{ang}^2}$$

$$p_{38} = \frac{\varepsilon\Psi \mathrm{k}_{e_{19}} k_{e_{16}} k_{G_{10}} \mathrm{k}_7}{\delta_{ERK}\delta_{ang}^2}$$

$$p_{39} = \frac{\varepsilon\Psi \mathrm{k}_{e_{19}} k_{e_{16}} \mathrm{k}_7}{\delta_{ERK}\delta_{ang}^2}$$

$$p_{40} = \frac{\varepsilon\Psi \mathrm{k}_{e_{19}} k_{e_{15}} k_6 \mathrm{k}_7}{\delta_{ERK}\delta_{ang}^2}$$

$$p_{41} = \frac{\varepsilon\Psi \mathrm{k}_{e_{19}} k_{e_{15}} k_{G_{10}} \mathrm{k}_7}{\delta_{ERK}\delta_{ang}^2}$$

$$p_{42} = \frac{\varepsilon\Psi \mathrm{k}_{e_{19}} k_{e_{15}} \mathrm{k}_7}{\delta_{ERK}\delta_{ang}^2}$$

$$p_{43} = \frac{\varepsilon\Psi \mathrm{k}_{e_{19}} k_{e_{14}} \mathrm{k}_7}{\delta_{ERK}\delta_{ang}}$$

$$p_{44} = \frac{\varepsilon\Psi \mathrm{k}_{e_{19}} k_8 k_{e_{17}} k_5 k_6 \mathrm{k}_7}{\delta_{ERK}\delta_{ON}\delta_R\delta_{ang}^2}$$

$$p_{45} = \frac{\varepsilon\Psi \mathrm{k}_{e_{19}} k_8 k_{e_{17}} k_5 k_{G_{10}} \mathrm{k}_7}{\delta_{ERK}\delta_{ON}\delta_R\delta_{ang}^2}$$

$$p_{46} = \frac{\varepsilon\Psi \mathrm{k}_{e_{19}} k_8 k_{e_{17}} k_5 \mathrm{k}_7}{\delta_{ERK}\delta_{ON}\delta_R\delta_{ang}^2}$$

$$p_{47} = \frac{\varepsilon\Psi \mathrm{k}_{e_{19}} k_8 k_{e_{17}} k_{G_{11}} \mathrm{k}_7}{\delta_{ERK}\delta_{ON}\delta_R\delta_{ang}}$$

$$p_{48} = \frac{\varepsilon\Psi \mathrm{k}_{e_{19}} k_{e_{20}} \mathrm{k}_7}{\delta_{ERK}\delta_{ang}}$$

$$p_{49} = \frac{k_{e\_13} k_{e\_16}\ k_6}{\delta_{ERK}\delta_{ang}}$$

$$p_{50} = \frac{k_{e\_13} k_{e\_16}\ k_{G\_10}}{\delta_{ERK}\delta_{ang}}$$

$$p_{51} = \frac{k_{e\_13} k_{e\_16}}{\delta_{ERK}\delta_{ang}}$$

$$p_{52} = \frac{k_{e\_13} k_{e\_15} k_6}{\delta_{ERK}\delta_{ang}}$$

$$p_{53} = \frac{k_{e\_13} k_{e\_15}\ k_{G\_10}}{\delta_{ERK}\delta_{ang}}$$

$$p_{54} = \frac{k_{e\_13} k_{e\_15}}{\delta_{ERK}\delta_{ang}}$$

$$p_{55} = \frac{k_{e\_13} k_{e\_14}}{\delta_{ERK}}$$

$$p_{56} = \frac{k_{e\_13} k_8 k_{e\_17} k_5 k_6}{\delta_{ERK}\delta_{ON}\delta_R\delta_{ang}}$$

$$p_{57} = \frac{k_{e\_13} k_8 k_{e\_17} k_5 k_{G\_10}}{\delta_{ERK}\delta_{ON}\delta_R\delta_{ang}}$$

$$p_{58} = \frac{k_{e\_13} k_8 k_{e\_17} k_5}{\delta_{ERK}\delta_{ON}\delta_R\delta_{ang}}$$

$$p_{59} = \frac{k_{e\_13} k_8 k_{e\_17} k_{G\_11}}{\delta_{ERK}\delta_{ON}\delta_R}$$

$$p_{60} = \frac{k_{e\_13} k_{e\_20}}{\delta_{ERK}}$$

$$p_{61} = \frac{k_{e\_18} k_6}{\delta_{ang}}$$

$$p_{62} = \frac{k_{e\_18} k_{G\_10}}{\delta_{ang}}$$

$$p_{63} = \frac{k_{e\_18}}{\delta_{ang}}$$

## BIBLIOGRAPHY


Aldridge, B.B., Burke, J.M., Lauffenburger, D.A., and Sorger, P.K., 2006. Physicochemical modelling of cell signalling pathways. Nat Cell Biol 8, 1195-203.

Altomare, D.A., and Testa, J.R., 2005. Perturbations of the AKT signaling pathway in human cancer. Oncogene 24, 7455-64.

Ando, K., and Fujita, T., 2006. Anti-diabetic effect of blockade of the renin-angiotensin system. Diabetes Obes Metab 8, 396-403.

Andreozzi, F., Laratta, E., Sciacqua, A., Perticone, F., and Sesti, G., 2004. Angiotensin II impairs the insulin signaling pathway promoting production of nitric oxide by inducing phosphorylation of insulin receptor substrate-1 on Ser312 and Ser616 in human umbilical vein endothelial cells. Circ Res 94, 1211-8.

Angeli, D., Ferrell, J.E., Jr., and Sontag, E.D., 2004. Detection of multistability, bifurcations, and hysteresis in a large class of biological positive-feedback systems. Proc Natl Acad Sci U S A 101, 1822-7.

Bagowski, C.P., and Ferrell, J.E., Jr., 2001. Bistability in the JNK cascade. Curr Biol 11, 1176-82.

Barkai, N., and Leibler, S., 1997. Robustness in simple biochemical networks. Nature 387, 913-7.

Becskei, A., and Serrano, L., 2000. Engineering stability in gene networks by autoregulation. Nature 405, 590-3.

Becskei, A., Seraphin, B., and Serrano, L., 2001. Positive feedback in eukaryotic gene networks: cell differentiation by graded to binary response conversion. EMBO J 20, 2528-35.

Bellacosa, A., Kumar, C.C., Di Cristofano, A., and Testa, J.R., 2005. Activation of AKT kinases in cancer: implications for therapeutic targeting. Adv Cancer Res 94, 29-86.

Blendea, M.C., Jacobs, D., Stump, C.S., McFarlane, S.I., Ogrin, C., Bahtyiar, G., Stas, S., Kumar, P., Sha, Q., Ferrario, C.M., and Sowers, J.R., 2005. Abrogation of oxidative stress improves insulin sensitivity in the Ren-2 rat model of tissue angiotensin II overexpression. Am J Physiol Endocrinol Metab 288, E353-9.

Boulton, T.G., Nye, S.H., Robbins, D.J., Ip, N.Y., Radziejewska, E., Morgenbesser, S.D., DePinho, R.A., Panayotatos, N., Cobb, M.H., and Yancopoulos, G.D., 1991. ERKs: a family of protein-serine/threonine kinases that are activated and tyrosine phosphorylated in response to insulin and NGF. Cell 65, 663-75.

Brandman, O., and Meyer, T., 2008. Feedback loops shape cellular signals in space and time. Science 322, 390-5.

Brands, M.W., and Fitzgerald, S.M., 2002. Blood pressure control early in diabetes: a balance between angiotensin II and nitric oxide. Clin Exp Pharmacol Physiol 29, 127-31.

Carracedo, A., Ma, L., Teruya-Feldstein, J., Rojo, F., Salmena, L., Alimonti, A., Egia, A., Sasaki, A.T., Thomas, G., Kozma, S.C., Papa, A., Nardella, C., Cantley, L.C., Baselga, J., and Pandolfi, P.P., 2008. Inhibition of mTORC1 leads to MAPK pathway activation through a PI3K-dependent feedback loop in human cancer. J Clin Invest 118, 3065-74.

Carvalho-Filho, M.A., Ueno, M., Hirabara, S.M., Seabra, A.B., Carvalheira, J.B., de Oliveira, M.G., Velloso, L.A., Curi, R., and Saad, M.J., 2005. S-nitrosation of the insulin receptor, insulin receptor substrate 1, and protein kinase B/Akt: a novel mechanism of insulin resistance. Diabetes 54, 959-67.

Ceriello, A., Assaloni, R., Da Ros, R., Maier, A., Quagliaro, L., Piconi, L., Esposito, K., and Giugliano, D., 2004. Effect of irbesartan on nitrotyrosine generation in non-hypertensive diabetic patients. Diabetologia 47, 1535-40.

Cong, L.N., Chen, H., Li, Y., Zhou, L., McGibbon, M.A., Taylor, S.I., and Quon, M.J., 1997. Physiological role of Akt in insulin-stimulated translocation of GLUT4 in transfected rat adipose cells. Mol Endocrinol 11, 1881-90.

Corbould, A., Zhao, H., Mirzoeva, S., Aird, F., and Dunaif, A., 2006. Enhanced mitogenic signaling in skeletal muscle of women with polycystic ovary syndrome. Diabetes 55, 751-9.

Crouthamel, M.C., Kahana, J.A., Korenchuk, S., Zhang, S.Y., Sundaresan, G., Eberwein, D.J., Brown, K.K., and Kumar, R., 2009. Mechanism and management of AKT inhibitor-induced hyperglycemia. Clin Cancer Res 15, 217-25.

Csibi, A., Communi, D., Muller, N., and Bottari, S.P., 2010. Angiotensin II inhibits insulin-stimulated GLUT4 translocation and Akt activation through tyrosine nitration-dependent mechanisms. PLoS One 5, e10070.

de Kloet, A.D., Krause, E.G., and Woods, S.C., 2010. The renin angiotensin system and the metabolic syndrome. Physiol Behav 100, 525-34.

Eguchi, S., Dempsey, P.J., Frank, G.D., Motley, E.D., and Inagami, T., 2001. Activation of MAPKs by angiotensin II in vascular smooth muscle cells. Metalloprotease-dependent EGF receptor activation is required for activation of ERK and p38 MAPK but not for JNK. J Biol Chem 276, 7957-62.

Elchebly, M., Payette, P., Michaliszyn, E., Cromlish, W., Collins, S., Loy, A.L., Normandin, D., Cheng, A., Himms-Hagen, J., Chan, C.C., Ramachandran, C., Gresser, M.J., Tremblay, M.L., and Kennedy, B.P., 1999. Increased insulin sensitivity and obesity resistance in mice lacking the protein tyrosine phosphatase-1B gene. Science 283, 1544-8.

Fan, Q., Liao, J., Kobayashi, M., Yamashita, M., Gu, L., Gohda, T., Suzuki, Y., Wang, L.N., Horikoshi, S., and Tomino, Y., 2004. Candesartan reduced advanced glycation end-products accumulation and diminished nitro-oxidative stress in type 2 diabetic KK/Ta mice. Nephrol Dial Transplant 19, 3012-20.

Ferrell, J.E., and Xiong, W., 2001. Bistability in cell signaling: How to make continuous processes discontinuous, and reversible processes irreversible. Chaos 11, 227-236.

Ferrell, J.E., Jr., 2002. Self-perpetuating states in signal transduction: positive feedback, double-negative feedback and bistability. Curr Opin Cell Biol 14, 140-8.

Frank, G.D., Eguchi, S., Yamakawa, T., Tanaka, S., Inagami, T., and Motley, E.D., 2000. Involvement of reactive oxygen species in the activation of tyrosine kinase and extracellular signal-regulated kinase by angiotensin II. Endocrinology 141, 3120-6.

Franke, T.F., Kaplan, D.R., and Cantley, L.C., 1997. PI3K: downstream AKTion blocks apoptosis. Cell 88, 435-7.

Freeman, M., 2000. Feedback control of intercellular signalling in development. Nature 408, 313-9.

Giovannucci, E., 2007. Metabolic syndrome, hyperinsulinemia, and colon cancer: a review. Am J Clin Nutr 86, s836-42.

Giovannucci, E., Harlan, D.M., Archer, M.C., Bergenstal, R.M., Gapstur, S.M., Habel, L.A., Pollak, M., Regensteiner, J.G., and Yee, D., 2010. Diabetes and cancer: a consensus report. Diabetes Care 33, 1674-85.

Giri, L., Mutalik, V.K., and Venkatesh, K.V., 2004. A steady state analysis indicates that negative feedback regulation of PTP1B by Akt elicits bistability in insulin-stimulated GLUT4 translocation. Theor Biol Med Model 1, 2.

Gookin, J.L., McWhorter, D., Vaden, S., and Posner, L., 2010. Outcome assessment of a computer-animated model for learning about the regulation of glomerular filtration rate. Adv Physiol Educ 34, 97-105.

Guertin, D.A., and Sabatini, D.M., 2005. An expanding role for mTOR in cancer. Trends Mol Med 11, 353-61.

Guo, W., Adachi, T., Matsui, R., Xu, S., Jiang, B., Zou, M.H., Kirber, M., Lieberthal, W., and Cohen, R.A., 2003. Quantitative assessment of tyrosine nitration of manganese superoxide dismutase in angiotensin II-infused rat kidney. Am J Physiol Heart Circ Physiol 285, H1396-403.

Guyton, A.C., Cowley, A.W., Jr., Coleman, T.G., DeClue, J.W., Norman, R.A., and Manning, R.D., 1974. Hypertension: a disease of abnormal circulatory control. Chest 65, 328-38.

Guyton, A.C.H., John E., 2006. Guyton and Hall Textbook of Medical Physiology. Philadelphia: Elsevier Saunders 11 th ed.

Hara, K., Yonezawa, K., Weng, Q.P., Kozlowski, M.T., Belham, C., and Avruch, J., 1998. Amino acid sufficiency and mTOR regulate p70 S6 kinase and eIF-4E BP1 through a common effector mechanism. J Biol Chem 273, 14484-94.

Henriksen, E.J., 2007. Improvement of insulin sensitivity by antagonism of the renin-angiotensin system. Am J Physiol Regul Integr Comp Physiol 293, R974-80.

Henriksen, E.J., Jacob, S., Kinnick, T.R., Teachey, M.K., and Krekler, M., 2001. Selective angiotensin II receptor antagonism reduces insulin resistance in obese Zucker rats. Hypertension 38, 884-90.

Hsu, I.R., Kim, S.P., Kabir, M., and Bergman, R.N., 2007. Metabolic syndrome, hyperinsulinemia, and cancer. Am J Clin Nutr 86, s867-71.

Inoguchi, T., Li, P., Umeda, F., Yu, H.Y., Kakimoto, M., Imamura, M., Aoki, T., Etoh, T., Hashimoto, T., Naruse, M., Sano, H., Utsumi, H., and Nawata, H., 2000. High glucose level and free fatty acid stimulate reactive oxygen species production through protein kinase C--dependent activation of NAD(P)H oxidase in cultured vascular cells. Diabetes 49, 1939-45.

Inoki, K., Corradetti, M.N., and Guan, K.L., 2005. Dysregulation of the TSC-mTOR pathway in human disease. Nat Genet 37, 19-24.

Izawa, Y., Yoshizumi, M., Fujita, Y., Ali, N., Kanematsu, Y., Ishizawa, K., Tsuchiya, K., Obata, T., Ebina, Y., Tomita, S., and Tamaki, T., 2005. ERK1/2 activation by angiotensin II inhibits insulin-induced glucose uptake in vascular smooth muscle cells. Exp Cell Res 308, 291-9.

Kahn, B.B., 1998. Type 2 diabetes: when insulin secretion fails to compensate for insulin resistance. Cell 92, 593-6.

Kim, J.R., Yoon, Y., and Cho, K.H., 2008. Coupled feedback loops form dynamic motifs of cellular networks. Biophys J 94, 359-65.

Kitano, H., 2002. Systems biology: a brief overview. Science 295, 1662-4.

Kurtz, A., and Wagner, C., 1998. Role of nitric oxide in the control of renin secretion. Am J Physiol 275, F849-62.

Kwon, Y.K., and Cho, K.H., 2008. Coherent coupling of feedback loops: a design principle of cell signaling networks. Bioinformatics 24, 1926-32.

Lansang, M.C., and Hollenberg, N.K., 2002. Renal perfusion and the renal hemodynamic response to blocking the renin system in diabetes: are the forces leading to vasodilation and vasoconstriction linked? Diabetes 51, 2025-8.

Laurent, M., and Kellershohn, N., 1999. Multistability: a major means of differentiation and evolution in biological systems. Trends Biochem Sci 24, 418-22.

Liao, Y., and Hung, M.C., 2010. Physiological regulation of Akt activity and stability. Am J Transl Res 2, 19-42.

Little, J.W., Shepley, D.P., and Wert, D.W., 1999. Robustness of a gene regulatory circuit. EMBO J 18, 4299-307.

Manning, B.D., 2004. Balancing Akt with S6K: implications for both metabolic diseases and tumorigenesis. J Cell Biol 167, 399-403.

Miller, J.A., 1999. Impact of hyperglycemia on the renin angiotensin system in early human type 1 diabetes mellitus. J Am Soc Nephrol 10, 1778-85.

Muscogiuri, G., Chavez, A.O., Gastaldelli, A., Perego, L., Tripathy, D., Saad, M.J., Velloso, L., and Folli, F., 2008. The crosstalk between insulin and renin-angiotensin-aldosterone signaling systems and its effect on glucose metabolism and diabetes prevention. Curr Vasc Pharmacol 6, 301-12.

National Diabetes Fact Sheet, 2011.

Nawano, M., Anai, M., Funaki, M., Kobayashi, H., Kanda, A., Fukushima, Y., Inukai, K., Ogihara, T., Sakoda, H., Onishi, Y., Kikuchi, M., Yazaki, Y., Oka, Y., and Asano, T., 1999. Imidapril, an angiotensin-converting enzyme inhibitor, improves insulin sensitivity by enhancing signal transduction via insulin receptor substrate proteins and improving vascular resistance in the Zucker fatty rat. Metabolism 48, 1248-55.

Nayak, S., Siddiqui, J.K., and Varner, J.D., 2011. Modelling and analysis of an ensemble of eukaryotic translation initiation models. IET Syst Biol 5, 2.

Ozbudak, E.M., Thattai, M., Lim, H.N., Shraiman, B.I., and Van Oudenaarden, A., 2004. Multistability in the lactose utilization network of Escherichia coli. Nature 427, 737-40.

Pacher, P., Beckman, J.S., and Liaudet, L., 2007. Nitric oxide and peroxynitrite in health and disease. Physiol Rev 87, 315-424.

Paz, K., Liu, Y.F., Shorer, H., Hemi, R., LeRoith, D., Quan, M., Kanety, H., Seger, R., and Zick, Y., 1999. Phosphorylation of insulin receptor substrate-1 (IRS-1) by protein kinase B positively regulates IRS-1 function. J Biol Chem 274, 28816-22.

Perkins, J.M., and Davis, S.N., 2008. The renin-angiotensin-aldosterone system: a pivotal role in insulin sensitivity and glycemic control. Curr Opin Endocrinol Diabetes Obes 15, 147-52.

Peti-Peterdi, J., Kang, J.J., and Toma, I., 2008. Activation of the renal renin-angiotensin system in diabetes--new concepts. Nephrol Dial Transplant 23, 3047-9.

Pinzar, E., Wang, T., Garrido, M.R., Xu, W., Levy, P., and Bottari, S.P., 2005. Angiotensin II induces tyrosine nitration and activation of ERK1/2 in vascular smooth muscle cells. FEBS Lett 579, 5100-4.

Pomerening, J.R., Sontag, E.D., and Ferrell, J.E., Jr., 2003. Building a cell cycle oscillator: hysteresis and bistability in the activation of Cdc2. Nat Cell Biol 5, 346-51.

Pueyo, M.E., Arnal, J.F., Rami, J., and Michel, J.B., 1998. Angiotensin II stimulates the production of NO and peroxynitrite in endothelial cells. Am J Physiol 274, C214-20.

Pulakat, L., Demarco, V.G., Whaley-Connell, A., and Sowers, J.R., 2011. The Impact of Overnutrition on Insulin Metabolic Signaling in the Heart and the Kidney. Cardiorenal Med 1, 102-112.

Raught, B., Gingras, A.C., and Sonenberg, N., 2001. The target of rapamycin (TOR) proteins. Proc Natl Acad Sci U S A 98, 7037-44.

Ravichandran, L.V., Chen, H., Li, Y., and Quon, M.J., 2001. Phosphorylation of PTP1B at Ser(50) by Akt impairs its ability to dephosphorylate the insulin receptor. Mol Endocrinol 15, 1768-80.

Reynolds, A.R., Tischer, C., Verveer, P.J., Rocks, O., and Bastiaens, P.I., 2003. EGFR activation coupled to inhibition of tyrosine phosphatases causes lateral signal propagation. Nat Cell Biol 5, 447-53.

Saltiel, A.R., and Kahn, C.R., 2001. Insulin signalling and the regulation of glucose and lipid metabolism. Nature 414, 799-806.

Scheen, A.J., 2004. Renin-angiotensin system inhibition prevents type 2 diabetes mellitus. Part 1. A meta-analysis of randomised clinical trials. Diabetes Metab 30, 487-96.

Smolen, P., Baxter, D.A., and Byrne, J.H., 1998. Frequency selectivity, multistability, and oscillations emerge from models of genetic regulatory systems. Am J Physiol 274, C531-42.

Sobie, E.A., 2011. Bistability in biochemical signaling models. Sci Signal 4, tr10.

Sowers, J.R., 1990. Insulin resistance and hypertension. Mol Cell Endocrinol 74, C87-9.

Tee, A.R., and Blenis, J., 2005. mTOR, translational control and human disease. Semin Cell Dev Biol 16, 29-37.

Teruel, M.N., and Meyer, T., 2002. Parallel single-cell monitoring of receptor-triggered membrane translocation of a calcium-sensing protein module. Science 295, 1910-2.

Thomas, G., and Hall, M.N., 1997. TOR signalling and control of cell growth. Curr Opin Cell Biol 9, 782-7.

Thron, C.D., 1997. Bistable biochemical switching and the control of the events of the cell cycle. Oncogene 15, 317-25.

Tian, Y., Smith, R.D., Balla, T., and Catt, K.J., 1998. Angiotensin II activates mitogen-activated protein kinase via protein kinase C and Ras/Raf-1 kinase in bovine adrenal glomerulosa cells. Endocrinology 139, 1801-9.

Ushio-Fukai, M., Alexander, R.W., Akers, M., and Griendling, K.K., 1998. p38 Mitogen-activated protein kinase is a critical component of the redox-sensitive signaling pathways activated by angiotensin II. Role in vascular smooth muscle cell hypertrophy. J Biol Chem 273, 15022-9.

Velloso, L.A., Folli, F., Perego, L., and Saad, M.J., 2006. The multi-faceted cross-talk between the insulin and angiotensin II signaling systems. Diabetes Metab Res Rev 22, 98-107.

Velloso, L.A., Folli, F., Sun, X.J., White, M.F., Saad, M.J., and Kahn, C.R., 1996. Cross-talk between the insulin and angiotensin signaling systems. Proc Natl Acad Sci U S A 93, 12490-5.

Wang, G., 2010. Singularity analysis of the AKT signaling pathway reveals connections between cancer and metabolic diseases. Phys Biol 7, 046015.

Wattanapitayakul, S.K., Weinstein, D.M., Holycross, B.J., and Bauer, J.A., 2000. Endothelial dysfunction and peroxynitrite formation are early events in angiotensin-induced cardiovascular disorders. FASEB J 14, 271-8.

Wei, Y., Sowers, J.R., Nistala, R., Gong, H., Uptergrove, G.M., Clark, S.E., Morris, E.M., Szary, N., Manrique, C., and Stump, C.S., 2006. Angiotensin II-induced NADPH oxidase activation impairs insulin signaling in skeletal muscle cells. J Biol Chem 281, 35137-46.

Wenzel, P., Schulz, E., Oelze, M., Muller, J., Schuhmacher, S., Alhamdani, M.S., Debrezion, J., Hortmann, M., Reifenberg, K., Fleming, I., Munzel, T., and Daiber, A., 2008. AT1-receptor blockade by telmisartan upregulates GTP-cyclohydrolase I and protects eNOS in diabetic rats. Free Radic Biol Med 45, 619-26.

Winter, J.N., Jefferson, L.S., and Kimball, S.R., 2011. ERK and Akt signaling pathways function through parallel mechanisms to promote mTORC1 signaling. Am J Physiol Cell Physiol 300, C1172-80.

World Health Organisation, August 2011. Fact sheet No 312

Xiong, W., and Ferrell, J.E., Jr., 2003. A positive-feedback-based bistable 'memory module' that governs a cell fate decision. Nature 426, 460-5.

Yasukawa, T., Tokunaga, E., Ota, H., Sugita, H., Martyn, J.A., and Kaneki, M., 2005. S-nitrosylation-dependent inactivation of Akt/protein kinase B in insulin resistance. J Biol Chem 280, 7511-8.

Yu, T., Jhun, B.S., and Yoon, Y., 2011. High-glucose stimulation increases reactive oxygen species production through the calcium and mitogen-activated protein kinase-mediated activation of mitochondrial fission. Antioxid Redox Signal 14, 425-37.

Zeng, G., Nystrom, F.H., Ravichandran, L.V., Cong, L.N., Kirby, M., Mostowski, H., and Quon, M.J., 2000. Roles for insulin receptor, PI3-kinase, and Akt in insulin-signaling pathways related to production of nitric oxide in human vascular endothelial cells. Circulation 101, 1539-45.

Zimmermann, S., and Moelling, K., 1999. Phosphorylation and regulation of Raf by Akt (protein kinase B). Science 286, 1741-4.

## VITA

Deniz was born in 1986 in Istanbul. In mid 2010, she graduated from Koc University with a double major in Chemistry and Chemical and Biological Engineering. In late 2010, she joined Koc University Computational and Quantitative Biology Lab. She was both research and teaching assistant at Koç University.